Investigation of RNA in Extracellular Vesicles

Investigation of RNA in Extracellular Vesicles

A dissertation presented

by

Dmitry Ter-Ovanesyan

to

The Department of Molecular and Cellular Biology

In partial fulfillment of the requirements

for the degree of

Doctor of Philosophy

In the subject of

Biology

Harvard University

Cambridge, Massachusetts

December 2018

Dissertation Advisors: George M. Church & Aviv Regev Dmitry Ter-Ovanesyan

Investigation of RNA in Extracellular Vesicles

Abstract

Extracellular vesicles (EVs) are small membrane packages that are released by all cells. About a decade ago, it was found that EVs contain RNA, and it was proposed that EVs may transfer RNA between cells as a mechanism of intercellular communication. In this thesis, I used human cell culture systems to develop new methods assessing whether EVs and RNA are transferred between cells, and also extensively characterized the RNA in EVs. Using EVs isolated from human cells, I developed single EV imaging methods and used high throughput RNA sequencing (RNA-Seq) to profile EV RNA. Additionally, I developed a new technique based on enzymatic treatments with proteinase and then RNase to differentiate what extracellular RNA is inside vesicles from that which is outside. Applying this technique, I performed RNA-Seq on RNA isolated from EVs in cell culture media and I found that the mRNA profile in EVs is highly correlated to that mRNA profile of the donor cells. This finding suggests that mRNA is generally packaged into EVs in a non-specific manner, and has significant implications for using EVs to non-invasively read out the transcriptome of human cells from biological fluids. Towards that end, I describe methods for isolating cell-type specific EV, using EVs from neurons as a proof of principle. My work highlights the potential of EVs for

diagnostics, but also casts doubt on the notion that EVs are used to physiologically transfer RNA between cells.

Acknowledgements

I'll start at the top. I am immensely grateful to my advisors, George and Aviv. The first person at Harvard I went to talk to after being admitted was George, due to his reputation for running, based on an article I found on the interwebs, a lab in a fashion akin to an artists' colony. George has created a unique environment for scientific research, and for a PhD in particular. Once one joins George's lab, one has true freedom in choosing what to work on. Such freedom is rare, even in academia. This freedom can be tremendously exciting for a new graduate student coming in with a lot of ideas, but, of course, also tremendously challenging as starting graduate students generally have no idea what they're doing or how challenging it is to actually carry out any of their proposed research ideas - I was certainly no exception. Nonetheless, George has qualities that are helpful in navigating a challenging research path: he is optimistic, encouraging and patient. I remember when I had my first meeting with George after joining the lab, I proposed a set of wildly ambitious, but as I now realize, completely unrealistic set of goals. George said, in response, "I bet you can do it." Although the goals, after acquiring unexpected data, changed, that simple phrase of encouragement kept me going for a while. I'd also like to thank George for his patience and support as I explored various directions and dead ends before finding my way.

I also owe a tremendous amount of gratitude to Aviv. When I started, Aviv's lab had a diverse set of projects, but it was nonetheless clear that my ideas were further from the lab's core interests than she prefers. Aviv took a chance on me, and

like George, was also encouraging and patient as I figured out the research that is ultimately described in this thesis. In particular, she was always quick to connect me to potential collaborators, and think of ways to move forward at times when I got stuck in non-productive interludes. There were many fortuitous cases where a problem I encountered was actually being worked on in some fashion in Aviv's lab, and I was able to greatly benefit. Additionally, Aviv's breadth of knowledge and ability to deeply understand both experimental and computational biology, are both qualities I still aspire to.

The person that has contributed most to helping me carry out the work described in this thesis is undoubtedly Emma Kowal. Emma joined me at the end of her Junior year of college and worked with me for two years: for a year as an undergrad and then, for a year afterwards. Usually, when one is at the end of one's third year as a PhD student and at a peak of general confusion about one's project, the solution is absolutely not to get an undergrad. I have seen many undergrads in the lab over the years and was also one myself. As an exception to this rule, the combination of youthful energy and hard work that Emma brought was crucial to moving the project forward. Within a few months of me teaching her all the techniques I knew, Emma not only mastered of them, but also started learning (and successfully applying) new techniques to solve some of the challenges we came across. The two years during which Emma and I worked together were definitely the most productive years for "Team Exosome," and also the most enjoyable.

There were many other people in the Church and Regev labs that were spectacularly helpful over the course of my PhD. I'll start with the Church lab.

Francois Vigneault helped me find my bearing in the Church lab when I was just getting started. Alex Ng and Seth Shipman were generous with helping me figure out how to work with iPS cells and make neurons. I greatly enjoyed interacting with Jon Scheiman in the lab, in particular, during heartfelt discussions very late at night in the tissue culture room. I enjoyed working with him and others in the Church lab on Cas9 activators. Dan Goodman was an inspirational grad student in the lab that I was fortunate to overlap with and whose comments were always insightful. I also had a chance to briefly work with Chris Guzman, and he helped clone constructs for live cell imaging. I shared a bay in the Church lab at various times with Joe Negri, Paul Reginato, and Eswar Iyer, and I greatly enjoyed the conversations and camaraderie I shared with them.

In the Regev lab, I started, in addition to working on my project, collaborating on RNA modifications with Schragi Schwartz and Max Mumbach. I benefited from Schragi's great intellect, and his criticism of my ideas and plans was incredibly helpful in becoming a clearer thinker. Max Mumbach was a delight to work with, and I learned a lot from him about making spectacular RNA-Seq libraries, among other life lessons. I started at the same time in the Regev Lab as Jenny Chen, and was fortunate to have my desk situated next to hers. I benefited greatly from Jenny's spectacular expertise on all things computational, as well as her general intelligence in far-reaching conversations on academia, psychology, politics, and a variety of other topics. I was also fortunate to overlap with Yarden Katz, whose idealism and expertise in a large number of disparate fields was inspirational. I'd also like to thank Sam Myers and Marko Jovanovic, who both gave me useful advice about

proteomics and were great to interact with in general. Additionally, I want to thank the Proteomics Platform at the Broad for help with mass spectrometry, in particular, Mike Burgess, Hasmik Keshishian, and Steve Carr.

I had a variety of crucial collaborators throughout my PhD. One that is particularly notable is Emanuele Coccuci. He taught me a lot about microscopy, membrane trafficking, and Italians. Our collaboration was a prime example of having two people interested in the same topic but bringing together different areas of expertise in a synergistic fashion. Additionally, working with Emanuele was a reminder that doing experiments can, and should, be fun. Another collaboration that I am extremely grateful for is that with David Walt's lab, in particular with Maia Kipman. David and Maia encouraged me to try to actually apply some of the methods I developed to try to create diagnostics, and I wouldn't have embarked on some of the latest experiments developing diagnostic methods were I not working with them.

There have been many people at Harvard who have been tremendously helpful during my PhD. My committee meetings were probably the most useful meetings I had to think about what I was doing. I am extremely grateful to Craig Hunter, Andrew Murray, and Sean Eddy. Craig was the first person at Harvard who gave me some assurance that I was not crazy for being interested in extracellular RNA. I always greatly enjoyed my interactions with him and the opportunity to work together with him and his former postdoc, Ken Pang, on some experiments testing the relationship between Sid1 and extracellular vesicles. Sean's clear thinking and insightful comments were also always appreciated - I'm glad he moved to MCB and

agreed to be on my committee before even getting here. Although Andrew's research interests are quite far removed from my thesis topic, his advice was generally spot-on. When ignored, it was often to my detriment. Furthermore, Andrew's idealistic and romantic perspective on science is rare these days, and he has clearly had a strong influence on a lot of the best things about the MCB department. Another person who I greatly enjoyed interacting with at MCB is John Calarco, who is one of the nicest people I met in the department. He orchestrated an RNA data club that had presentations and discussions at a spectacularly high level of quality, and made me feel that choosing RNA as my general area of scientific interest was the correct decision. Another inspirational figure in my PhD was Vlad Denic, who made me glad I chose MCB for grad school, and also made me giggle.

Some of the people who helped my training before grad school continued to be there for me during my PhD. Eric Wang and Robin Friedman were two graduate student in Chris Burge's lab who I still view as role models, and who, whenever I met with them and described various hardships, were energizing and encouraging. I am grateful to Clotilde Thery (as well as her graduate student, Marina Colombo) and Johan Skog, who I had the opportunity to work with before grad school. Receiving training from leaders in the field was incredibly helpful preparation for venturing off into ExosomeLand on my own. I enjoyed continuing my interactions with them during my PhD.

Finally, I'm grateful for all the people in my life outside of science. Friends (Rich, Jamie, Praveen, Cinjon, Nina, Mei Mei, Marco): thank you. And most of all, I'd

like to thank my family for their unequivocal support: my parents, grandparents, and brother.

This thesis is dedicated to the memory of my grandfather, Anatol Rozenberg.

Contributions

I have worked with several collaborators on the work described in this thesis.

In Chapter 2, electron microscopy and enzymatic treatment experiments were done together with Emma Kowal.

In Chapter 3, TIRF microscopy experiments were performed together with Emma Kowal and Emanuele Coccuci.

In Chapter 4, mass spectrometry of neuron-derived EVs was performed at the Broad Institute Proteomics Platform by Mike Burgess, under the supervision of Hasmik Keshishian and Steve Carr. The immuno-isolation protocol was developed together with Emma Kowal.

In Chapter 5, live cell imaging was performed together with Emanuele Coccuci. Chris Guzman assisted with cloning of plasmid constructs for live cell imaging. RNA-Seq data for mouse-human co-culture experiment was analyzed by Schragi Schwartz.

Table of Contents

List of Tables and Figures

Chapter 2:

Chapter 3:

Chapter 4:

Chapter 5:

Chapter I

Introduction

Ribonucleic Acid (RNA) is a central player in the normal functioning of the cell. Although all of the described functions of RNA are inside the cell, it was demonstrated 70 years ago that RNA is also found outside of the cell in human plasma, the cell-free portion of blood (1). For the subsequent 60 years, this finding was largely ignored as plasma is known to have a large amount of RNase activity, and it was unclear how RNA could be protected from RNases outside of the cell. It is well established that adding *in-vitro* transcribed or chemically synthesized RNA to plasma causes rapid degradation. The RNA that is found in the extracellular portion of biological fluids, however, appears to be stable (2, 3). Thus, there must be a mechanism of protecting RNA outside of the cell from RNases. Such a mechanism was described in the form of extracellular vesicles (EVs) (4-7). Although these EVs, also called exosomes or microvesicles, were first described in the late 1970's and early 1980's, the finding that they contain RNA came more than 25 years later (8).

The discovery that EVs contain RNA led to excitement (particularly among impressionable young RNA biologists), about the possibility of EVs transferring functional RNA between cells as a form of intercellular communication (9). RNA transfer between cells was first postulated to happen long before the discovery of EVs in 1971 (10), but EVs provided a potential mechanistic explanation to how this process could occur. Namely, the fact that EVs contain transmembrane proteins theoretically opened up the possibility that certain EV ligands could interact with certain cellular receptors in a specific fashion. Soon, a large number of studies started to declare that EVs facilitate various physiological functions through transfer of RNAs in processes as diverse as cancer metastasis, longevity, and insulin resistance (11). Intercellular

communication through EVs is an enticing notion as EVs could serve as specific packages of RNAs and protein that could encode messages far more complex and precise than the signal transduction cascades induced by hormones or extracellular signaling proteins. For example, transfer of an mRNA would allow for the upregulation of one specific protein in the recipient cell (9).

As tempting as it is to speculate about a previously unknown mechanism of intercellular communication, all of these studies suffered from serious and systematic shortcomings. Firstly, it is not possible to isolate just EVs and not other contaminating biomolecules (free proteins, etc.) from a given biological fluid or cell culture media preparation. This makes it difficult to determine whether a molecule presumed to be inside of EV is really inside or present in the EV preparation but actually stuck to the outside of EVs (11). This is particularly a problem for microRNAs (miRNAs), as it has been shown that miRNAs are protected from RNAse degradation in plasma through binding to proteins such as Argonaute2 (12, 13). Furthermore, the inability to isolate just EVs is also a problem for functional studies. When EVs are added to a certain type of cell and a phenotype is measured, it is not possible to conclude that the phenotype is from the EV cargo and not the contaminants in the EV preparation. Additionally, as EVs are heterogeneous and contain many different cargos, it is not possible to attribute the phenotype to any given cargo molecule, whether it is an RNA or protein (11).

Another problem that has plagued the field is the inability to distinguish EVs released by live cells from those coming from dead cells. In the early days of EV research, there were questions of whether EVs are released from live cells at all or whether they come exclusively from dead cells (14). Although it is currently impossible

to answer what proportion of EVs in culture or a biological fluid come from live vs. dead cells, there is strong evidence that live cells do release EVs (8, 15). To evaluate this evidence, it is useful to consider how EVs were first discovered.

In the late 1970's and early 1980's, EVs were discovered by electron microscopy (16-20). The term "exosome" was first coined in 1981 (17), but EVs were purified and visualized by electron microscopy even earlier (16). The mechanism of EVs release was first studied in detail in the course of studying the transferrin receptor in erythrocytes by electron microscopy with immune-gold labeling. It was found that the transferrin receptor is released from cells in vesicles. By looking at different electron microscopy images, a novel cellular mechanism was reconstructed whereby the endosome forms inward budding (to become the multivesicular body), and then fuses with the plasma membrane, releasing its intraluminal vesicles. These cross-sections showed cells releasing vesicles into the extracellular space (18, 21).

Additional evidence for EV release is observed upon examining scanning electron microscopy images of the cell surface, which show budding of a large number of vesicles out of a cell directly from the membrane (7). Initially, there have been attempts to differentiate EVs that come from the MVB from those that bud directly from the plasma membrane by calling EVs that originate from the MVB "exosomes" and EVs that originate at the plasma membrane "microvesicles." This, however, has not been a fruitful direction given that no protein markers (or other distinguishing features) exist that separate one from the other (22). Therefore, I will define EVs in this thesis as any vesicle outside of cells (regardless of mechanism of biogenesis) of an arbitrary size (or example, <~200 nm in diameter, if a 0.22 μm filter is used). Although most of what we know about

EV biogenesis comes from electron microscopy, more recently, there have been studies reporting the imaging of EV release from live cells using fluorescent reporters (23).

One direction to try to understand the function of EVs has been to investigate the molecular mechanism of EV secretion. If genes involved in EV biogenesis could be found, the hope was that these genes could be inhibited. Then, EV function could theoretically be interrogated by shutting off EV function (24). Although RNAi screens for genes involved in EV biogenesis have been attempted (25, 26), a crucial limitation to performing such a screen is that there are no methods to directly and reliably quantify vesicles (27, 28). Furthermore, the candidate genes that are involved in EV biogenesis are very likely that they play other roles in various membrane trafficking pathways (24).

Although EVs seem to be released by all cell types studies, figuring out where they go *in vivo* is largely unknown (29). One strategy has been to isolate EVs from cell culture in vitro, label them, and then to inject them into mice. These studies show that EVs accumulate primarily in the liver and spleen, as is the case with liposomes or other synthetic nanoparticles (30-32). Of course, isolated EVs that are then injected into the bloodstream may not necessarily travel the same path or have the same properties as those generated in vivo. Another approach has been to label cells with reporters and see if the reporter travels between cells. This approach has the advantage of being more physiological than injecting EVs, but has the disadvantage of not being able to directly prove that the reporter is transported through EVs. In this approach, a transgenic mouse is used in which there is a reporter gene that is flanked by LoxP sites. The reporter is only activated in the event of recombination by the Cre recombinase. When cells from a mouse transgenically expressing Cre are injected into mice transgenically expressing the

LoxP reporter, recombination of the reporter can be observed, suggesting that Cre was transferred from a donor cell to a different recipient cell (29).

As a first demonstration of the Cre-Lox approach, Stefan Momma's group performed a bone marrow transplant from a Cre-expressing mouse to a LoxP reporter-expressing mouse. They were able to detect some recombined cells in the liver and also in the brain. The authors were able to rule out cell-cell fusion between the Cre and LoxP cells by also tagging the Cre cells with GFP and checking that the recipient recombined cells do not express GFP. The study also reported recombination in Purkinje neurons after injecting EVs isolated from the blood of Cre-expressing mice directly into the brains of LoxP reporter mouse brains, albeit at very low levels (33). The same group performed similar experiments observing Cre transfer between transplanted tumor cells and myeloid LoxP reporter cells in the tumor microenvironment (34). The van Rheenen group also used a similar Cre-Lox reporter system in mice to show transfer of Cre between different tumor cells using *in vivo* intravital imaging (35).

For the studies investigating the intercellular transfer of Cre or other reporters, it has not been possible to definitely prove that the transfer is through EVs, and also that the transfer is of the mRNA encoding the reporter and not the protein. The authors of both studies made claims that the transfer of Cre was through mRNA and not protein by isolating EVs, and detecting Cre mRNA by RT-PCR but not the protein by an antibody-based method such as ELISA or western blot (33, 35). However, as RT-PCR is much more sensitive than ELISA or western blot in terms of its limit of detection, this is not a particularly convincing argument (11). Furthermore, as one is merely studying what happens to a reporter in a recipient cell, it is not possible in these experiments to

definitely prove that the transfer is through EVs (29). Despite these limitations, the finding that a cytosolic protein (or mRNA encoding it) can be transferred between cells is a significant result that makes it theoretically plausible that EVs physiologically transfer RNA or protein between cells.

One experiment to try to differentiate between mRNA and protein transfer of a reporter involved the translation-inhibiting drug cycloxhexamide. EVs were isolated from donor cells expressing luciferase and added to recipient cells with or without cyclohexamide. There was considerably less luciferase expression in recipient cells when cyclohexamide was added, and the authors concluded that the luciferase was transferred in the form of mRNA as opposed to protein (36). Using cyclohexamide, however, is not an ideal control, as global inhibition of translation in a cell is likely to have a wide variety of indirect effects that could affect the experiment. Furthermore, more generally, seeing transfer of an exogenous reporter between cells does not necessarily mean that endogenous RNAs are transferred between cells (11). Studying endogenous transfer of RNA between cells, however, is very challenging since the sequence of RNAs is the same in donor and acceptor cells and it is impossible to differentiate in any given condition (such as dropping isolated EVs from one cell type on another cell type) whether a change in RNA levels is due to potential RNA transfer or a change in transcription of the corresponding genes.

While many studies have attempted to investigate the complex and (and, at least for now, largely intractable) question of whether EVs are involved in intercellular communication, many fundamental questions remain regarding EV released by a given cell type (28). These questions are more tractable as investigating these does not

necessitate the knowledge of whether EVs are functional, and if so, which cells are the target cells for EVs released by certain donor cells. Furthermore, these questions may be studies *in vitro* in mammalian cell culture systems. One such question is that of selectivity. Are specific cargo molecules packaged into EVs or does the RNA profile reflect that of donor cells? Ideally, one would be able to answer this question *in vivo*. However, this is not readily possible as isolating EVs from blood or another biological fluids represents a mixture from different cell types. Thus, using an *in vitro* system with a single type of cell in culture is a more appropriate approach. In principle, the experiment to determine how the RNA profile of EVs compares to that the RNA profile of cell is simple: isolate EVs and extract their RNA at the same time as extracting the RNA from the donor cells. Then, the cell RNA can be directly compared to the EV RNA by a high-throughput RNA profiling method such as RNA-Seq.

The first papers identifying RNA in EVs performed this basic experiment using gene expression microarrays. Their results indicated that for both mRNA and miRNAs, expression in EVs is uncorrelated to that of donor cells, suggesting that cells may have a mechanism for sorting specific RNAs into EVs (6, 7). A large number of studies followed profiling both coding and non-coding RNAs of EVs from different cell types. The results were wildly variable, with some groups reporting that the profiles were correlated while others reported that the profiles were uncorrelated. Some studies went on to suggest they found a packaging mechanism for a specific RNAs (37).

Upon deeper inspection, it is clear that determining the relationship between EV RNA and that of donor cells is actually non-trivial. The main challenge lies in the imperfection and lack of standardized in available techniques for EV isolation. As all EV

isolation techniques have some non-vesicular contaminants, it is important to ascertain whether these contaminants include RNAs outside of EVs (11). If so, these RNAs would influence the comparison of cell to EV RNA profiles since the contaminating RNAs would erroneously be attributed to the EV RNA repertoire (37).

In addition to differing amount of non-vesicular contaminants, various isolation procedures also capture different subpopulations of EVs. For example, some EV isolation procedures include a filtration step (often using a 0.22 μm filter) where others omit it. As there are EVs of all different sizes (including ones larger than one μm in size), isolating different EV subpopulations may yield different answers regarding their RNA contents (11). Furthermore, certain isolation procedures (such as those without the use of a size filter) are more likely than other to co-purify dead cells or apoptotic bodies in the EV preparation, again potentially skewing the results of RNA profiling.

Lastly, EVs contain a very small amount of RNA relative to cells, and this poses significant challenges for analysis. For example, it was shown that there are biases when extracting microRNAs from different amounts of cells (a large number of cells vs. a small number of cells) when using Trizol, as opposed to Phenol-Chloroform. Specifically, the extraction efficiency is different for miRNAs with more GC content relative to other miRNAs when isolating RNA from differing numbers of cells (38). These findings certainly affect many studies investigating EV miRNAs, as the amount of RNA in EVs is several orders of magnitude less than the amount of RNA in the corresponding donor cells (37).

Despite the challenges in both characterizing EVs and studying their potential function in intercellular communication, the EV field presents an exciting opportunity.

As EVs have been described not only in mammals but also in many other organisms (including unicellular ones) (39), they represent a fundamental aspect of cell biology that we do not understand. If EVs do transfer functional RNA between cells, this would represent a fundamentally new way of thinking about intercellular communication (9). The findings that exogenous RNA molecules such as double-stranded RNA can clearly be transferred between cells in plants (40) and the worm Caenorhabditis elegans (41), makes this worthy of investigation in other organisms, including mammals. Lastly, regardless of their function, EVs are already showing signs of great promise as diagnostic biomarkers of disease (42, 43).

In this thesis, I explore several aspects of EV biology, particularly focusing on the RNA in EVs. Most of my work focuses on EVs isolated from mammalian cell culture systems, as studying EVs is much more tractable *in vitro*. In Chapter II, I describe the development of new techniques for RNA isolation and profiling, and apply them to profile RNA in EVs. In Chapter III, I describe the development of new methods to image single EVs by fluorescent microscopy and our application of this method to studying RNA in EVs. In Chapter IV, I describe general approaches for isolating cell type-specific EVs towards the goal of non-invasively measure transcriptomes in humans, and apply this framework for isolating neuron-specific EVs. In Chapter V, I describe new experimental approaches I developed to study whether EVs transfer RNA between cells. Lastly, in Chapter VI, I summarize my work and indulge in uninhibited speculation about the potential roles of EVs in biology.

Chapter II

Characterization of the RNA contents of EVs

Introduction

Cells release extracellular vesicles (EVs), and these vesicles are found in all human bodily fluids. EVs can be released by fusion of the multivesicular body (MVB) with the plasma membrane or by direct budding from the plasma membrane (8). Interest in extracellular vesicles has increased since the discovery that they contain RNA (4-7). This discovery led to the use of extracellular RNA in EVs as a novel biomarker in a wide range of medical applications. It has also led to excitement regarding the possibility that RNA could be transferred between cells as a mechanism of intercellular communication (44). Although there have been studies detailing RNA transfer through EVs and certain reporters have been shown to be secreted in one cell and functional in another, it remains unclear whether EVs transfer functional RNA under physiological conditions (29).

One of the main challenges in studying the RNA in EVs has been purifying EVs without co-isolating contaminating RNA protected by protein complexes. In the case of extracellular microRNAs (miRNAs) in human serum, it has been shown that the majority of extracellular miRNAs are in ribonuceoprotein (RNP) complexes as opposed to vesicles, and common EV isolation techniques such as ultracentrifugation isolate large amounts of contaminating RNPs along with EVs (12, 13). Due to this technical challenge, answering the question of which RNAs are actually in EVs has remained unanswered since many of the RNAs analyzed after various EV isolation procedures were probably from contaminating RNPs (11).

A central question in EV biology is whether the contents of EVs (RNAs and proteins) are specifically packaged or whether their contents reflect the contents of the

cell. This question is of paramount importance for both the utility of EVs as diagnostic biomarkers and for understanding the role of EVs in intercellular communication. Previous attempts to answer the question of whether EVs package specific RNAs have yielded inconsistent results due to differences in EV isolation techniques, contamination with non-vesicular RNPs, and varying RNA profiling methods (37).

We set out to analyze the RNA in EVs. In particular, we focused on using high-throughput sequencing to analyze messenger RNA (mRNA), which has been much less studied than miRNAs in EVs. Furthermore, we developed a method to separate RNA inside of vesicles from RNA that is outside based on enzymatic treatments with proteinase and then RNase. We analyzed the RNA from EVs in cell culture and found that the mRNA profile of EVs is highly correlated to that of cells. This finding indicates that EVs may be used as a non-invasive "read out" of a cell's transcriptome.

Results

Characterization of EVs

In order to study the RNA contents of EVs, we decided to turn to a cell culture system. We isolated EVs from the K562 human leukemia cell line using the widely used differential ultracentrifugation method (45). After spinning down the cells at 300g, taking the supernatant through a 2000g spin to pellet dead cells and 16,500g spin to remove large vesicles, we perform a filtration through a 0.22 μm filter and then ultracentrifugation at 120,000g. We have previously described (46) our

version of this protocol in great detail (also included as Appendix S2). We were able to characterize our EVs using Dynamic Light Scattering (DLS) and visualize our EVs using transmission electron microscopy (**Fig 2.1**).

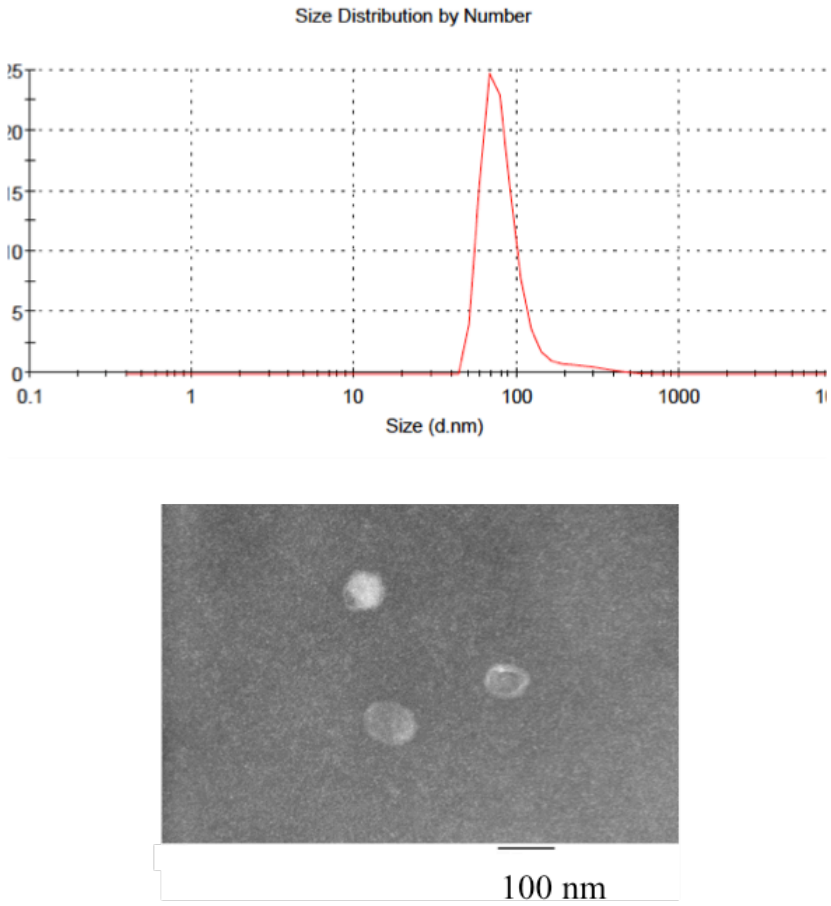

Figure 2.1: Characterization and visualization of differential ultracentrifugation isolation reveals EVs
Dynamic Light Scattering (DLS) via Malvern Zetasizer reveals the preparation of EVs contains objects with diameter averaging slightly less than 100 nm **(top)**. Transmission Electron Microscopy of EVs allows visualization of individual EVs **(bottom)**.

Comparing RNA-Seq profiles of cells and EVs

Characterization of EVs Next, we isolated total RNA from EV preparation as well as the donor K562 cells. We first analyzed the RNA using the Bioanalyzer and found that the size distribution of RNAs is very different between cells and EVs (**Figure 2.2**). In particular, the RNA in EVs does not have large ribosomal RNA peaks as is the case in cells. To compare the RNA profiles of EVs and the corresponding donor cells, we made libraries for high throughput RNA sequencing (RNA-Seq). As

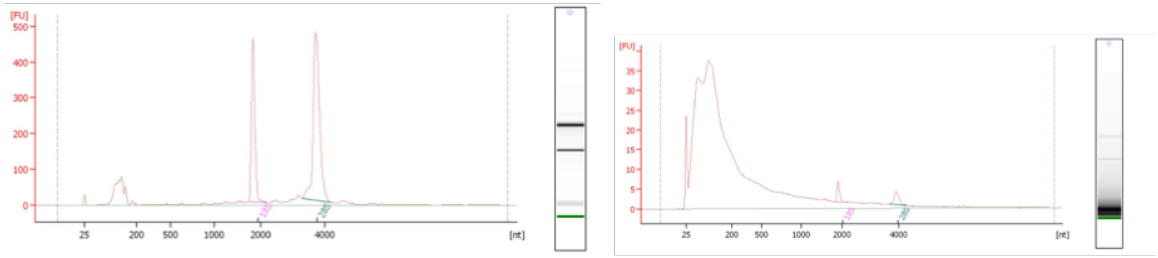

Figure 2.2: RNA size analysis shows marked differences between cell and EV RNA
Cell RNA (left) and EV pellet RNA (right) size profiles were determined using Agilent Bioanalyzer. The EV pellet RNA contents have small ribosomal RNA peak relative to the cell RNA.

we were interested in mRNA in EVs, we isolated PolyA+ RNA in both cells and EVs after DNase treatment. We performed RNA-Seq and assessed the correlation of mRNA expression between cells and EVs. Our results indicate a high correlation between the expression of mRNAs in cells and EVs (**Figure 2.3**).

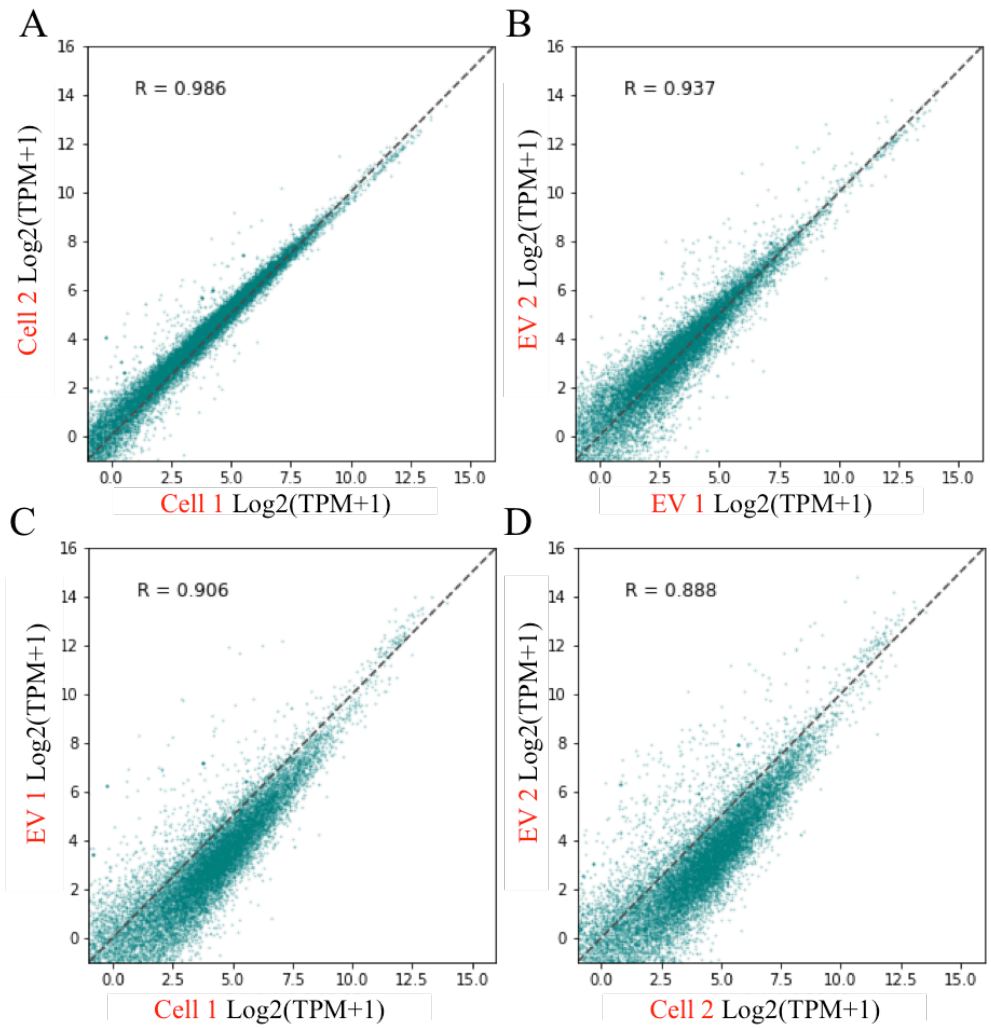

Figure 2.3: RNA-Seq of cells and EVs from K562 cells shows correlation in mRNA profiles
RNA-Seq results of the correlation (R = Spearman Correlation) between gene expression of coding mRNAs in Transcripts Per Million (TPM) for **A.** two replicates of K562 cells, Cell 1 and Cell 2. **B.** two replicates of EVs isolated from K562 cells , EV 1 and EV 2. **C.** donor K562 cells and K562 EVs, replicate 1 **D.** donor K562 cells and K562 EVs, replicate 2.

Although on the whole the mRNA profiles were very correlated, there were some outlier mRNAs that were enriched in EVs relative to cells. We looked at the

RNA-Seq reads for a few of these mRNAs in the Integrated Genomics Viewer (IGV) (47) to see how the reads line up relative to the gene structure. In addition to confirming the enrichment, we observed that the mRNAs appeared to be full length and had normal exon splicing patterns, as in the cell (**Figure 2.4**).

As we are working with a cancer cell line, we were also interested in whether we would get similar results if we looked at primary cells. While we were conducting our study, Stefano Pluchino's group reported RNA-Seq results of EVs or "Exosomes" (defined in their paper as EVs that are subjected to an additional density gradient ultracentrifugation step) obtained from primary mouse neural precursor cells (NPCs) (48). They also repeated the experiment after treating their NPCs with a pro-inflammatory Th1-like cytokine cocktail (which they refer to as "Th1") or an anti-inflammatory Th2-like cytokine cocktail (which they refer to as "Th2"). Although they did not list the correlation between RNA expression in cells and EVs, they made their data publicly available so we downloaded the raw data and reanalyzed it to determine the correlation between RNA in cells and EVs from primary cells. The results indicate a strong correlation between cells and EVs (whether or not purified with density gradient ultracentrifugation) in both basal and stimulated conditions (**Figure 2.5**), agreeing with our results in K562 cells.

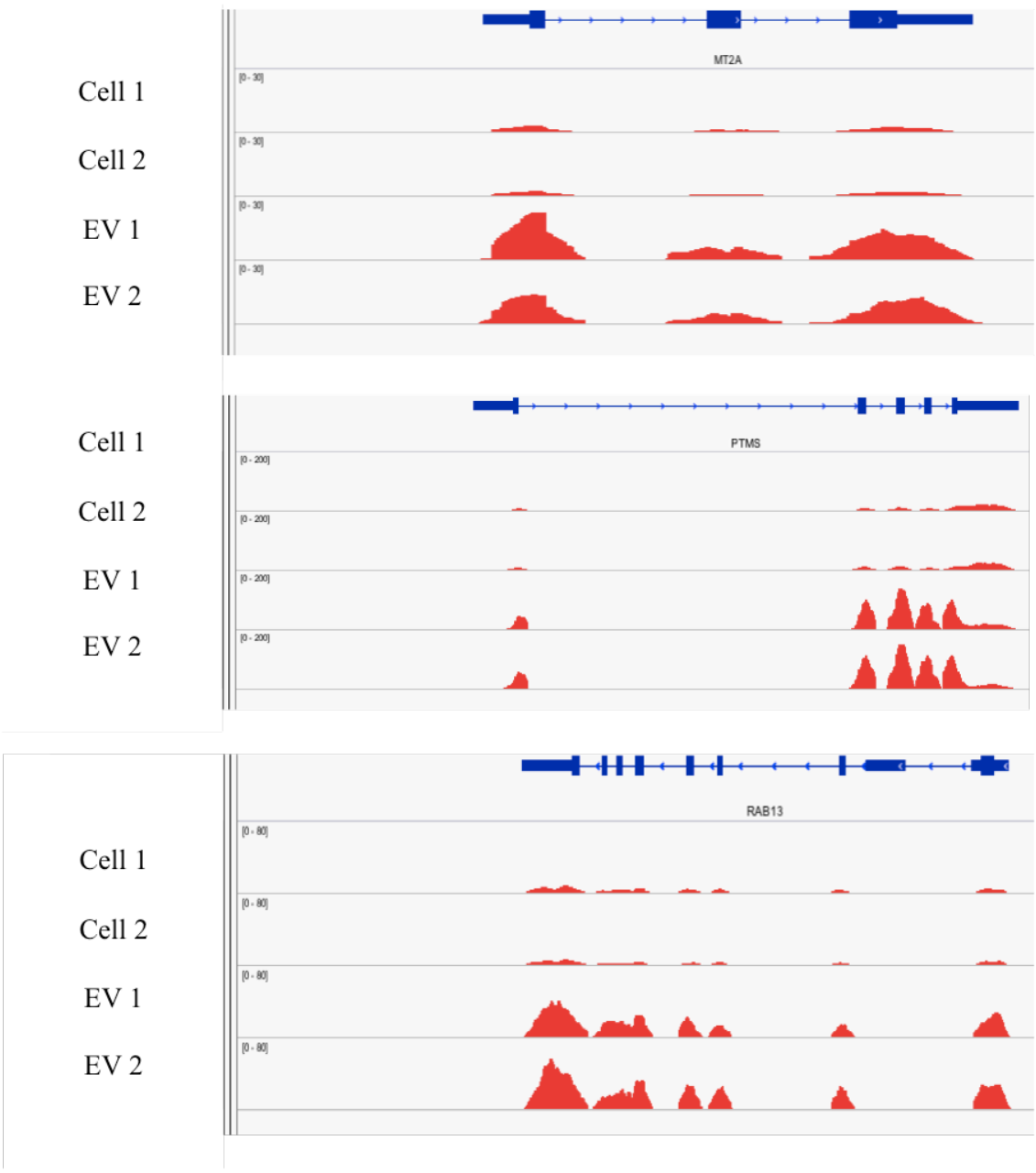

Figure 2.4: IGV analysis of RNA-Seq reads confirms enriched outlier mRNAs exist
Previously published (Cosseti *et al*, 2014) RNA-Seq dataset of primary mouse neural precursor cells (NPCs) and EVs shows strong correlation between Transcripts Per Million (TPM) expression levels of coding mRNAs (R = Spearman Correlation).

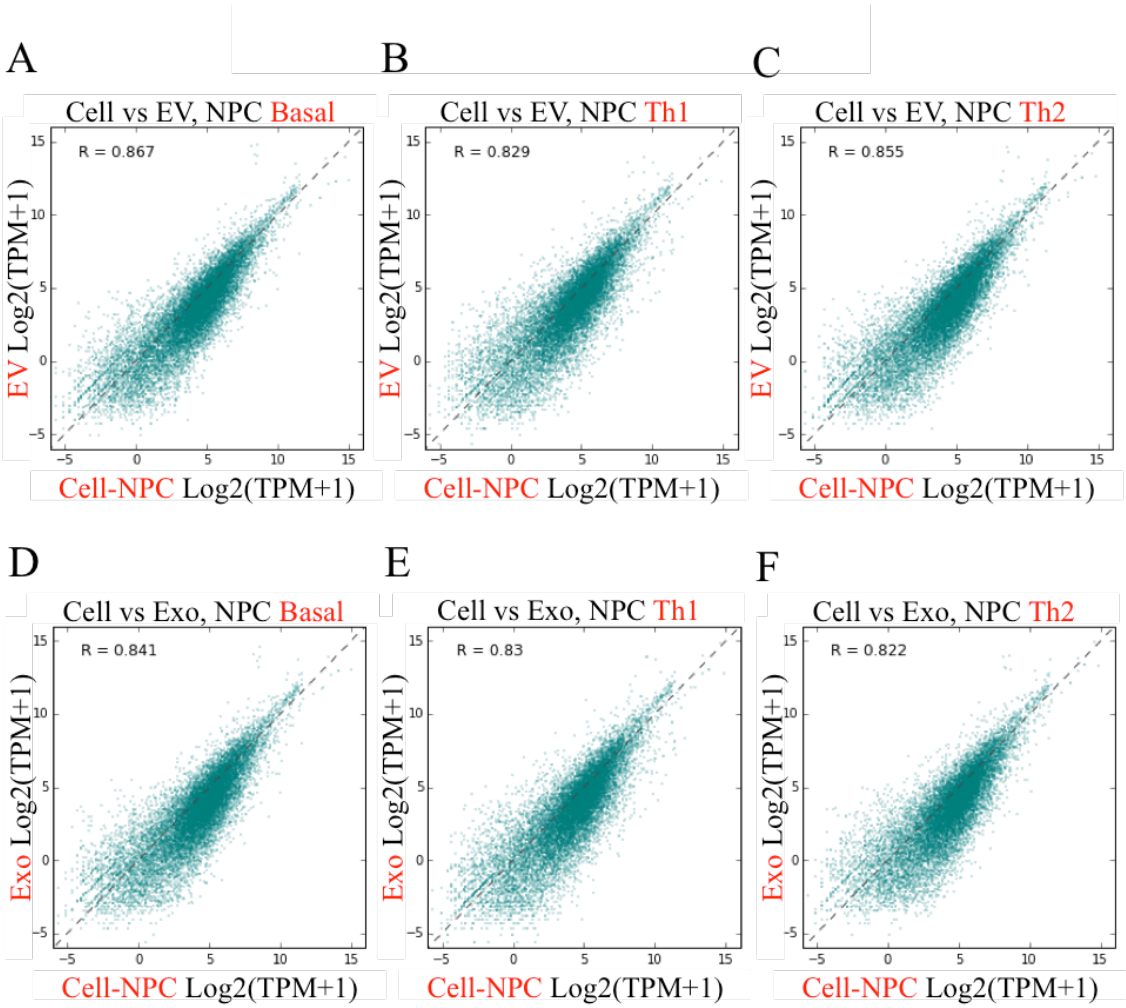

Figure 2.5: Available RNA-Seq dataset of neural precursor cells and EVs shows correlation in mRNA profiles
Previously published (Cosseti *et al*, 2014) RNA-Seq dataset of primary mouse neural precursor cells (NPCs) and EVs or Exosomes (Exos), defined in the paper as EVs that go through additional density gradient centrifugation step for extra purification, shows strong correlation between Transcripts Per Million (TPM) expression levels of coding mRNAs (R = Spearman Correlation). In each experiment, RNA-Seq was performed on NPCs that were not stimulated (basal) and their **A.** EVs or **D.** Exos, NPCs that were stimulated with Th1 and their **B.** EVs or **E.** Exos, or NPCs that were stimulated with Th2 and their **C.** EVs or **F.** Exos.

Development of proteinase-RNase method

One problem with all current EV isolation methods is that they are unable to fully purify contaminating proteins away from EVs. It has previously been shown

that the majority of extracellular miRNA in the blood are present in protein complexes that prevent the miRNAs from being degraded by RNAses. Furthermore, these protein-bound miRNAs co-purify with EVs during EV isolation by ultracentrifugation (12, 13). Although it is not known whether larger miRNAs such as mRNAs can also exist outside of the cell in protein-bound complexes, we figured that this possibility could confound our results. Thus, we decided to develop a method to separate RNA that is inside EVs from contaminating RNA that is stuck to the outside of EVs and is co-purified during the isolation. Although there are a variety of available methods that can be used in conjunction with differential ultracentrifugation (including density-gradient ultracentrifugation, size-exclusion chromatography, and immuno-isolation), none of these are perfect at removing contaminating free proteins (49).

We decided to develop a method to degrade all RNAs that are outside of EVs based on enzymatic treatments with proteinase and then RNase. We figured that if we could degrade all proteins that are not protected by the lipid membrane of the EVs, this would expose RNAs in protein complexes to RNAse activity. The RNAs that are inside of EVs, however, should still be protected (**Figure 2.6**). One question we had to resolve was how to remove or inactivate the proteinase after allowing it to degrade free proteins to prevent the subsequent degradation of the RNase enzyme. In one of the original papers that first described RNA in EVs, the authors added the proteinase Trypsin to EVs and then ultracentrifuged the EVs to separate them from the Trypsin (which is then expected to end up in the supernatant) (6).

When we tried this strategy (but with Proteinase K, which is a more aggressive proteinase than Trypsin), we were surprised to find a strong decrease in

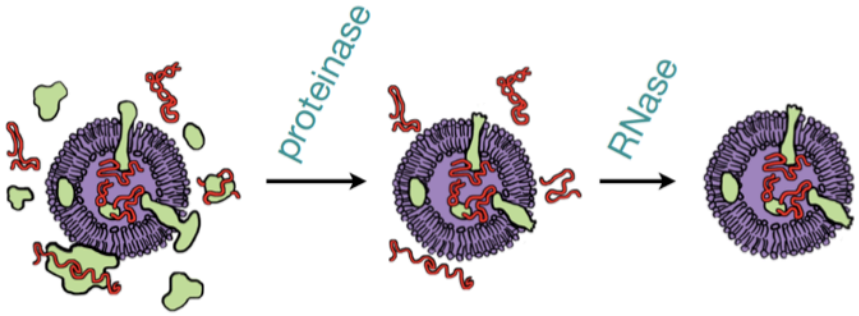

Figure 2.6: General strategy for Proteinase-RNase enzymatic treatment method
As we do not know whether our EV pellet after our differential ultracentrifugation protocol contains exclusively RNA that is in EVs or also protein-bound RNA that is outside of EVs, we decided to develop a method to degrade all proteins not protected by the lipid membrane, inactivate the proteinase, add RNase to degrade all RNA not protected by the lipid membrane, and then inactivate the RNase, being left with only RNA inside EVs

the amount of RNA in EVs relative to untreated EVs (**Figure 2.7A,B**). We reasoned this proteinase result could represent the liberation of non-vesicular RNAs that stuck to EVs via the proteins they were otherwise bound to. Alternatively, we considered the possibility that the proteinase treatment was somehow breaking our EVs and releasing RNA that is actually inside. As we generally do when we are worried, we decided to follow up with a series of controls. Using the proteinase inhibitor, phenylmethane sulfonyl (PMSF), we added inactivated proteinase to EVs before the final spin to rule out that there may be potential detergent in the

proteinase enzyme solution that could lyse EVs (**Figure 2.7C**). Finding that this was not the case, we tried another control where added proteinase to the EVs after the

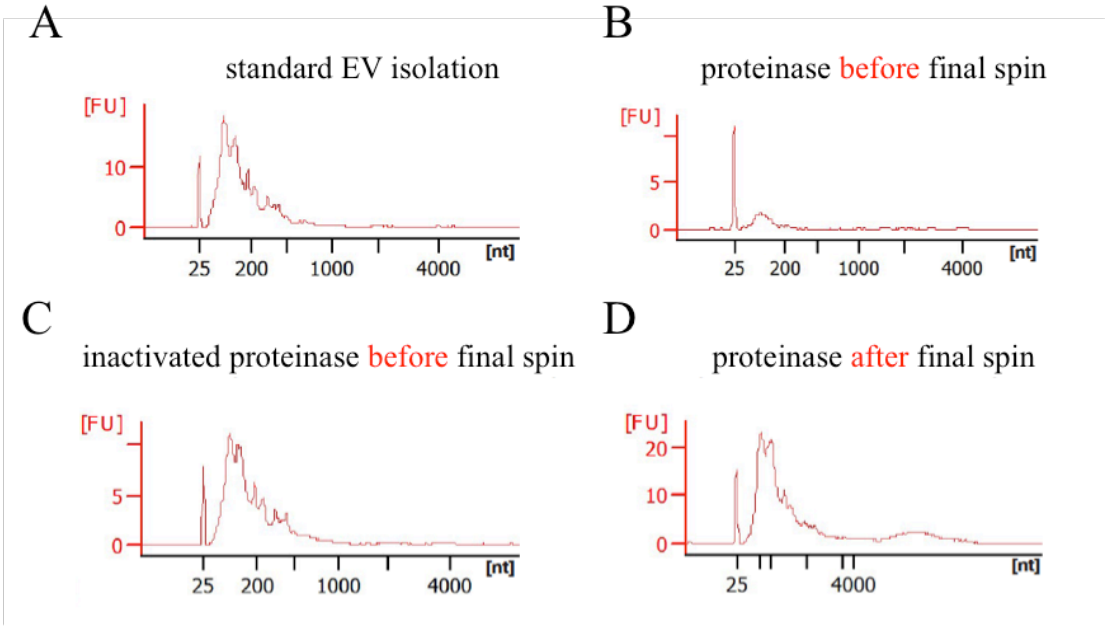

Figure 2.7: Different proteinase treatments alter EV RNA profiles
RNA was isolated and analyzed by Agilent Bioanalyzer for: **A.** normal EV isolation from K562 cell **B.** EV isolation where EVs were treated with Proteinase K before the final ultracentrifugation **C.** EV isolation where EVs were treated with inactivated Proteinase K (using the chemical PMSF) before the final ultracentrifugation **D.** EV isolation where EVs were treated with Proteinase K after the final ultracentrifugation spin

final spin, and then analyzed the RNA. The RNA in this treatment looked similar to the untreated EVs (**Figure 2.7D**).

We were able to conclude that it was the proteinase activity before the final spin that was causing a decrease in RNA, but we still did not know if this was because the EVs were breaking when treated with proteinase and then

ultracentrifuged or whether protein-RNA complexes were removed from the EVs but the EVs were intact. Given that this was a crucial question, we turned to transmission electron microscopy (TEM) to see if we could observe morphological changes to the EVs upon proteinase treatment. We compared EV samples where proteinase was added before or after the final ultracentrifugation spin (**Figure 2.8**). We were able to see a striking difference where the EVs treated with proteinase before the ultracentrifugation step were much smaller than untreated EVs (as seen in Figure 2.1) and had a non-smooth "popcorn" morphology. In contrast, the EVs where proteinase was added after the ultracentrifugation looked similar to untreated EVs.

We concluded that adding proteinase before the final ultracentrifugation breaks EVs, potentially because they are more fragile during the ultracentrifugation step without having the full-length transmembrane proteins to provide structural integrity. We thus settled on an optimized protocol where we add proteinase to EVs after the final ultracentrifugation step, inhibit the proteinase with PMSF, and then add RNase. We then inactivate the RNase with harsh lysis buffer and extract the resulting protected RNA. As an additional control, we checked that the lysis buffer inactivates the RNase by incubating the RNase with the buffer and then adding purified RNA. The RNA was not degraded.

With this optimized proteinase-RNase protocol in hand, we applied it to EVs isolated from K562 cells by differential ultracentrifugation. When we compared the Bioanalyzer profiles of untreated EVs, EVs treated with the proteinase-RNase protocol, and EVs treated with proteinase before spins (as a control), we were

surprised to see that there was much less RNA in the proteinase-RNAse EVs relative to the untreated control (**Figure 2.9A-C**). This was similar to the proteinase between spins treatment that we knew from electron microscopy was breaking the

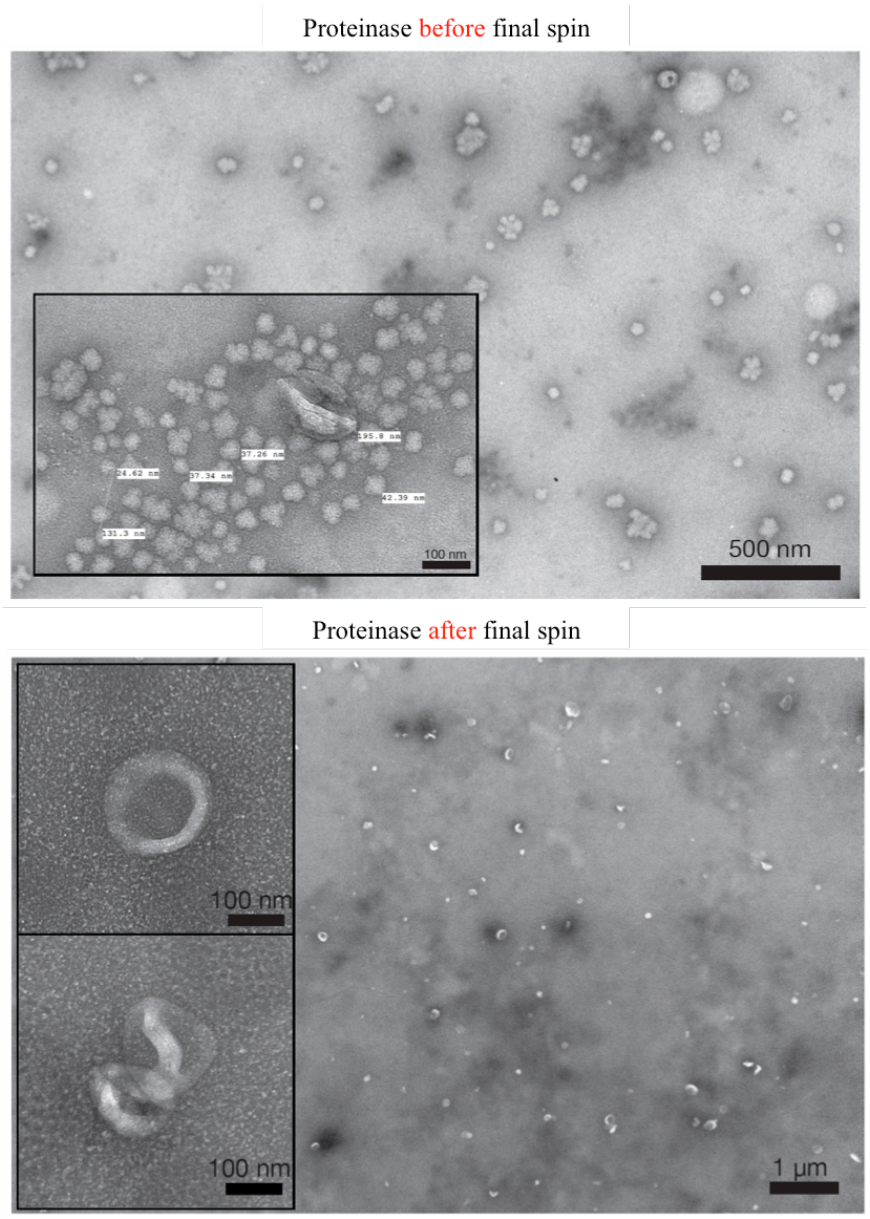

Figure 2.8: Electron microscopy of EVs treated with proteinase before, but not after, final spin show broken EVs
Transmission electron microscopy (TEM) of EVs treated with Proteinase K before (top) or after (bottom) the final ultracentrifugation spin. Treating with proteinase before the final spin leads to what looks like smaller broken vesicles whereas treating with proteinase after the final spin leads to EVs with normal morphology.

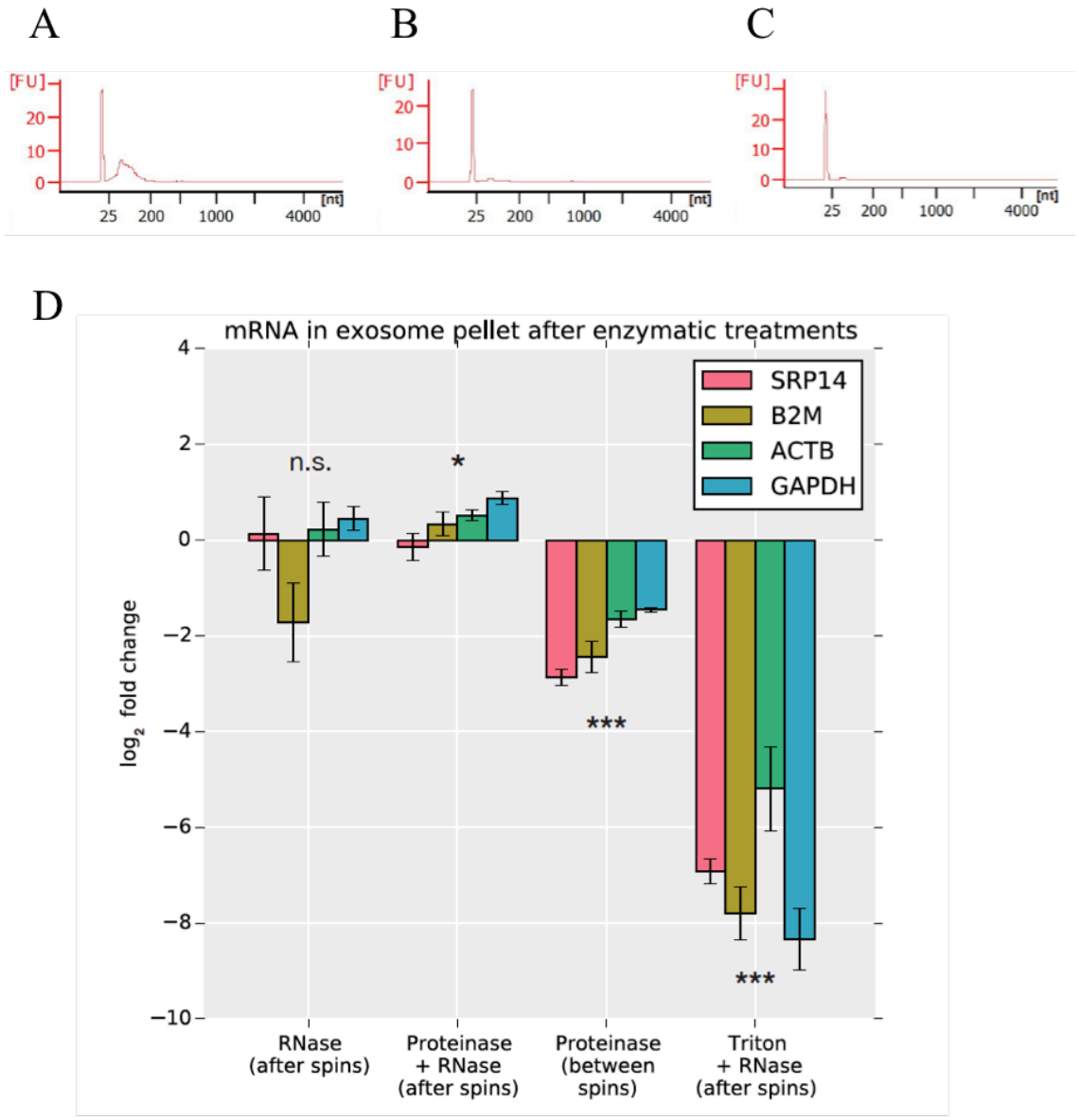

Figure 2.9: qRT-PCR after optimized Proteinase-RNase protocol shows mRNAs are inside EVs
Bioanalyzer profiles of RNA isolated from EV isolation after A. no treatment, B. optimized Proteinase-RNase treatment after final ultracentrifugation spin, C. proteinase treatment before the final ultracentrifugation spin D. quantitative Reverse Transcription PCR (qRT-PCR) was performed on four different mRNAs after each treatment expression was normalized and compared to the no treatment EV control. Error bars represent +/- standard error of the mean (n=4). n.s. = not significant, * = $p < 0.05$, *** = $p < 1e\text{-}7$.

vesicles. It also looked like there was less RNA in the untreated EVs than usual in this experiment, but we figured this could be because we put the untreated EV samples through the same incubations as the treated samples. Thus, it could be that some RNA is degraded upon incubation at 37C. Nonetheless, there was clearly less RNA in the proteinase-RNAse EVs relative to the untreated EVs.

Despite the emotional tumultuousness caused by the possibility that all EV RNA is not actually in EVs but rather in contaminating protein complexes, we decided to explore further. By Bioanalyzer, most of the EV RNA is less than 200 nucleotides. On the other hand, messenger RNA is greater than 200 nucleotides and not easily seen on the Bioanalyzer as it is of various sizes, thereby not forming a clear peak. We decided it may be possible that smaller RNAs are mostly present in protein complexes outside of EVs but the larger RNAs (which we can't really visualize on the Bioanalyzer are inside of EVs).

We thus turned to quantitative Reverse-Transcription PCR (qPCR) to measure the levels of four mRNA in the EVs treated by different conditions. We chose four mRNA that are highly expressed in K562s and are often used as housekeeping genes: B2M, SRP14, ACTB, and GAPDH. We measured the levels of these four mRNAs in EVs treated with a variety of conditions, and compared them to the levels in untreated EVs (**Figure 2.9D**). Our results, indeed, suggested that these mRNAs are inside EVs, and not outside since when we treated with proteinase-RNAse, we saw no decrease in RNA levels (we even saw a slight increase, probably due to experimental noise or error). We also saw no decrease in RNA levels relative to untreated EVs when we treated EVs with just RNase. This was expected since

extracellular RNases should degrade free RNA not bound by proteins. Nonetheless, it was a nice control to confirm that the RNase we add is being inactivated upon lysing of the EVs. In the proteinase between spins condition, we saw a significant decrease in EV RNA. This finding is in accordance with the electron microscopy results that EVs in this condition are likely breaking. Importantly, we see RNA levels drop precipitously when we add the detergent Triton-X together with RNAse. This is an important control confirming the mRNA inside of EVs.

Having confirmed by qRT-PCR that the levels of four mRNA are the same in proteinase-RNase treated and untreated EVs, we then wanted to go back to the RNA-Seq and look at all transcripts. We sequenced the RNA of cells, untreated EVs, and proteinase-RNase treated EVs (**Figure 2.10**). We found that the proteinase-RNAse EV profile is very correlated to the untreated EV profile for coding mRNAs,

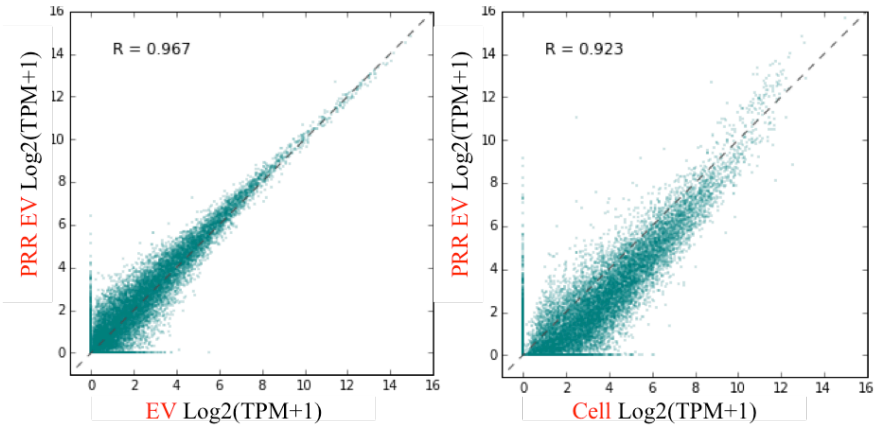

Figure 2.10: RNA-Seq after optimized proteinase-RNase protocol shows mRNAs are inside EVs and correlated to mRNAs in cells
EVs from K562 cells were isolated and split into two samples. One sample was untreated (EV) while the other sample was treated with the optimized proteinase-RNase protocol (PRR EV). K562 cell RNA, EV RNA and PRR EV RNA were sequenced using an RNA-Seq method that uses PolyA priming. Correlation of expression levels in Transcripts Per Million (TPM) of coding mRNAs are shown for: **A.** untreated EVs relative to proteinase-RNase treated EVs (PRR EV) and **B.** K562 cells relative to proteinase-RNase treated EVs (PRR EV) confirming that mRNA is inside of EVs and correlated between cells and EVs (R = Spearman Correlation).

suggesting that mRNAs obtained by differential ultracentrifugation are all inside of EVs. As expected from our previous RNA-Seq experiments, the RNA profile of proteinase-RNase EVs was very correlated to the K562 cell RNA profile.

Assessing DNA content of EVs

After finding all of the mRNAs found in cells in our EVs, we wondered what else is in EVs. Are all cellular components in EVs? We decided to investigate DNA in EVs. Several groups have reported isolating DNA from EVs (50-52), including from the EVs released by K562 cells (52). Using the same differential ultracentrifugation procedure as before, we performed a DNA extraction from the EV pellet isolated from K562 cell culture media. We ran the resulting DNA on a gel, and found a smear of DNA of various sizes but mostly between 1 and 10 kilobases. Following the general idea of what we did with RNA, we then decided to treat the EV preparation with DNase. We inactivated the DNase with EDTA and then performed a DNA extraction on the resulting preparation (which we assumed to be any DNA inside of EVs, which should be protected from DNase activity). We found that there was no detectable DNA in this condition by gel electrophoresis, suggesting that DNA in the EV preparation is stuck to the outside of EVs and is not actually inside the EVs (**Figure 2.11A**).

We performed several controls to help us gain confidence in our interpretation of the data. First, we also treated the DNA from the EVs with RNAse to ensure that the

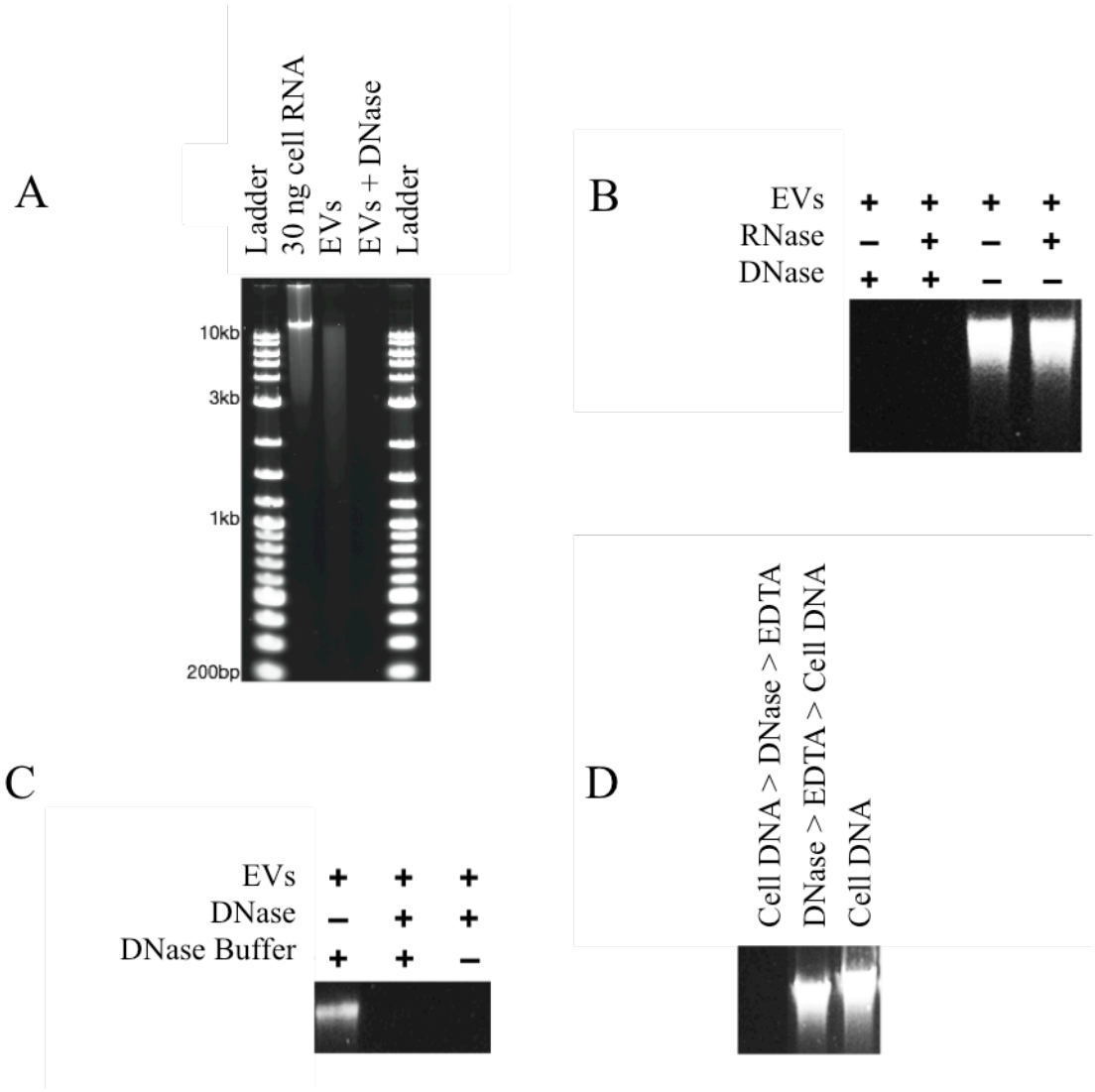

Figure 2.11: DNase treatment shows DNA co-isolates, but is outside of EVs
DNA is isolated and run on an agarose electrophoresis gel (stained with SYBRGold) for: **A.** K562 cells, an isolation of EVs, and an isolation of EVs treated with DNase. **B.** EVs treated with RNase and/or DNase to show that we visualizing DNA, not RNA. **C.** EVs treated with DNAse and/or DNase buffer to show that DNase buffer alone is not causing degradation of DNA. **D.** Cell DNA is treated with DNase that has been first inactivated by DNAse to show that our EDTA inactivation works (DNAse is inactivated with EDTA prior to extracting DNA).

SYBR Gold nucleic acid gel stain is not actually staining RNA instead of DNA. This was not the case (**Figure 2.11B**). We also wanted to ensure that the DNase buffer is not somehow leading to degradation of DNA. This was also not the case (**Figure 2.11C**). Lastly, we checked the DNase inactivation with EDTA by adding purified cell DNA to

the inactivated enzyme to make sure it wasn't being degraded (**Figure 2.11D**). This was to ensure the DNase was incapable of degrading DNA when we break open the vesicles during the DNA extraction (theoretically, the DNA lysis buffer should also inactivate the DNase but the EDTA was for extra assurance). After the expected results in all of these controls, we conclude that the vast majority of DNA in EV preparations is not actually inside of EVs, but most likely sticks to the outside of EVs during the isolation.

Discussion

We have used a simple cell culture model to compare the RNA profile in cells to the RNA profile of the EVs they produce. We found that the mRNAs levels in cells are highly correlated to those of EVs. Our results suggest that mRNAs are generally packaged into EVs in a non-specific manner. These results are in disagreement with the first two papers analyzing RNA expression in EVs, which found very specific mRNAs get packaged into EVs (6, 7). The procedure in those studies and our study used to isolate EVs was the same (differential ultracentrifugation), but there are two major differences. One difference was that each study analyzed EVs from different cell types. The other difference was that these studies used microarrays while we used RNA-Seq. When we analyzed RNA-Seq data from a report investigating EVs from mouse primary neural precursor cells (NPCs) (48), we also found a very strong correlation between the mRNA profile of cells and EVs, giving us more confidence in our conclusions. Nevertheless, EVs from more cell types need to be analyzed to determine how general this result is. Additionally, it would be interesting to see

whether changes in RNA profiles upon exposure of cells to stimuli are reflected in the RNA profiles of EVs. In the one study that addressed this question by stimulating NPCs with cocktails of cytokines and then analyzing RNA in EVs, the differences in a cell's gene expression profile were reflected in EVs (48).

As with any RNA-Seq experiment, there were some outliers. Although the RNA-Seq profiles of cells and EVs were very correlated, generally arguing against a packaging mechanism, there were some RNAs in EVs that were enriched relative to cells. Looking at some of RNA-Seq reads for these, they are full-length mRNAs. This is in contrast to some studies that EVs do not carry full length mRNA (53, 54). There are various technical articles that could lead to results that look like certain RNAs are enriched in EVs compared to cells (55, 56), but it's also possible that there is a subset of EVs package specific RNA while most EVs do not package RNA. This possibility would be difficult to follow up unless the subset of EVs had a clear defining feature that could be used to isolate them (such as a specific surface protein). Intriguingly, one of the mRNAs we found to be highly enriched, Rab13, was also recently found to be enriched in EVs isolated from colorectal cancer cells (57).

A central challenge in the EV field has been the inability to isolate EVs away from other components in cell culture media or biological fluid. This has hampered previous studies from being able to distinguish whether a given protein or nucleic acid is truly inside EVs or outside and merely stuck to EVs as an artifact of the isolation procedure (11). This has been a particular problem for RNA as it has been reported that a majority of extracellular miRNAs are in protein-RNA complexes as opposed to inside of EVs, but co-purify during many EV isolation procedures (12,

13). Although there have been a variety of biochemical approaches applied to purify more stringently than just differential ultracentrifugation (including density-gradient ultracentrifugation, size-exclusion chromatography, and immuno-isolation), none of these are perfect for separating EVs away from free proteins or RNA-protein complexes (49). We believe our new approach of enzymatic treatments of EVs with proteinase and then RNase in a fashion that does not break open the EVs solves the problem of not knowing whether a given RNA is inside or outside. We use our approach to confirm that EVs contain mRNA and that mRNA levels in EVs are, indeed, correlated to mRNA levels in cells. We expect our approach to be applicable to understanding the miRNA and protein content of EVs as well.

We found that in our K562 cell culture system, EVs do not contain DNA since treating the outside of EVs with DNase (without proteinase) gets rid of all DNA (visible by gel). Thus, we think that previous reports claiming the presence of DNA in EVs (50-52) may have actually been isolating DNA from the outside of EVs that became associated with EVs during the isolation procedure. The most likely explanation for this DNA is that it found its way outside of the cell after cell death. This is also a likely explanation for the biogenesis of extracellular Ago2-miRNA found outside of EVs. Secreted proteins generally go through the Golgi, where they would presumably not have a chance to interact with RNA.

Our result that the transcriptome of cells is reflected in EVs, if generalizable, has widespread implications for the use of EVs in studying human biology and diagnosing disease. As most cell types in the human body are inaccessible to biopsy, isolating EVs from biological fluids may represent a non-invasive way to read out

the RNA profiles of cells. We expect EVs in biological fluids to carry different RNA signatures in the context of different physiological and disease processes. Although previous reports have performed RNA-Seq on cell-free RNA (not specifically by isolating EVs) (58, 59), it is unclear whether this RNA correlates to RNA from cells. One particular advantage of isolating RNA from EVs relative to total cell-free RNA is that EVs have membrane proteins that can be used for immuno-isolation. Thus, it should theoretically be possible to isolate EVs from a particular cell type using antibodies against a cell type-specific transmembrane protein found on a subset of EVs in a biological fluid such as plasma. This possibility, combined with our finding that EVs reflect the mRNA profile of cells, holds promise for both better understanding biological processes in humans in general and assessing health and disease in individuals.

Chapter III

Single EV Imaging

Introduction

A major challenge in the EV field is that EVs are heterogeneous. When isolating a population of EVs, there are many proteins and RNAs detected and it is unclear if there are specific subpopulations of EVs. This question is of great importance for trying to decipher the potential functions of EVs, as well as for using EVs diagnostically (29). Although, theoretically, individual EVs can be characterized by flow cytometry, the fact that EVs are much smaller than cells presents a large number of technical challenges for this technique (60, 61). We set out to develop methods to image and characterize single EVs using fluorescence microscopy.

We were particularly interested in imaging RNA in EVs to understand questions such as whether a subpopulation of EVs contains RNAs or whether RNA is evenly distributed in EVs. We also wanted to assess how well our proteinase-RNase method worked using additional techniques. We developed a method of imaging isolated EVs using by Total Internal Reflection Fluorescence (TIRF) Microscopy, and explored its utility in investigating the EV RNA at the single EV level.

Results

Imaging EVs labeled with lipid and RNA dye

In order to imagine single EVs with microscopy, which requires great sensitivity, we used TIRF. The main defining characteristic of EV is the presence of

membrane, so we used a hydrophobic membrane dye to visualize them. We had success labeling EVs with a variety of lipid dyes, but found that different dyes had varying degrees of brightness and different propensities to aggregate into micelles (which could then be confused for EVs). For each EV treatment, we also tested the dye without EVs. We started by labeling EV membranes with the red fluorescent dye, BODIPY TR Ceramide. After labeling EVs, we assessed various methods of removing excess unbound dye. Although previous reports have used ultracentrifugation to separate EVs from unbound lipid dye, ultracentrifugation itself can cause the lipophilic dye to form aggregates of similar size to EVs (62). We found a gel-containing spin column was able to efficiently remove unbound dye and recover labeled EVs. We then were able to attach EVs to the surface of charged glass and image EVs by TIRF microscopy.

After establishing our EV membrane labeling method, we then wanted to characterize the RNA in EVs using with an RNA dye. We were interested in co-localizing EVs and RNA to see the RNA distribution among isolated EVs. We started by using a membrane permeable RNA dye, SYTO RNASelect. We wanted the dye to be membrane permeable so that it would be able to label RNA inside EVs in addition to outside. For all of the imaging experiments, we used EVs isolated from K562 cells. We incubated the EVs with both BODIPY TR Ceramide (10 μM final concentration) and SYTO RNASelect (10 μM final concentration), removed excess dye, applied EVs to a charged glass coverslip and then imaged the EVs using TIRF (**Figure 3.1**). We were able to see many spots corresponding to EVs, a fraction of which co-localized with the RNA. Although we could not discriminate whether the RNA was inside or

outside of the EVs, this was encouraging. However, we also observed RNA some RNA dye spots that did not co-localize with the lipid dye. We reasoned that there could be several reasons that we observe RNA without lipid. One reason could be that we are not staining all EVs. Another reason could be that not all EVs are being labeled.

We tried increasing the concentration of the Bodipy TR Ceramide lipid dye to see if higher concentrations of dye would label more EVs, but at those higher

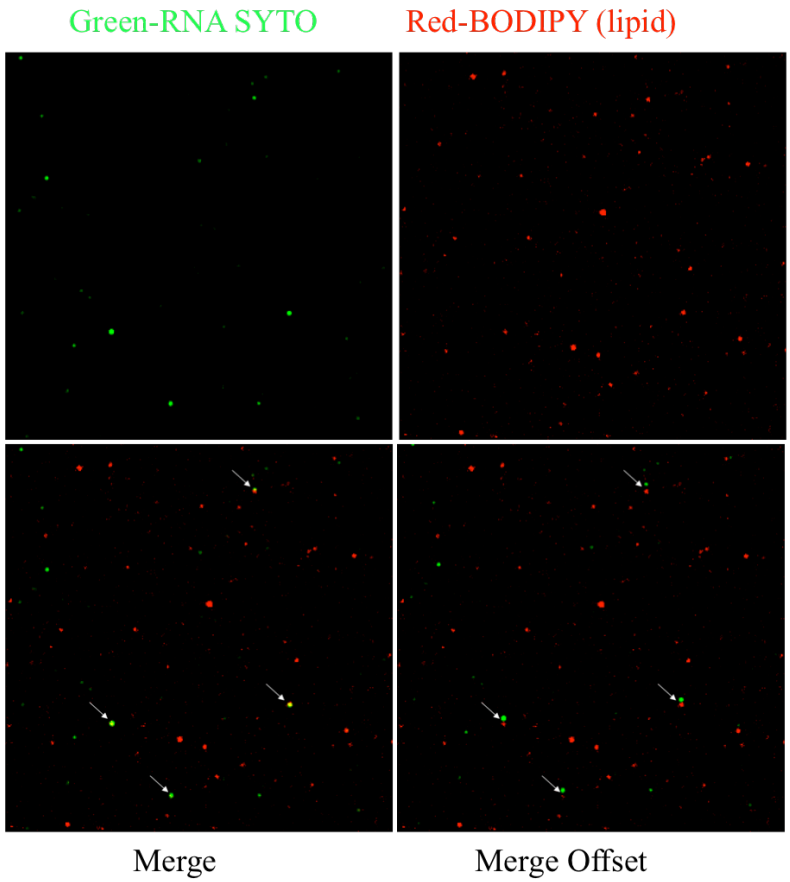

Figure 3.1: Imaging EVs with BODIPY TR Ceramide lipid dye and SYTO RNA Select dye reveals some co-localization
EVs stained with BODIPY TR Ceramide (10 μM) lipid dye and SYTO RNASelect dye (10 μM) and imaged using TIRF microscopy. **Top left**: EVs imaged in green channel. **Top right:** EVs imaged in red channel. **Bottom left:** merge of red channel and green channel images. Arrows point to co-localization events. **Bottom right:** merge and offset of red channel and green channel images for easier visualization of co-localization. Arrows point to co-localization events.

concentrations the dye starting forming objects in the PBS only (no EV) control. This is likely due to the formation of micelles. After trying several other dyes to see if we could find a brighter one which would potentially label more EVs, we had the best results with DiD, a lipophilic carbocyanine with fluorescence in the far-red range. DiD is weakly fluorescent in water but highly fluorescent and photo stable upon incorporation into membranes. After checking that DiD does not form micelles at 10 μM, we repeated the lipid and RNA co-localization experiment. As before, we incubated the EVs with both DiD (10 μM final concentration) and SYTO RNASelect (10 μM final concentration), removed excess dye, applied EVs to a charged glass coverslip and then imaged the EVs using TIRF (**Figure 3.2A**).

Our results imaging EVs labeled with both DiD and SYTO RNASelect showed very high co-localization between the lipid and RNA dyes. Suspicious by the extremely high percentage of co-localized events, we set out to perform a variety of controls. We identified the problem when we did a DiD (with no SYTO RNASelect) EV labeling control. Despite the difference in emission spectra between the two dyes, we saw bleed-through of DiD into the green channel (used for detection of RNA) (**Figure 3.2B**). This was surprising since one of the reasons we picked DiD is that it emits in the far-red range. We reasoned this would be ideal for double-labeling application with the RNA dye since SYTO RNASelect is green, far away from the emission of the far-red DiD dye. However, since we are exposing much longer in the SYTO RNASelect channel than the DiD channel (since the amount of RNA is very low relative to lipid), bleed-through still occurs at some rate despite having the

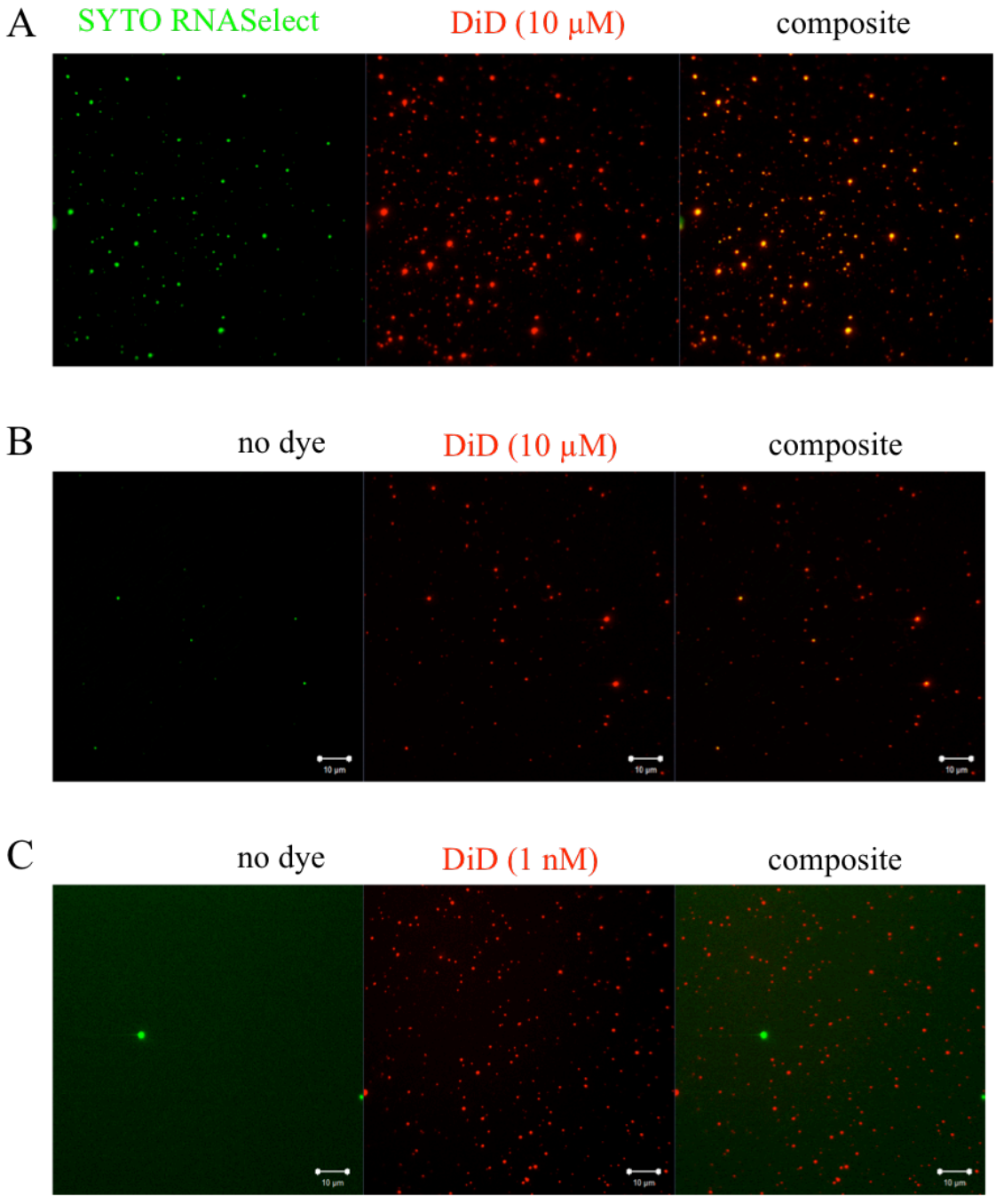

Figure 3.2: DiD lipid dye bleeds through at high concentrations
EVs are imaged by TIRF using: **A.** DiD (10 µM) lipid dye and SYTO RNASelect (10 µM). **B.** Just DiD (10 µM) with no RNA dye, showing some bleed-through of DiD into the green channel (used for RNA). **C.** Just DiD (1 nM) with no RNA dye, now showing no bleed-through. The two bright green objects are GFP beads used to find the focal plane at the surface of the glass slide. Left: green channel, middle: far-red channel, right: composite (merge of two channels).

correct filter on our microscope and the dyes having emission spectra that are far away from each other.

We were able to solve this problem by lowering the DiD concentration and checking for absence of signal in the green channel with a DiD only staining control (**Figure 3.2C**). Satisfied that we were now staining EVs such that our DiD lipid dye does not spontaneously form micelles (with a PBS only DiD control) and that our DiD dye does not bleed through into the green channel used to image the RNA dye, we turned back to the task of co-localizing EVs with RNA. We again imaged EVs with both DiD (1 nM final concentration) and SYTO RNASelect (10 μM final concentration). We were able to see EVs and several spots of RNA, but there was now very low co-localization between the EVs and the RNA dye (**Figure 3.3**). We reasoned that this could be because most of the RNA in the EV pellet we obtained by our standard

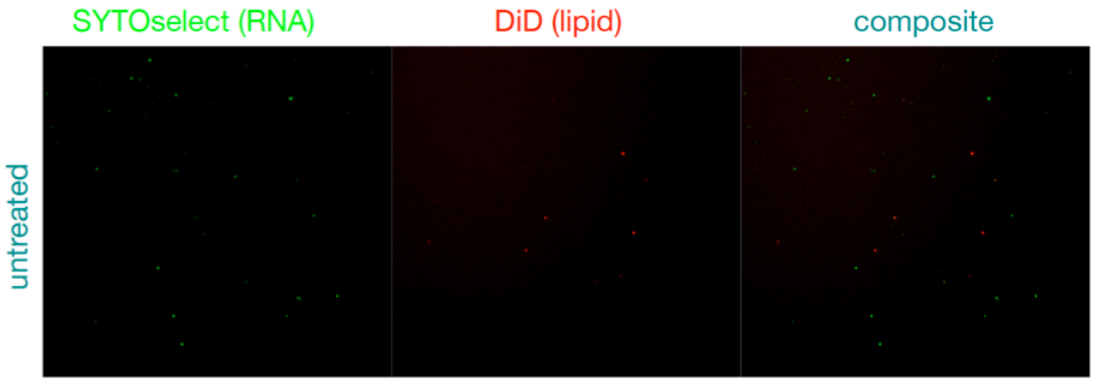

Figure 3.3: EVs labeled with DiD lipid dye and SYTO RNASelect show low number of co-localizations
EVs are imaged by TIRF using DiD (1 nM) lipid dye and SYTO RNASelect (10 μM). Left: green channel, middle: far-red channel, right: composite (merge of two channels).

differential ultracentrifugation protocol is in RNA-protein complexes and not EVs. This would be consistent with our finding that most of the RNA in EVs (less than 200 nucleotides in length, not the mRNA) goes away after proteinase and RNase treatment according to the BioAnalyzer.

Imaging of Proteinase-RNAse treated EVs

To test if the RNA spots that do not co-localize with the lipid dye are protein-RNA complexes, we decided to treat our EVs with our proteinase-RNase protocol and then image them. When we imaged EVs with either proteinase or proteinase-RNase treatment with both DiD (1 nM final concentration) and SYTO RNASelect (10 μM final concentration), we still found several RNA dye spots that were not co-localizing with lipid (**Figure 3.4**). At first, we went back to the thought we are not labeling all EV at the lowered DiD concentration where there is no bleed-through into the RNA channel. Although we did observe that we label more EVs when we increase the DiD concentration, we then also started having bleed-through into the green channel.

We then considered another explanation for the large number of spots of RNA dye without co-localized lipid dye. Since the amount of RNA in our EV sample is very low, we wondered whether the RNA dye was binding non-specifically to other molecules in the sample. We reasoned this was possible given that SYTO RNASelect is a membrane permeable dye, which means that it has considerable hydrophobic character. We figured this might make it more likely to bind to molecules other than RNA. To test this possibility we, decided to repeat the proteinase-RNase experiment with DiD and a

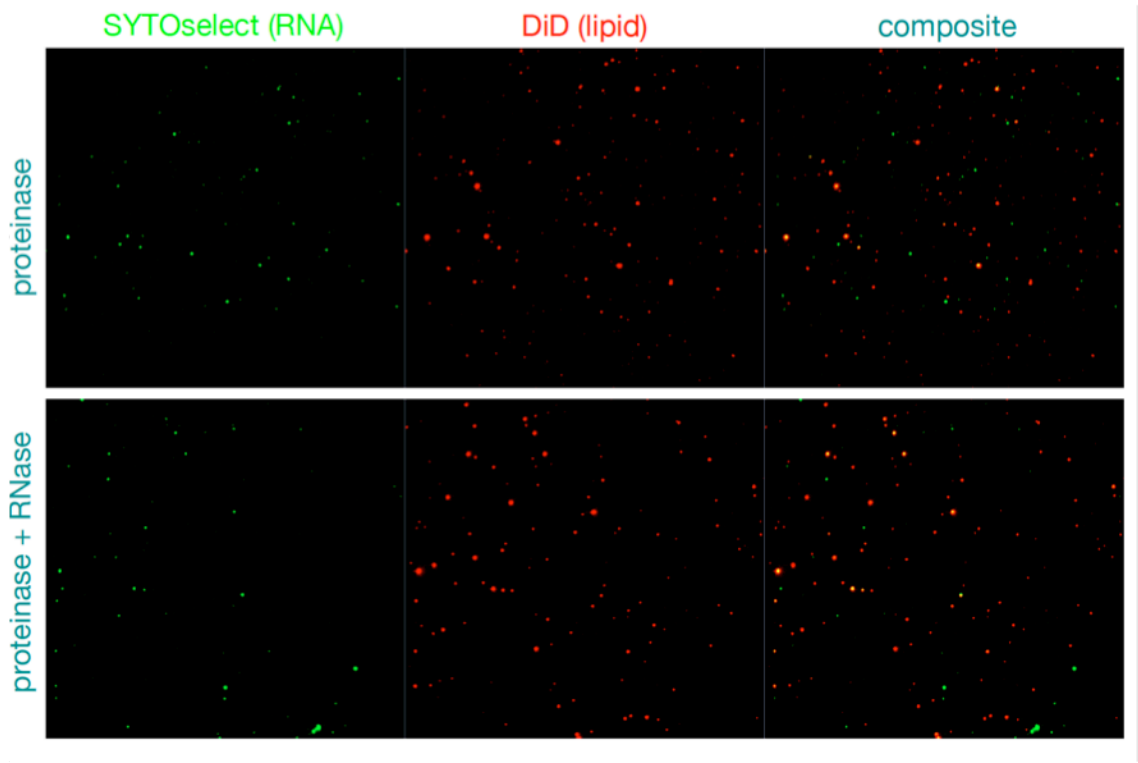

Figure 3.4: Proteinase-RNase treated EVs labeled with DiD lipid dye and SYTO RNASelect show low number of co-localizations
Proteinase-RNase or proteinase treated EVs are imaged by TIRF using DiD (1 nM) lipid dye and SYTO RNASelect (10 μM). Left: green channel, middle: far-red channel, right: composite (merge of two channels).

different green RNA-binding dye, TOTO-1. When we incubated both untreated EVs and proteinase-RNase treated EV with DiD and TOTO-1, we observed almost a complete disappearance of green spots of RNA dye in the proteinase-RNase sample compared to the control (**Figure 3.5**). This result was in strong disagreement with the SYTO RNASelect result, suggesting that SYTO RNASelect could be binding non-specifically. The TOTO-1 imaging result reassured us that our proteinase-RNase protocol was effective. However, since TOTO-1 is not membrane permeable, we were unable to conclude anything about RNA inside EVs.

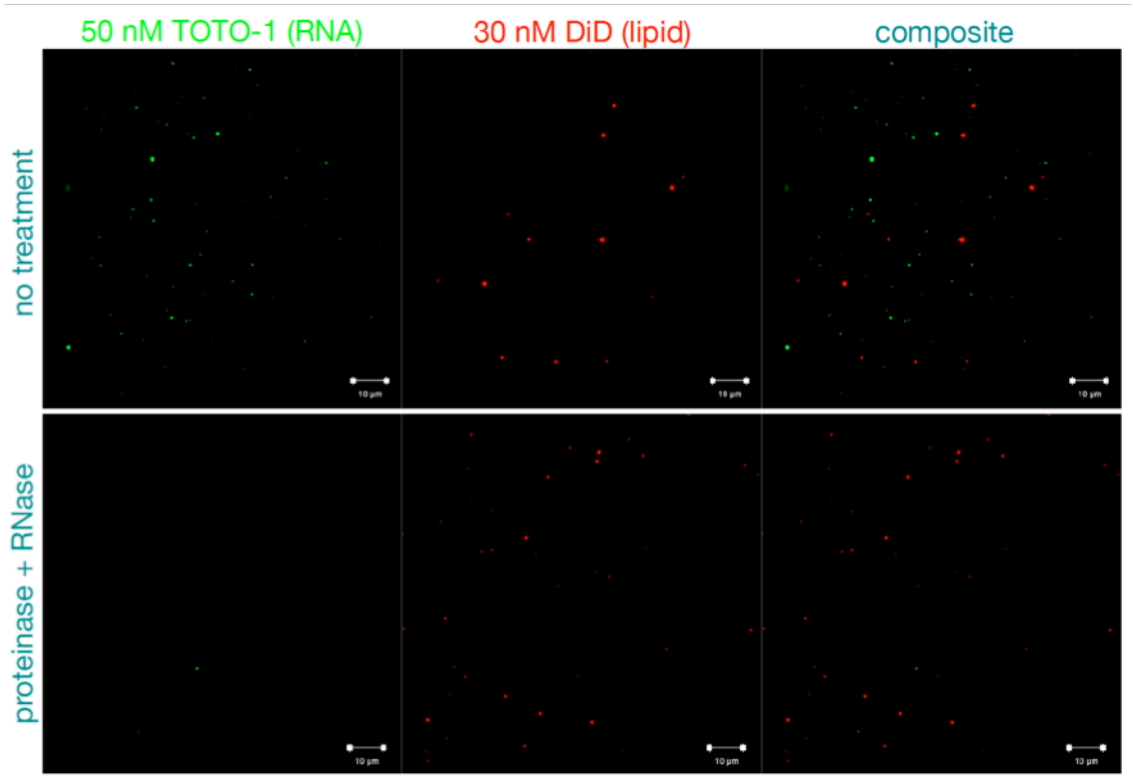

Figure 3.5: Proteinase-RNase treated EVs labeled with DiD lipid dye and TOTO-1 RNA dye reveal degradation of non-vesicular RNA
Proteinase-RNase or proteinase treated EVs are imaged by TIRF using DiD (30 nM) lipid dye and TOTO-1 RNA dye (50 nM). Left: green channel, middle: far-red channel, right: composite (merge of two channels).

Discussion

The ability to characterize individual EVs and their cargo molecules would greatly advance the EV field. We set out to develop methods to image isolated, individual EVs using TIRF microscopy. We applied this method to the study of EV RNA in order to figure out how RNA is distributed among EVs or what proportion of RNA in our EV preparation is truly inside EV. We were hoping that we would be able to gather quantitative answers to these questions, but found ourselves faced with several challenges

that prevented us from this goal. Although we believe imaging individual EVs is a promising approach to characterize EV heterogeneity, we encountered a number of challenges that need to be overcome for this technique to be reliable and informative.

One problem we encountered is that lipid dyes can, by themselves, assemble into micelles if they are at a sufficiently high concentration. We were able to solve this problem by performing a "no EV" PBS control to ensure that this is not happening at the dye concentration we use. However, as we lowered the dye concentration, we also became less confident in our ability label all of the EV. Not being able to label EVs would obviously prevent this technique from providing quantitative answers in co-localization experiments.

Another problem we encountered is bleed-through of dyes during our co-localization experiments with lipid and RNA dyes. This is a particular problem with regard to labeling EV RNA since the amount of RNA in EVs is very low. Thus, it is necessary to always do a control staining the EVs with just a lipid dye and not the RNA dye to insure that the lipid dye does not bleed-through into the channel of the other dye. Yet another problem that we encountered, also likely due to the amount of RNA being very low in EVs, is that it difficult to find a dye that is sufficiently specific. This is particularly the case for dyes that are also membrane permeable, since the moiety that makes it permeable to membranes is likely to make it less specific for RNA.

One other consideration that must be taken into account if one is to use this technique to obtain quantitative information. Since EVs are smaller than the diffraction limit, for a given diffraction-limited spot, we cannot distinguish one EV from two EVs stuck together. By electron microscopy, we see an identical preparation of EVs as used

here fairly dispersed on a grid (such that the EVs are generally not stuck together). Nevertheless, further experiments mixing half of a preparation of EVs labeled with a membrane dye of one color and half labeled with a membrane dye of another color could determine whether mostly single EVs are being imaged or not.

Despite all of the challenges, we still believe single EV imaging will prove to be a useful technique. There is still no technique to reliably address very basic questions such as what percentage of EVs contain a given protein marker. Using single EV imaging, for example by co-localizing lipid dye together with a fluorescently–labeled antibody, should theoretically be able to answer such a question and many others.

Chapter IV

Isolation of Cell-Type Specific EVs

Introduction

A grand challenge in maximizing the potential of EVs in molecular diagnostics is the isolation of cell-type specific EVs. Although the total population of EVs can be isolated from a biological fluid such as plasma and the RNA can be analyzed, this approach does not distinguish which RNA comes from which cell type. Analyzing RNA in total EVs can certainly be diagnostically useful, since RNA-Seq would yield on the order of tens of thousands of different measurements. But, in theory, it would be even more useful to be able to distinguish a population of EVs by their cell type of origin. If EVs from a given cell type can be isolated, then proteins and RNAs can from inside those EVs can be analyzed as a non-invasive "window" into that cell type. If our cell culture results that the RNA profile of EVs reflects that of cells is broadly applicable, analyzing cell type-specific EVs would allow the non-invasive measurement of a cell type's transcriptome.

Isolating cell type-specific EVs would have broad applications in both the study of biological processes in humans and as a novel class of biomarkers for diagnosing disease. Although there have been reports claiming to isolate cell type-specific EVs (63-70), none of them have assessed whether the marker they use is unique to the cell type of origin and how efficient and specific their immuno-isolation technique is. Thus, we set out to develop a rigorously validated and optimized immuno-isolation technique. We also set out to identify a general framework for identifying cell type-specific EV markers.

To test our methods, we decided to focus on neurons as a proof of principle. We applied our framework for choosing cell type-specific EV markers to figure out markers

for the isolation of neuron-specific EVs from human CSF. We then developed a general EV immuno-isolation method to capture EV subpopulations with a specific marker, and applied it to the isolation of neuron-specific EVs.

Isolation and proteomics of EVs from human iPS-derived neurons

To study neuron-derived EVs, we differentiated human neurons from induced pluripotent stem (iPS) cells. We figured having an *in vitro* model of EVs from our target cell type would be very useful for both identifying which proteins are found on neuron-derived EVs and, also, developing or optimizing our immuno-isolation procedure. We used a system previously developed in our lab based on doxycycline-inducible expression of the transcription factors Neurogenin-1 and Neurogenin-2. This system of inducible Neurogenin (iNGN) iPS cells allows for the rapid (as little as 4 days) differentiation of iPS cells into neurons at a very high (>90%) efficiency (71).

After validating the expected morphological differences in cells in iPS colonies spreading out and forming long processes (**Figure 4.1**), we isolated EVs from the cell culture media of the neurons. We followed the same protocol of EV isolation from cell

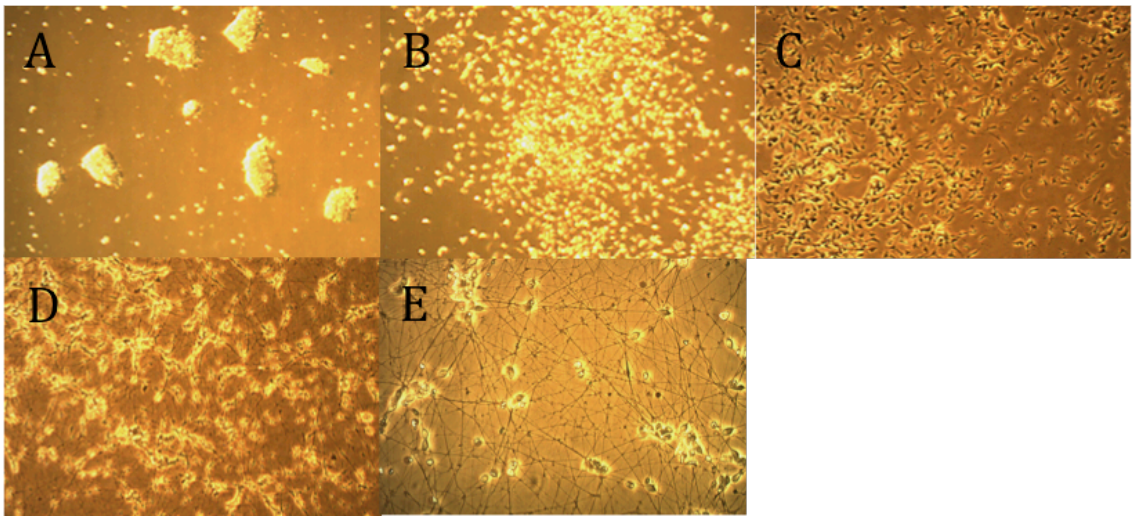

Figure 4.1: Microscopy of iPS iNGN cell differentiation into neurons
(A) iPS NGN cells before doxycycline addition (40x magnification) **(B)** iPS NGN cells 1 day after doxycycline addition (40x magnification) **(C)** iPS NGN cells 2 days after doxycycline addition (40x magnification) **(D)** iPS NGN cells 4 days after doxycycline addition (40x magnification) **(E)** iPS NGN cells 5 days after doxycycline addition (200x magnification)

culture media (**Appendix S2**) that we used for the K562 cells and other cell lines. We then wanted to identify all of the transmembrane proteins in the neuron EVs, and turned to mass spectrometry. We had to optimize the mass spectrometry sample prep to maximize the number of proteins detected. In particular, as cell culture media has a large amount of Albumin, we had to devise ways of albumin depletion from our sample. The method we found most successful was cutting out the Albumin band from the protein gel and using the rest of the proteins for downstream analysis.

To ensure that the proteins we characterize are truly neuronal and not from undifferentiated iPS cells, we used EVs from undifferentiated iPS cells as a control in the proteomics experiments. We restricted our analysis to only transmembrane proteins so that we could pull on them with antibodies to isolate the corresponding EVs. We were able to also detect proteins that were not transmembrane in our mass spectrometry results

but for those proteins we could not be confident that the proteins are truly inside the lumen of EVs as opposed to being stuck to the outside. We found 197 transmembrane proteins found in EVs from neurons that were not also found in EVs from undifferentiated iPS cells

Framework for identifying cell type-specific EV markers

We decided to implement a simple, unbiased framework for determining which markers to use for cell-type specific EV isolation from a specific biological fluid. The frameworks starts by finding markers that are transmembrane, expressed in the given cell type of interest at the gene expression level, and found in the biological fluid of interest. We applied this framework for determining candidate markers for isolating neuron-specific EVs from human CSF.

First, we start with only transmembrane proteins (so that we could use them for immuno-isolation) based on annotations from the UniProt database (72). Next, we look at existing mass spectrometry data of all proteins that have been found in the biofluid of interest - in this case, cell-free CSF. This step is to ensure that the candidate EV marker is actually expressed and gets into biofluid of interest. We found two studies that performed mass spectrometry on pooled samples of human cell-free CSF (73, 74) and filtered the subset of those that are annotated as transmembrane. Lastly, we overlap these hits (of which there are 1819) with proteins that are neuron-specific at the gene expression level from RNA-Seq data (75, 76). We picked a cutoff of 3-fold enrichment in neurons over average expression in other cell types of the CNS in both human and mouse (although we are only working with human samples, using markers that are also neuron-specific in

mouse gives us higher confidence that they are truly neuron specific). Overlapping these three lists, we end up with 78 candidate transmembrane markers, found in cell-free CSF, and specific to neurons at the gene expression level.

We then overlapped the set of 78 candidate markers from our computational analysis of publicly available data with the mass spectrometry data we generated. This yielded 15 candidates that were transmembrane, found in CSF, neuron-specific at the gene expression level (in both human and mouse), and also found on EVs isolated from our iNGN neurons (**Figure 4.2**). From these 15 candidates, we prioritized seven candidates to screen antibodies for based on how well they satisfy the criteria relative to each other (**Table 3.1**). We were able to find specific antibodies (as evidenced by giving a single band of the predicted size by western blot) for the three top markers: L1CAM, SYT1, and CACNA2B1 and confirmed the presence of the marker in both cells and EVs (**Figure 4.3**). Individual inspection of their gene expression profiles in various cell types in the brain from the published reference studies (75, 76) confirmed that they were, indeed, neuron-specific in both mice and humans (**Figure 4.4**).

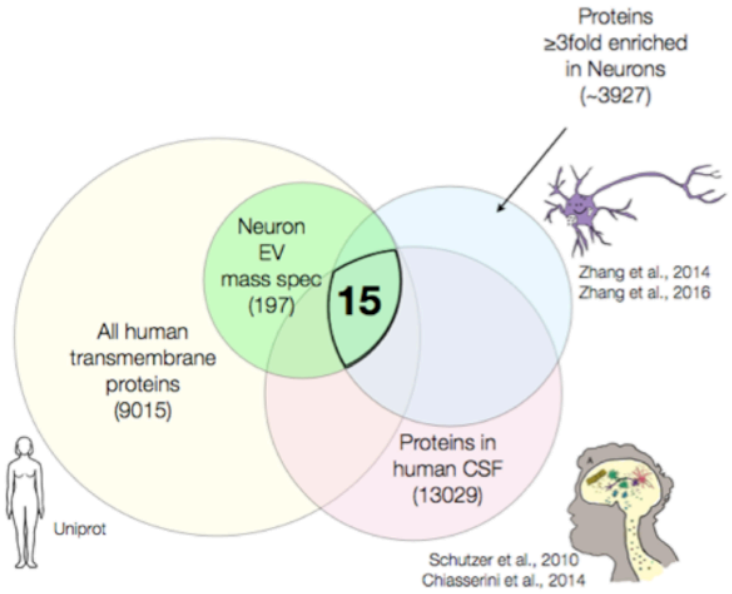

Figure 4.2. Framework for choosing neuron-specific EV markers
Transmembrane proteins are selected that have been found in human cell-free CSF by mass spectrometry and are also specific to neurons at the gene expression level (greater than three-fold enriched in neurons relative to average of other cell types) in both human and mouse RNA-Seq reference data sets.

Table 4.1: Prioritization of top EV neuron-specific candidate markers

Gene Name	Neural Enrichment (Human)	Neural Enrichment (Mouse)	Detected in Schutzer CSF Mass Spec?	Detected in Chiasserini CSF Mass Spec?	Enrichment in iPS Neurons over iPSCs by RNA-seq	Peptides detected in iPS Neuron Exo Mass Spec
SYT1	58.8	47.04	TRUE	TRUE	4.53	25
ROBO2	39.3	53.1	TRUE	FALSE	73.36	139
RTN1	31.5	5.75	TRUE	FALSE	142.97	26
PLXNA4	16.9	4.07	TRUE	FALSE	10.72	61
ATP2B3	16.5	6.69	FALSE	TRUE	182.75	40
SCN3A	14.3	3.7	TRUE	FALSE	0	18
FLRT3	14.3	7.37	TRUE	FALSE	10.92	5
L1CAM	13.4	57.52	TRUE	TRUE	19.51	51
FXYD6	9.9	3.49	TRUE	FALSE	1.76	9
CACNA2D1	8.2	20.44	TRUE	TRUE	5.63	50
ATP2B1	6.5	3.01	TRUE	TRUE	1.32	62
ATP2B2	5.3	5.83	FALSE	TRUE	36.29	20
ROBO1	3.4	3.73	TRUE	TRUE	5.15	26
VAMP2	3.2	3.92	TRUE	TRUE	8.63	18
SEZ6L2	3.2	7.71	TRUE	TRUE	3.79	8

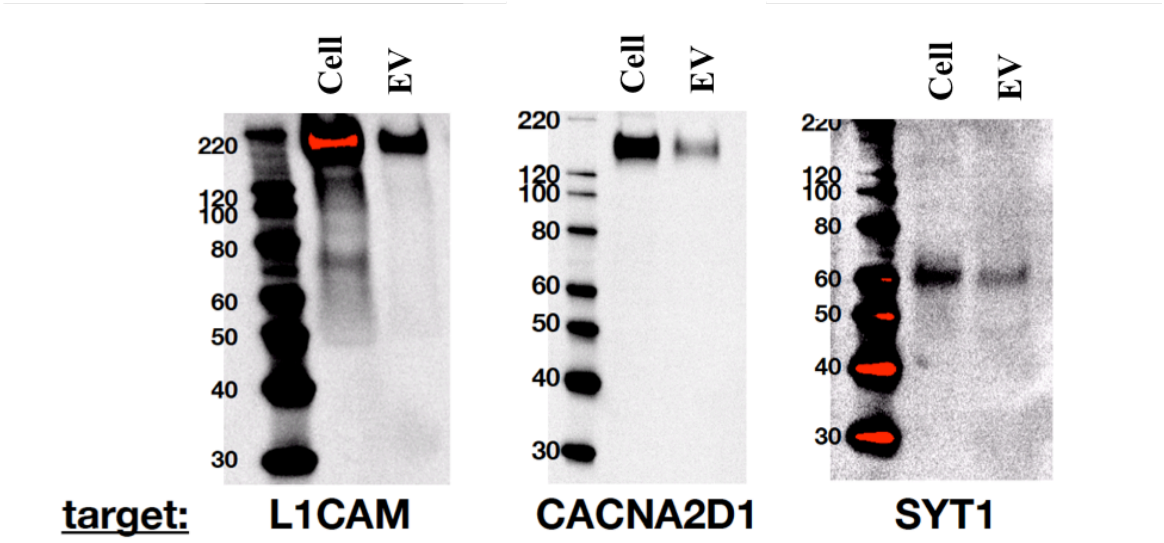

Figure 4.3: Western blot detects presence of candidate markers in neurons and neuron EVs
For the proteins L1CAM (left), CACNA2D1 (middle), and SYT1 (right), western blotting was performed on cell lysate from the iNGN neurons or EVs isolated from the media of iNGN neurons

Figure 4.4: Gene expression profiles show top three candidate markers are specifically expressed in neurons
Gene expression profiles (obtained from Source: http://web.stanford.edu/group/barres_lab/brainseq2/brainseq2.html) show that the genes L1CAM (left), SYT1 (middle), and CACNA2D1 (right) are expressed specifically in neurons in both mouse and human.

Development of EV immuno-isolation method

We set out to develop a method for immuno-isolation of EVs based on antibody capture of specific EV transmembrane proteins. Such a method would be useful for both the study of EVs subsets from a given cell type in culture (in order to study EV heterogeneity), as well as for the capture of cell type specific EVs from a human biological fluid such as plasma. The basic idea of the method is to capture EVs containing the specific marker with antibodies against that marker. By using conjugating the antibodies to magnetic beads, the antibody-bound EVs could then be isolated using a magnet.

We decided to start by developing a protocol for immuno-isolation of EVs using the tetraspanin proteins and common EV markers, CD63 and CD81. We first established the read-out of our method using western blotting to detect the target proteins used for the immuno-isolation. We performed western blotting to confirm that both CD63 and CD81 are present in K562 cells and EVs (**Figure 4.5**). We figured that to evaluate how various parameters affect the immuno-isolation, we first need a clear way to assess how our protocol is performing. In particular, we need to measure the efficiency our capture, which we define as the percentage of marker detected in the pulldown fraction compared to the flow-through fraction when adding EVs to beads with antibody against the target. We also needed to evaluate the specificity of our capture, to ensure that we are not binding EVs non-specifically to our beads regardless of whether they have the target protein or not (77). For this, we used an equal amount of EVs (as with the target

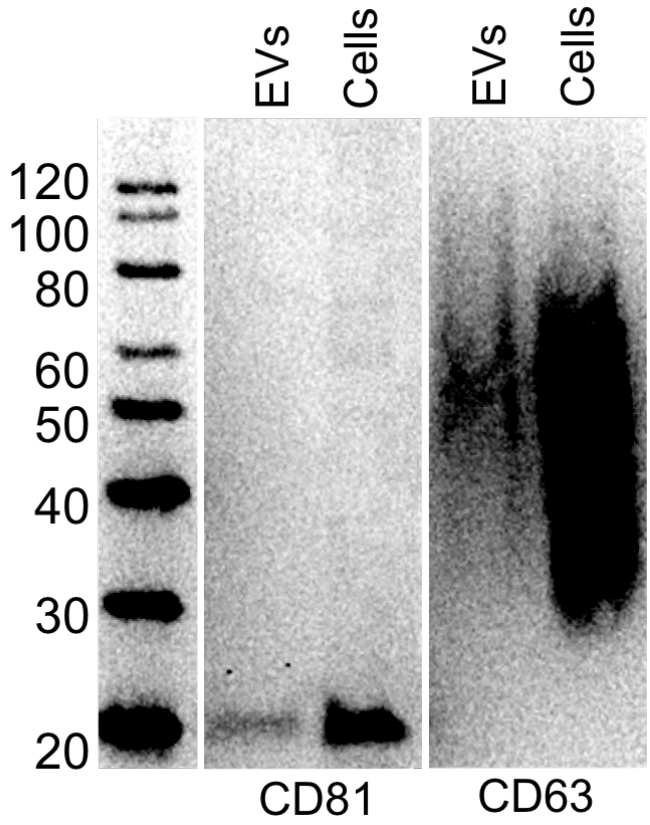

Figure 4.5: Western blot of K562 cells and EVs shows presence of CD81 and CD63
Lysate from cells and EVs was run on a denaturing gel and western blotting was performed against CD81 and CD63. The expected size of CD81 is ~26 kDa but we see it closer to the 20 kDa ladder marker. CD63 is also ~26kDa in size but is expected to be a larger smear between 30 and 60 kDa due to it's variable glycosylation patterns, giving rise to proteins of different sizes.

antibody) with a non-specific antibody (against a protein not expressed on the EVs such as GFP or mCherry).

After testing a variety of antibodies, we performed immuno-isolations on EVs isolated by differential ultracentrifugation from K562 cells. One problem we had in the beginning was that after immuno-isolating EVs and adding lysis buffer to the beads to recover EV lysate, the primary antibody came off the beads in the lysis buffer. It was then detected (on the denaturing gel) as prominent bands by the secondary antibody. This was

particularly problematic as the light chain of the antibody is close in size to CD81. We were able to largely remedy this problem by using a special secondary antibody (called TrueBlot) that preferentially detects the native, disulfide form of IgG over the denatured form (**Figure 4.6**).

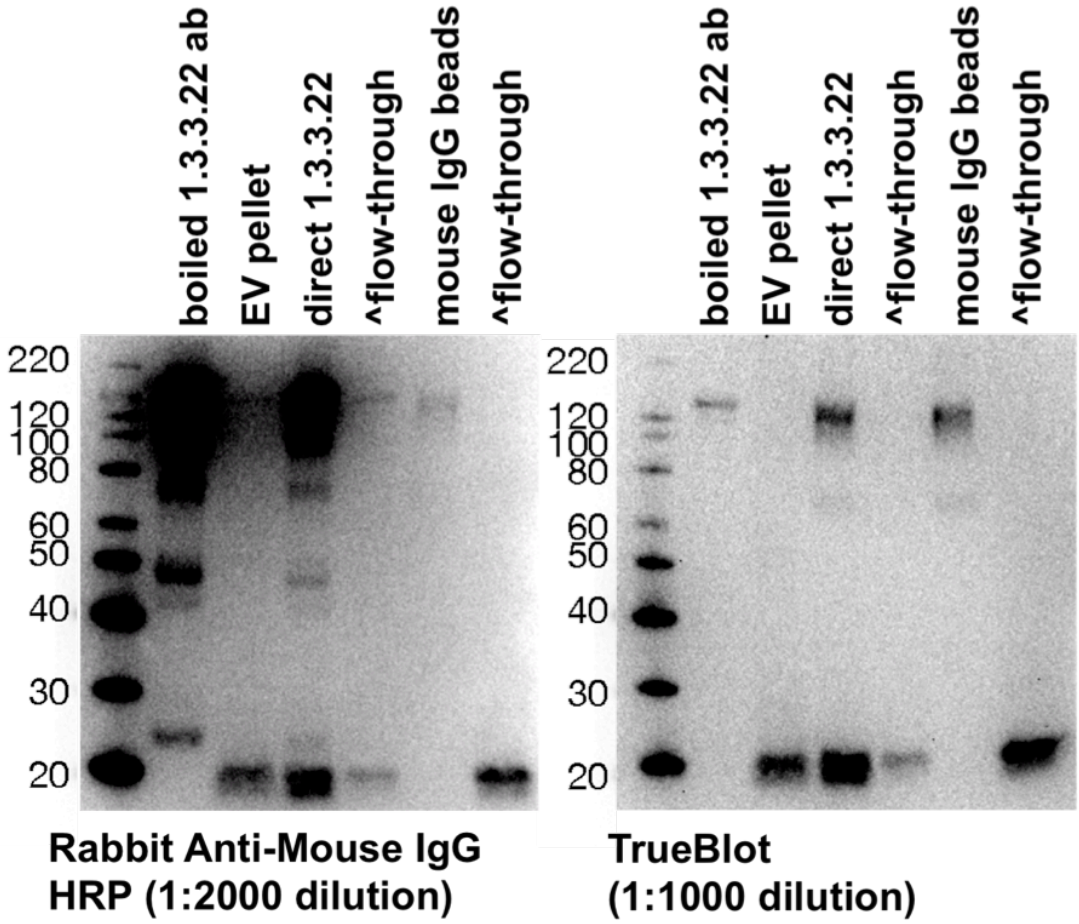

Figure 4.6: TrueBlot secondary antibody reduces binding to primary antibody conjugated to beads
CD81 western blot comparing regular secondary Rabbit Anti-Mouse IgG HRP antibody to the TrueBlot secondary antibody. TrueBlot greatly reduces the signal seen at 150 kDa of the primary antibody that is conjugated to the beads coming off during the EV lysis. Lysate was used from K562 EVs (EV pellet) or EV pulldown using beads conjugated to antibody (clone 1.3.3.22)

With our western blots now working well, we started comparing different parameters and conditions for immuno-isolation. We first compared direct (primary antibody conjugated to beads and then added to sample) vs. indirect (primary antibody is added to sample first and then added to beads) immuno-isolation methods using two different antibodies (clones M38 and 1.3.3.22) against CD81 (**Figure 4.7**). Finding that the direct method worked better, we stuck with it for the subsequent optimizations. Next,

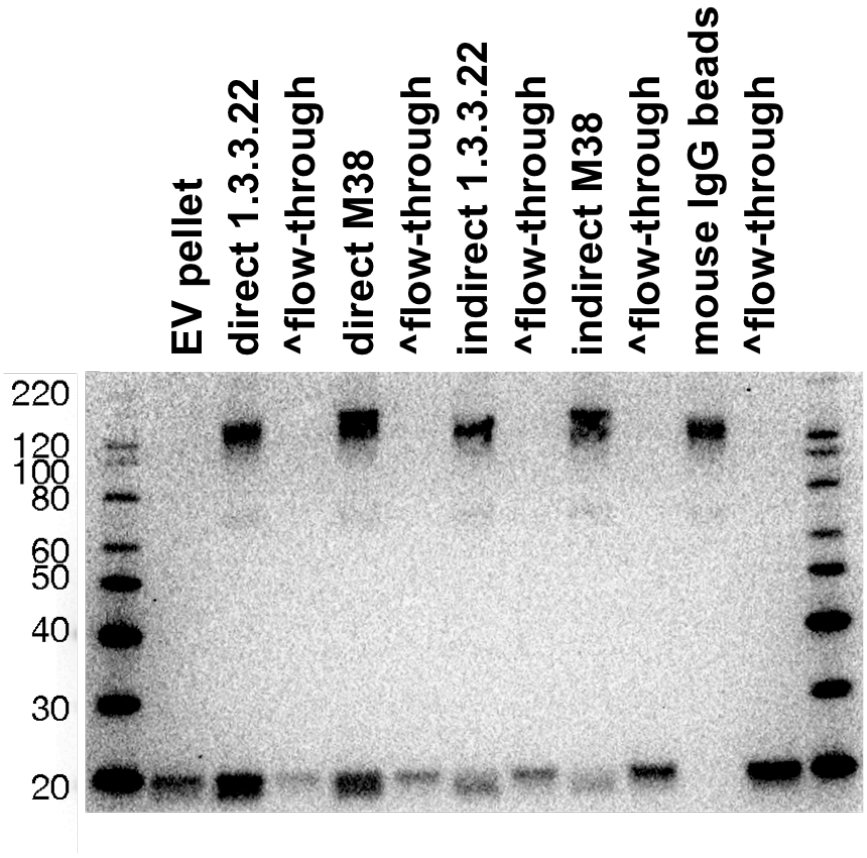

Figure 4.7: Direct immuno-isolation of EVs works better than indirect for CD81
Direct (primary antibody conjugated to beads and then added to sample) vs. indirect (primary antibody is added to sample first and then added to beads) pulldown methods are compared for CD81 immuno-isolation using two different antibodies (clones M38 and 1.3.3.22). Note: band at 150 kDa is primary antibody coming off of beads.

we tried different incubation times and temperatures, finding that changing these variables has a large effect on the CD81 capture efficiency (**Figure 4.8**).

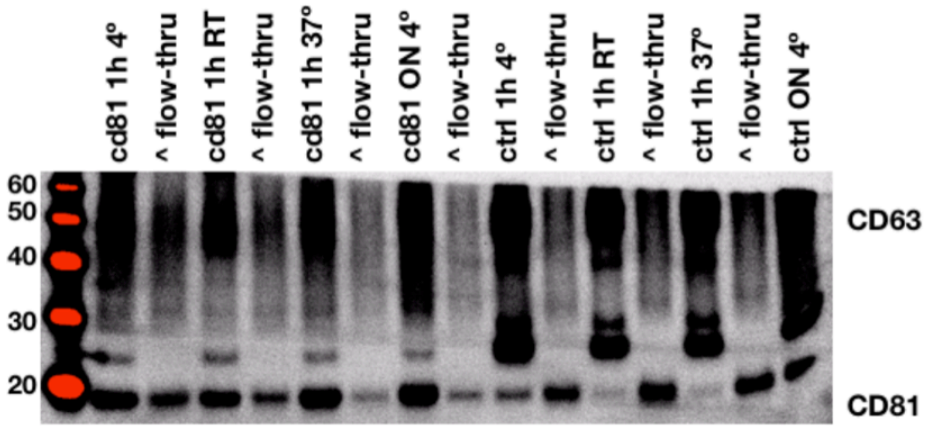

Figure 4.8: Immuno-isolation incubation time and temperature affects CD81 capture efficiency
Western blot against CD81 and CD63 after EVs were incubated with beads for either 1 hour or overnight (ON), at different temperatures (4C, room temperature, or 37C) using beads conjugated to either CD81 or a control (ctrl) non-specific antibody (against mCherry)

After some more optimization, we were able to get highly efficient and specific immuno-isolations for CD81 and CD63. Additionally, we tested the topology of CD81 and CD63 in EVs using a proteinase protection assay. We treated the EVs with Proteinase K or Triton and Proteinase K and performed a western blot against CD63 or CD81 using antibodies that recognize the extracellular domain. We confirmed CD81 has the expected topology as the protein was fully degraded upon treatment of EVs using proteinase. CD63 was not fully degraded upon proteinase treatment, but that may be because its heavy glycosylation protects it from proteinase cleavage. We also checked that after lysing EVs on the beads to recover the lysate we don't leave any EVs behind (by reboiling the beads and assessing if any further protein is removed) (**Figure 4.9**). Our

best protocol yielded a capture efficiency of 98% for CD81 and a specificity of 100% (as measured by western blot).

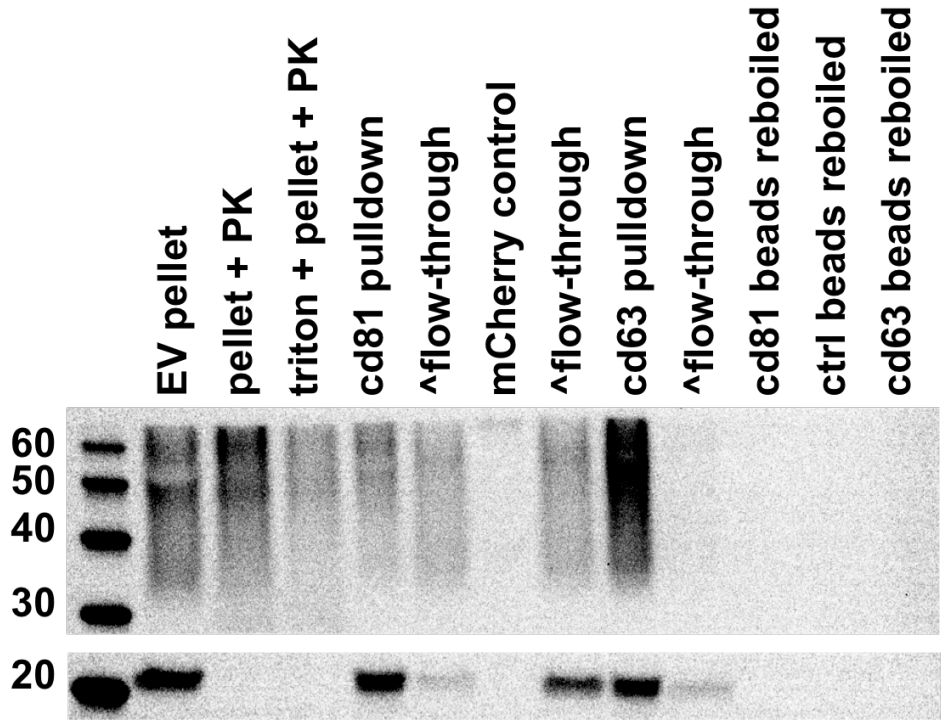

Figure 4.9: Optimized immuno-isolation protocol is efficient and specific against K562 EVs with CD81 or CD63
Western blot against CD81 and CD63 after EVs were incubated with beads for 1 hour at 37C using beads conjugated to antibody against CD81, CD63 or mCherry. As an extra control to ensure that all EVs came off of beads during lysis, beads were reboiled after lysis to see if more material was left. Additionally, EV pellet was treated with Proteinase K (PK) or Triton X and Proteinase K.

Immuno-isolation of EVs isolated from neurons

After developing an immuno-isolation protocol against the general EV markers CD63 and CD81, we set out to adapt the protocol for neuron-specific EV markers. We first tested a variety of antibodies against our top three candidate markers (L1CAM,

SYT1, and CACAN2D1). Although we found one or more antibodies for each of the three proteins that were specific by western blot, we only found one antibody (against L1CAM, Clone 5G3) that worked well for immuno-isolation. It is not entirely surprising that antibodies that work for western blot do not often work for immuno-isolation since a western blot is performed after running a gel under denaturing conditions, whereas the immuno-isolation is performed using native conditions.

We also tested the topology of L1CAM. We were worried that some of the proteins we were using for immuno-isolation could have the opposite topology. For example, if there are contaminating synaptic vesicles from dying cells, and we isolate them using our protocol, the domain of the protein that is normally extracellular would be inside of the synaptic vesicle and inaccessible to our antibody. A proteinase protection assay (with a antibody used for western blot that recognizes the extracellular domain of L1CAM) showed that L1CAM has the expected topology on EVs with the extracellular domain exposed (**Figure 4.10**).

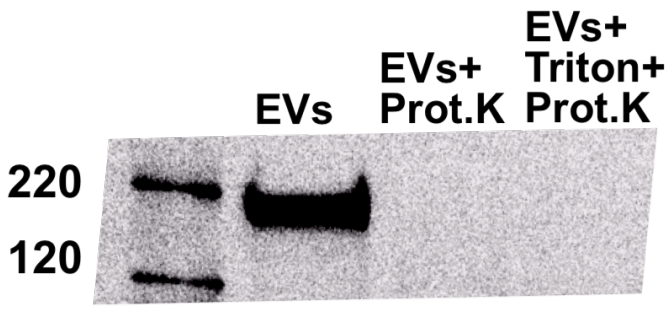

Figure 4.10: Proteinase protection assay shows L1CAM has expected topology in neuron EVs
Western blot against L1CAM using antibody that recognizes extracellular domain. Lysate is used from neurons EVs that are untreated (EVs), treated with Proteinase K (EVs+ Prot. K) or treated with Proteinase K and Triton X (EVs+Triton+ Prot. K)

Using the best-performing antibody, we were able to demonstrate a highly specific immuno-isolation against L1CAM using EVs isolated form the media of the iNGN neurons. This took some additional optimization, as conditions that worked best for the CD81 antibody did not work as well for the L1CAM antibody (**Figure 4.11**).

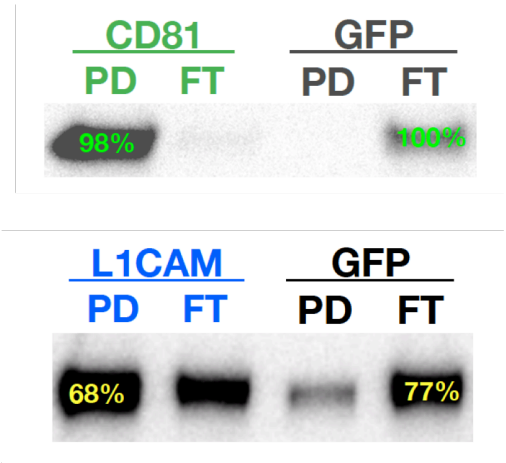

Figure 4.11: Optimal immuno-isolation conditions for CD81 not optimal for L1CAM
Immuno-isolation for 1 hour at 37C was performed on K562 EVs using CD81 (or control GFP antibody) and neuron EVs using L1CAM (or control GFP antibody) and corresponding western blot was performed against CD81 (**Top**) or L1CAM (**Bottom**). Intensity of bands on western blot was quantified as percentage of band relative to sum of pulldown (PD) + flow-through (FT) for that condition.

Using EVs from the iNGN neurons, we went back to trying different temperatures, volumes, and incubation times for the immuno-isolation (**Figure 4.12**). Then, holding those parameters constant but further optimizing the number of antibody-conjugated beads led us to find the optimal conditions for the L1CAM immuno-isolation. We were able to achieve 89% efficiency (comparing how much L1CAM was in pulldown vs. flow-through fraction when using L1CAM antibody) and 100% specificity (comparing how

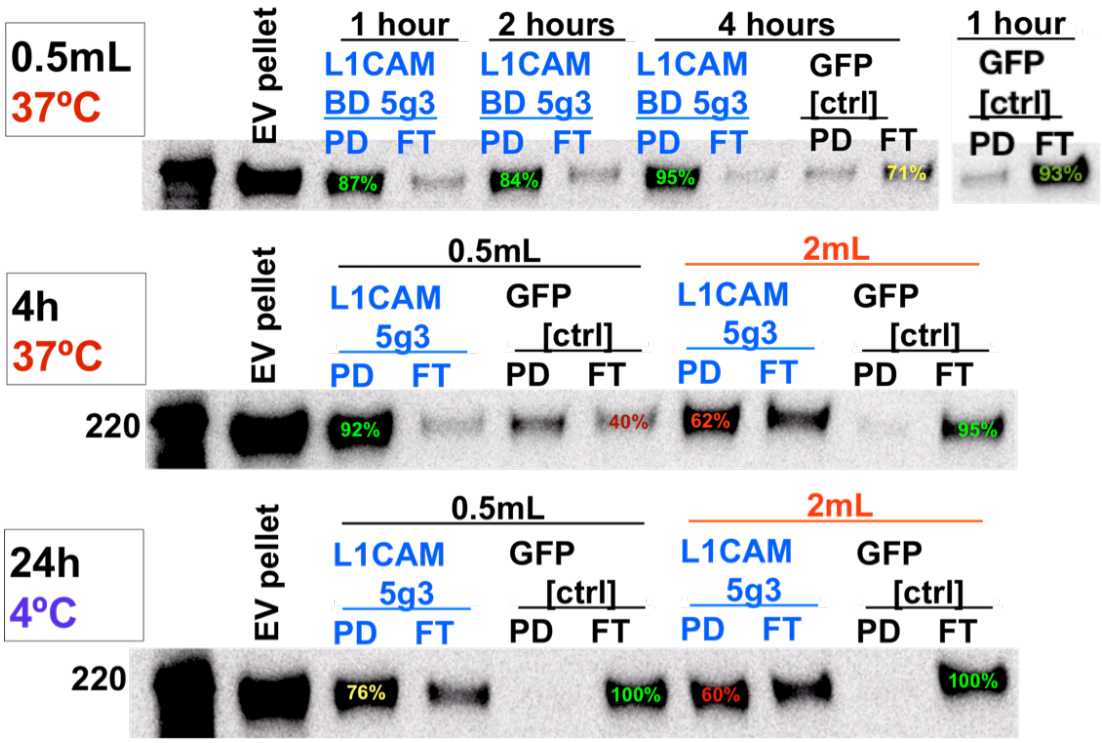

Figure 4.12: Immuno-isolation incubation time, volume and temperature affects L1CAM capture efficiency
Western blot against L1CAM after neuron EVs were incubated with antibody conjugated beads (against L1CAM or GFP) for different times (1, 2, 4, or 24 hours), in different volumes (0.5 mL or 2 mL) at different temperatures (4C or 37C). Intensity of bands on western blot was quantified as percentage of band relative to sum of pulldown (PD) + flow-through (FT) for that condition.

much L1CAM was in flow-through fraction vs. pulldown fraction when using non-specific antibody) (**Figure 4.13**).

After we optimized the L1CAM immuno-isolation to be highly efficient and specific in the neuron EVs, we wanted to see if it would work for a more complex mixture of EVs. We thus decided to perform a mixing experiment where we mix EVs

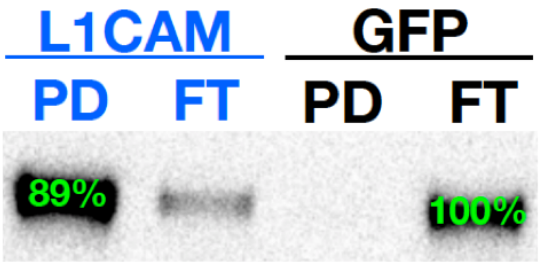

Figure 4.13: Optimized immuno-isolation protocol is efficient and specific against neuron EVs with L1CAM
Western blot against L1CAM after neuron EVs were incubated with beads for 24 hours at 4C using beads conjugated to either an antibody against L1CAM or GFP. Intensity of bands on western blot was quantified as percentage of band relative to sum of pulldown (PD) + flow-through (FT) for that condition.

from neurons and EVs from a different cell type that does not express L1CAM. For this purpose, we chose undifferentiated iPS cells. We first confirmed that the iPS EVs do not express L1CAM. We also found a marker from our mass spectrometry data, GJA1, which is expressed only in iPS cells but not in neurons. We figured we could follow this marker as additional control that our L1CAM immuno-isolation is specific.

Performing the L1CAM immuno-isolation on a mixture of neuron and iPS EVs mixed at an equal ratio (normalized to cell number), we found that our immuno-isolation protocol was still highly efficient and specific (**Figure 4.14**). Although we do not know what percentage of EVs from neurons or in CSF have L1CAM, we expect that percentage to low. Thus, we wanted to insure that our protocol still works when there is an even lower percentage of L1CAM-positive EVs. We repeated the mixture experiment again but with a lower ratio of neuron EVs to iPS EV and assured ourselves that our immuno-isolation protocol still works with a lower percentage of EVs (**Figure 4.15**).

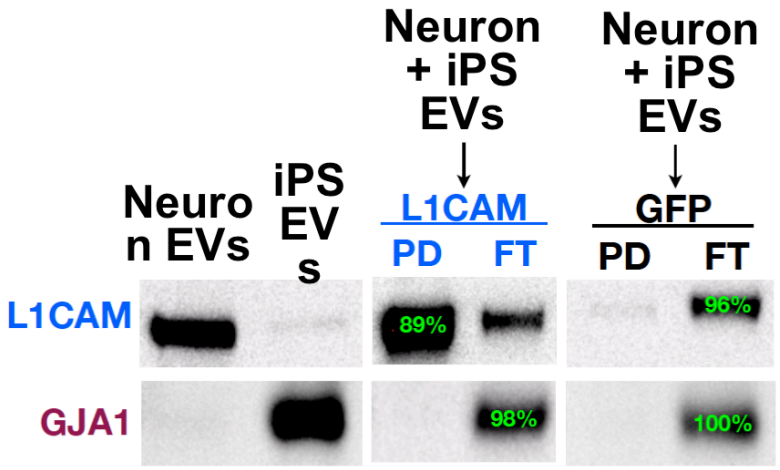

Figure 4.14: Mixing experiment with equal ratio of both neuron and iPS EVs shows high efficiency and specificity of L1CAM immuno-isolation
Western blot against L1CAM and GJA1 using lysate from neuron EVs, iPS EVs, or an immuno-isolation (using L1CAM or GFP antibody) on a mixture of neuron EVs and iPS EV. An equal ratio of neuron or iPS EVs was used in the mixture (normalized to cell number). Intensity of bands on western blot was quantified as percentage of band relative to sum of pulldown (PD) + flow-through (FT) for that condition.

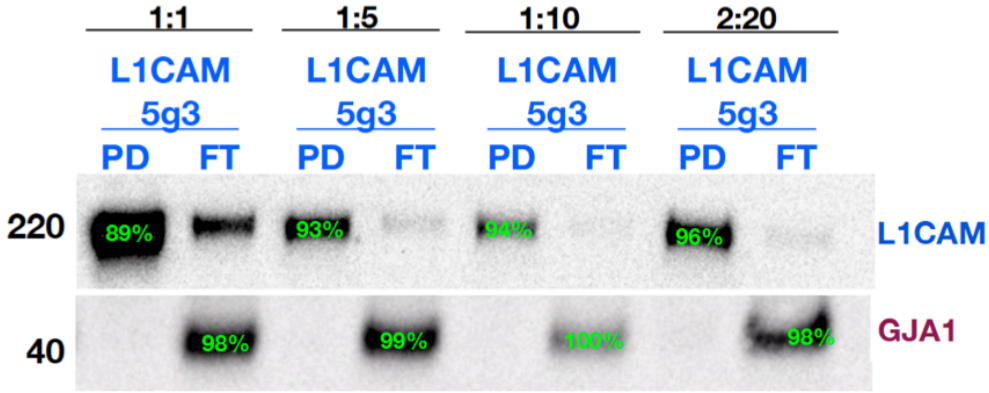

Figure 4.15: Mixing experiment with different ratios of neuron and iPS EVs shows high efficiency and specificity of L1CAM immuno-isolation
Western blot against L1CAM and GJA1 on EV lysate recovered from L1CAM immuno-isolation on mixtures of neuron EVs and iPS EVs. Different ratios were used of neuron EVs to iPS EVs (normalized to cell number). Ratio of 1:10 is equivalent 1 part neuron EVs to 10 parts iPS EVs. Ratio of 2:20 is same as 1:10 but twice as much of each is used (so that bands on western blot are less faint). Intensity of bands on western blot was quantified as percentage of band relative to sum of pulldown (PD) + flow-through (FT) for that condition.

Immuno-isolation of neuron-specific EVs from human CSF

Having convinced ourselves that our immuno-isolation protocol is robust in EVs isolated from cell culture, we then turned to human CSF. We performed the protocol on 0.5 mL of human CSF and performed RNA-Seq using an ultralow input RNA-Seq library construction protocol used for single cell RNA-Seq (78). When we sequenced the libraries, it did not look like the method worked, likely due to not getting enough RNA to sequence. There were several possibilities that we considered as to why we did not get enough RNA to sequence. It could be that the immuno-isolation worked but there were not sufficient EVs (or RNA in EVs) to be able to sequence. It also could be that the immuno-isolation did not work in CSF.

We decided to first see if we could detect L1CAM in EVs isolated from CSF. We pooled 3 mL of human CSF and isolated EVs by ultracentrifugation. We then performed a western blot to detect L1CAM. We were able to detect L1CAM but found that a majority of it was a cleaved product much shorter than the full length transmembrane L1CAM (**Figure 4.16**). We had previously considered that L1CAM could be proteolytically cleaved since cleavage products have been reported before. The full length L1CAM is 200-220 kDa in size (there is some variability due to glycosylation) but much smaller, soluble fragments have been reported both in the brain and in some cancer cells (79). However, our western blot (**Figure 4.3**) of L1CAM in neuron EVs suggested that L1CAM was full length as we saw only one prominent band corresponding in size to the full-length protein. Our CSF results, nonetheless, suggest that L1CAM may bot be a good

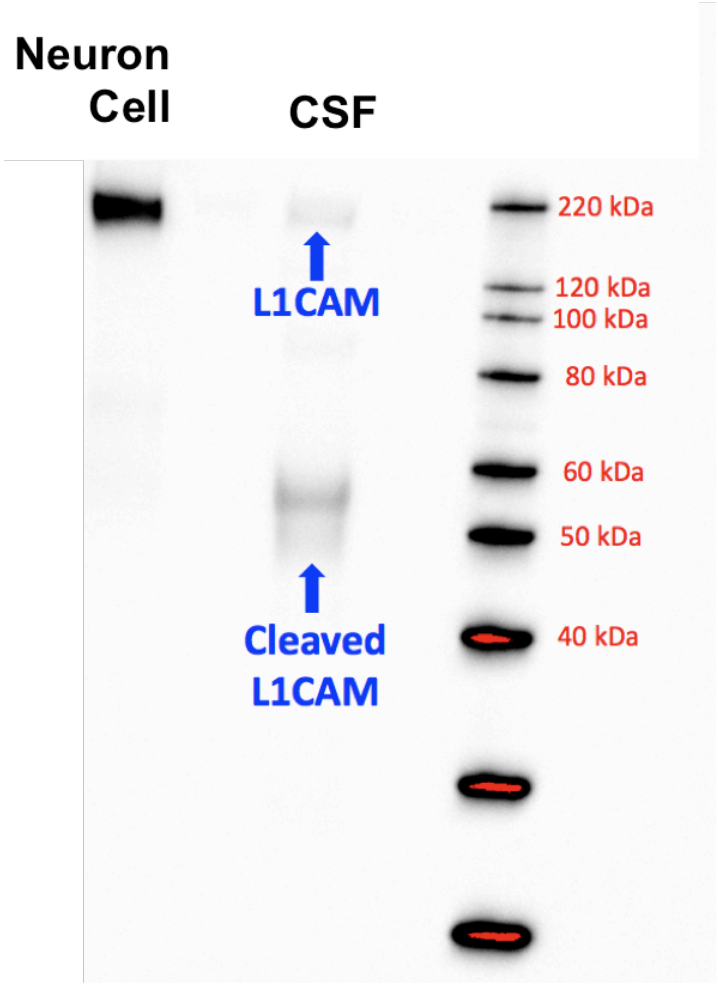

Figure 4.16: L1CAM western blot in human CSF shows predominant form of L1CAM is cleavage product
Western blot against L1CAM on lysate from: neuron cells, and EVs isolated from 3mL human CSF.

marker for immuno-isolation as a large majority of it in CSF is cleaved and, therefore, not associated with EVs.

Discussion

One of the greatest challenges in studying EVs, whether in a biological fluid such as blood, or in cell culture media, is that they are heterogeneous. One reasonable way to try to characterize subsets of EVs is through which proteins are on their surface (29). Analyzing EV surface proteins represents a way of characterizing EVs, as well as a means to isolate them (through antibody capture). Furthermore, isolating EV subsets using cell type specific markers from biological fluids in humans would have tremendous utility in clinical diagnostics as it would allow for the analysis of RNAs and intracellular proteins RNAs that come from specific cell types that are inaccessible to biopsy (most cell types in humans).

We demonstrate how to go about choosing markers for the isolation of cell type-specific EVs, using neurons as a proof of principle. We also develop and validate an immuno-isolation method using EVs in cell culture, and apply it to neuron EVs. Although previous groups have attempted to isolate cell-type specific EVs from plasma, including neuron-specific EVs, these studies did not show validation that their immuno-isolation method was successful. Furthermore, these studies did not take into account global gene expression data when picking their marker. Thus, they didn't could not conclude the EVs they obtained, even if their immuno-isolation was actually efficient and specific for the marker of interest, were coming from the cell type of interest and not a different cell type that also expressed that marker.

For example, one group claimed to isolate neuron-derived EVs from blood using either NCAM1 or L1CAM. Although both of these proteins are expressed in neurons,

NCAM1 is not specific to neurons. Gene expression data in both human mouse brains shows that it is also expressed in astrocytes (**Figure 4-17**). Currently, we only have organ-level body-wide gene expression data (as opposed to cell type specific) for humans. Thus, it is difficult to know how cell type specific a given EV marker is when isolated from blood (where presumably all cell types of the body can contribute EVs).

Figure 4.17: Gene expression profiles show NCAM1 is not expressed specifically in neurons
Gene expression profiles (obtained from Source: http://web.stanford.edu/group/barres_lab/brainseq2/brainseq2.html) show that the NCAM1 is not expressed specifically in neurons in both and human (top) and mouse (bottom).

We focused on isolating neuron EVs from CSF as opposed to blood. We made the assumption that the large majority of EVs in CSF are coming from the brain and not the periphery. This simplifies the problem of choosing cell type specific EV markers since there is good cell type specific gene expression data available for the brain (75, 76). As

more cell type-specific gene expression data becomes available, for example, through the Human Cell Atlas Initiative (80), our computational framework can easily be adapted to use this data. We would then also be able to better predict EV markers (whether from neurons or other cell types) for EV isolation in blood, which is, of course, a more accessible biofluid than CSF.

Our work demonstrates the utility of using simple cell culture systems for developing new methods to isolate and characterize EVs. By using EVs from cell culture, we were able to obtain large amount of material in a reproducible fashion. We validated our EV immuno-isolation method using a variety of cell culture experiments before applying it to the isolation of neuron-specific EVs from human CSF. Our attempts to isolate neuron-specific EVs and perform RNA-Seq on their contents in order to measure the human neuronal transcriptome were, alas, not successful. Our investigation into potential reasons why we did not get enough RNA for RNA-Seq led us to the finding that the large majority of cleaved L1CAM in CSF is cleaved, and therefore not associated with EVs. This likely means that L1CAM is not a good marker for isolating EVs and other markers will need to be tried. We have provided, for future attempts, a framework for choosing other markers and a method for immuno-isolating EVs.

Chapter V

Investigation of EV and RNA transfer between cells

Introduction:

The main question in the EV field is whether EVs are involved in intercellular communication. The excitement regarding EVs largely stems from the possibility that EVs carry cargo, in the form of RNA and protein, which is sent from a donor cell to a recipient cell. Whether this actually happens under physiological conditions, however, is not known and heavily debated (11, 29). This question has been difficult to study since it is unclear where EVs are transferred, if at all. Does a cell type A, maybe a dendritic cell, send EVs specifically to cell type B, maybe a particular T cell? And is this transfer mediated by a particular receptor-ligand interaction that mediates cell type specificity? Although it was initially assumed that some of the transmembrane proteins on EV are ligands for particular cell type specific receptors, none such ligand-receptor interactions have been convincingly identified (11).

Some of the challenges of studying EV transfer in mammalian systems are inherent to studying any intercellular communication. The general problem of trying to figure out a complex *in vivo* process is difficult to reduce to a simple *in vitro* system, particularly when it is unclear which pair of cells should be studied. There have been some attempts at investigating EVs *in vivo*. One clever approach involves the use of the Cre-Lox system in mice. In this approach, donor cells expressing Cre are injected into mice with LoxP reporters such that recombination only occurs if Cre is transferred between donor and acceptor cells. Although these experiments showed a very low level of recombination, and were unable to conclusively differentiate whether the Cre was transferred as mRNA or protein, they nonetheless demonstrated the possibility of a

functional reporter transferring between different cells (33-35). Demonstrating the transfer of Cre is different than showing transfer of endogenous RNA since Cre is an exogenous reporter, and also one that is incredibly sensitive (only one molecule of Cre protein is enough to induce recombination in the recipient cell). Nonetheless, this was an important demonstration for the field (29).

The first study to undertake the investigation of RNA transfer between cells was devised in 1971 by Gerald Kolodny. In a spectacularly elegant set of experiments, Kolodny realized he could use metabolic labeling to detect transferred RNAs. Specifically, Kolodny added the radioactive nucleotide, 3H-uridine, to one set of (donor) human 3T3 fibroblast cells. He waited for the radioactive (monomeric) nucleotide to incorporate in polymeric RNAs during transcription and then washed away the excess free radioactive nucleotide. He then co-cultured the donor cells (with radioactive RNA) with a different set of acceptor cells (also 3T3 fibroblasts). The acceptor cells had never seen the radioactive nucleotide and thus did not have any radioactivity. The acceptor cells were could also be separated from the donor cells as heavy tantalum beads were added to the culture media of donor cells. The cells took up the beads by phagocytosis and were consequently heavier than cells that had not taken up by beads. This principle was then used to be able to separate the donor cells (containing beads) from acceptor cells (that had never seen beads).

Kolodny then co-cultured the donor cells (containing radioactive RNA and heavy beads) with the acceptor cells (containing no radioactivity). Next, Kolodny separated the acceptor cells away from donor cells using centrifugation on a Ficoll gradient due to the

fact that the donor cells were heavier (having previously taken up the beads). RNA was subsequently extracted from the acceptor cells and radioactivity was detected (10).

We decided to investigate whether EVs and RNAs are transferred between cells in vitro using a co-culture system. We devised an experiment to study whether EVs are transferred between cells using fluorescent reporters and live cell imaging. We also devised two different approaches to investigate whether RNAs are transferred between cells. In one approach, we used metabolic labeling using the click-chemistry compatible modified nucleotide, Ethylene Uridine (EU). In a second approach we co-cultured human and mouse cells and looked for mouse transcripts in human cells by RNA-Seq.

Results:

Live cell imaging of EV transfer

To investigate whether EVs are transferred between cells, we decided to use a simple co-culture system and perform live cell imaging. To label EVs, we made fusion protein constructs with membrane proteins fused to a fluorescent protein. Specifically, we fused GFP or RFP to the C terminus of either CD63 or CD9. Both of these proteins are considered to be general EV markers that enriched in EVs and are members of the tetraspanin family. Tetraspanins are a class of proteins with four transmembrane domains, with both the N and C domains facing into the cytosol (81). Thus, in EVs, a tetraspanin fused to a fluorescent protein would orient the fluorescent protein inside the vesicle, decreasing the chance that the fusion protein would interfere with potential

interactions between EVs and recipient cells. We made lentiviral constructs of CD9-GFP, CD9-RFP, and CD63-RFP, and then infected three batches of A549 lung adenocarcinoma cells with the different constructs.

We set up co-culture experiments with cells expressing CD9-GFP and either CD9-RFP or CD63-RFP. Using spinning disk confocal microscopy, we were able to observe EV exchange between live cells in the co-culture system. One advantage of this system is that we don't isolate EVs, thereby eliminating the possibility of studying an artifact of the purification procedure (such as cells or larger particles being broken up into smaller vesicles during a centrifugation or filtration step). We made live cell imaging movies of co-cultures using either CD9-GFP cells and CD63-RFP cells (**Figure 5.1**) or CD9-GFP and CD9-RFP cells (**Figures 5.2 and 5.3**). In these movies, a Z plane was found such that we were looking at a slice through the middle of the cells and the Z plane was held constant. We also made a movie where a Z stack was taken over time going from the bottom of the cells to the top (**Figure 5.4**) in a co-culture of CD9-GFP cells and CD63-RFP cells. This was to ensure that the EVs we observed were truly inside the cells.

In each movie, we were clearly able to see GFP-labeled EVs in RFP–expressing cells and RFP-labeled EVs in GFP-labeled cells. The results were similar regardless of whether CD9-GFP cells were used together with CD9-RFP cells or CD63-RFP cells. We could observe, however, that the CD9 is much more localized to the membrane whereas CD63 is more heavily expressed in endosomes and multivesicular bodies. Due to the restricted movement of most donor EVs in recipient cells, it is likely they are in endosomes and therefore taken up by endocytosis. We also saw cells extrude protrusions or tubes of this membrane and contact other cells. We often were able to see EVs transfer

close to the area, suggesting that EVs may be more likely to transfer between cells at areas where cells contact each other.

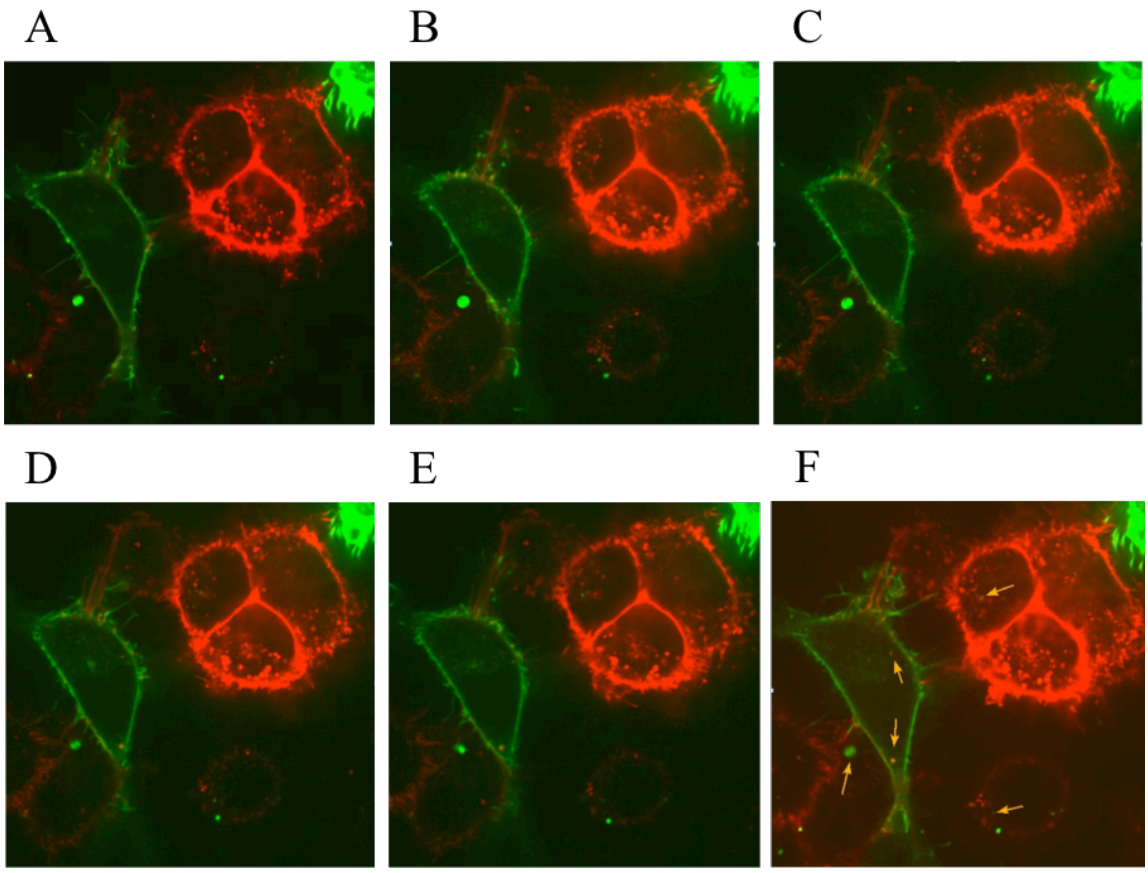

Figure 5.1: Live cell imaging of CD9-GFP and CD63-RFP cells over time shows EV exchange
Live cell imaging of CD9-GFP A549 cells co-cultured with CD63-RFP A549 cells over time. Z plane was held constant and cells were recorded over time. **A-E**: Still images from live cell imaging movie with each still 1 second apart. **F**: Image from live cell imaging movie at 1 second with arrows indicating EVs from one cells inside another cell.

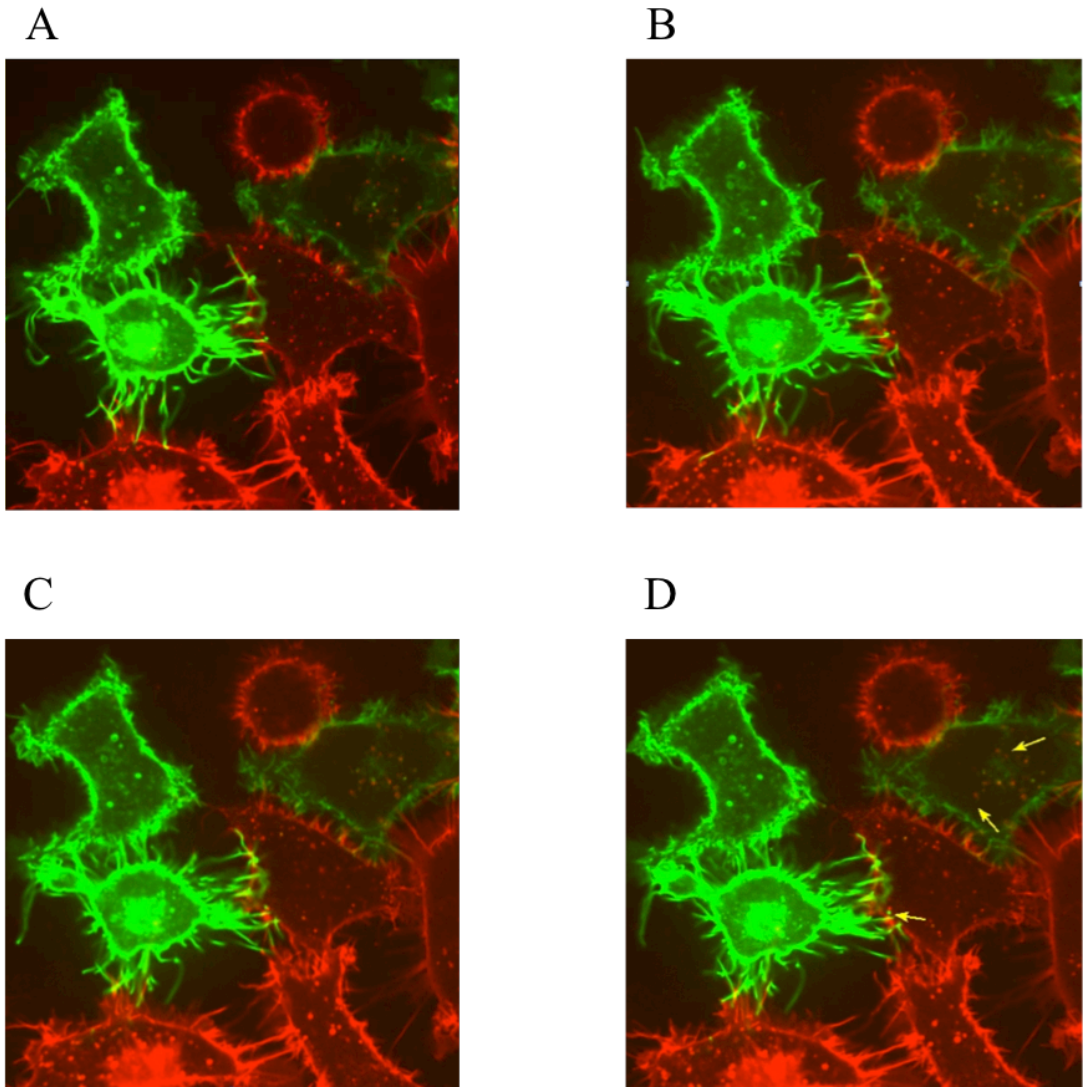

Figure 5.2: Live cell imaging of CD9-GFP and CD9-RFP cells over time shows EV exchange
Live cell imaging of CD9-GFP A549 cells co-cultured with CD9-RFP A549 cells over time. Z plane was held constant and cells were recorded over time. **A-C**: still images from live cell imaging movie with each still 1 second apart. **D**: Image from live cell imaging movie at 2.25 second with arrows indicating EVs from one cells inside another cell.

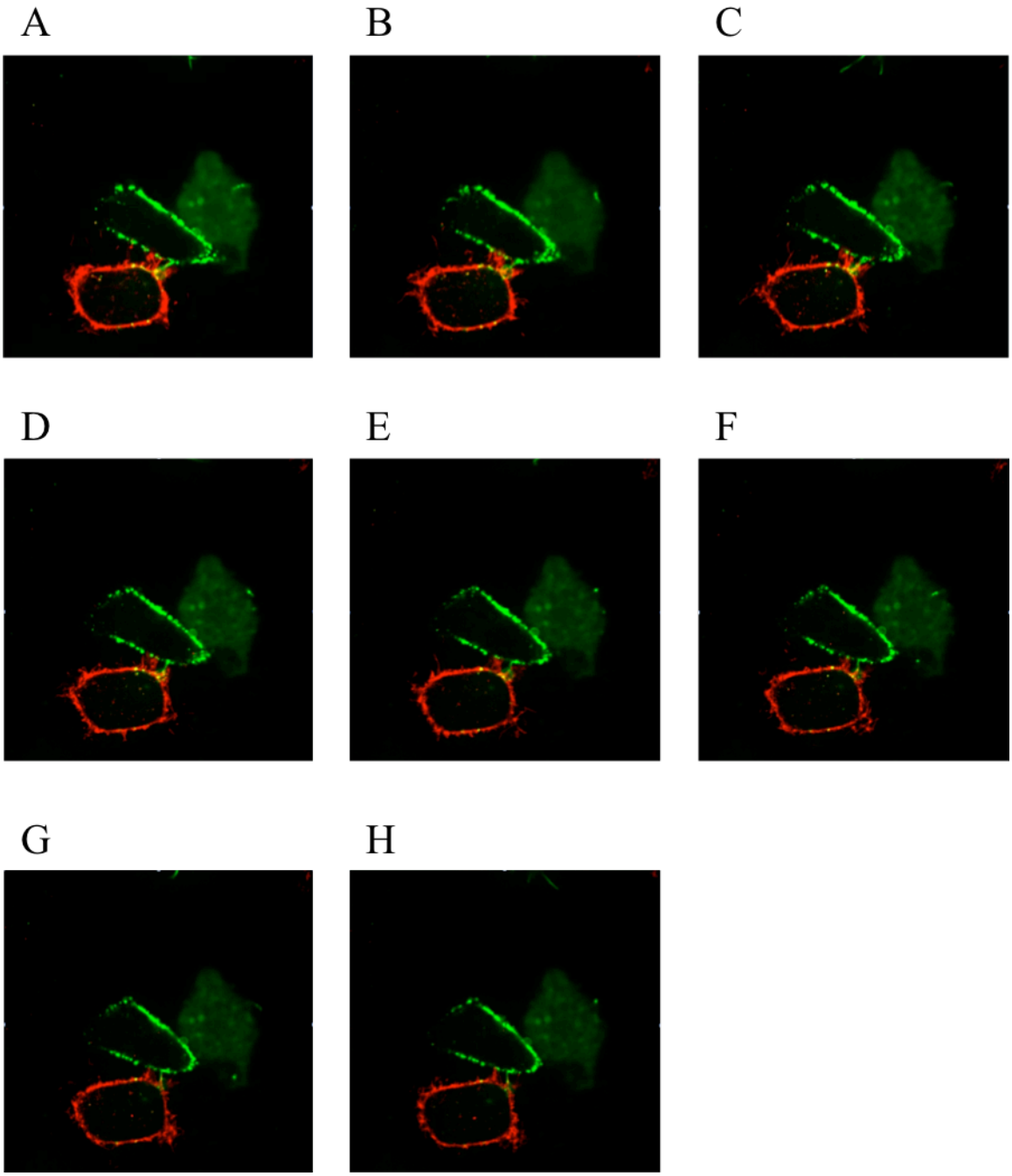

Figure 5.3: Live cell imaging of CD9-GFP and CD9-RFP cells shows EVs close to intercellular membrane contact sites
Live cell imaging of CD9-GFP A549 cells co-cultured with CD9-RFP A549 cells over time. Z plane was held constant and cells were recorded over time. **A-H**: still images from live cell imaging movie with each still 1 second apart.

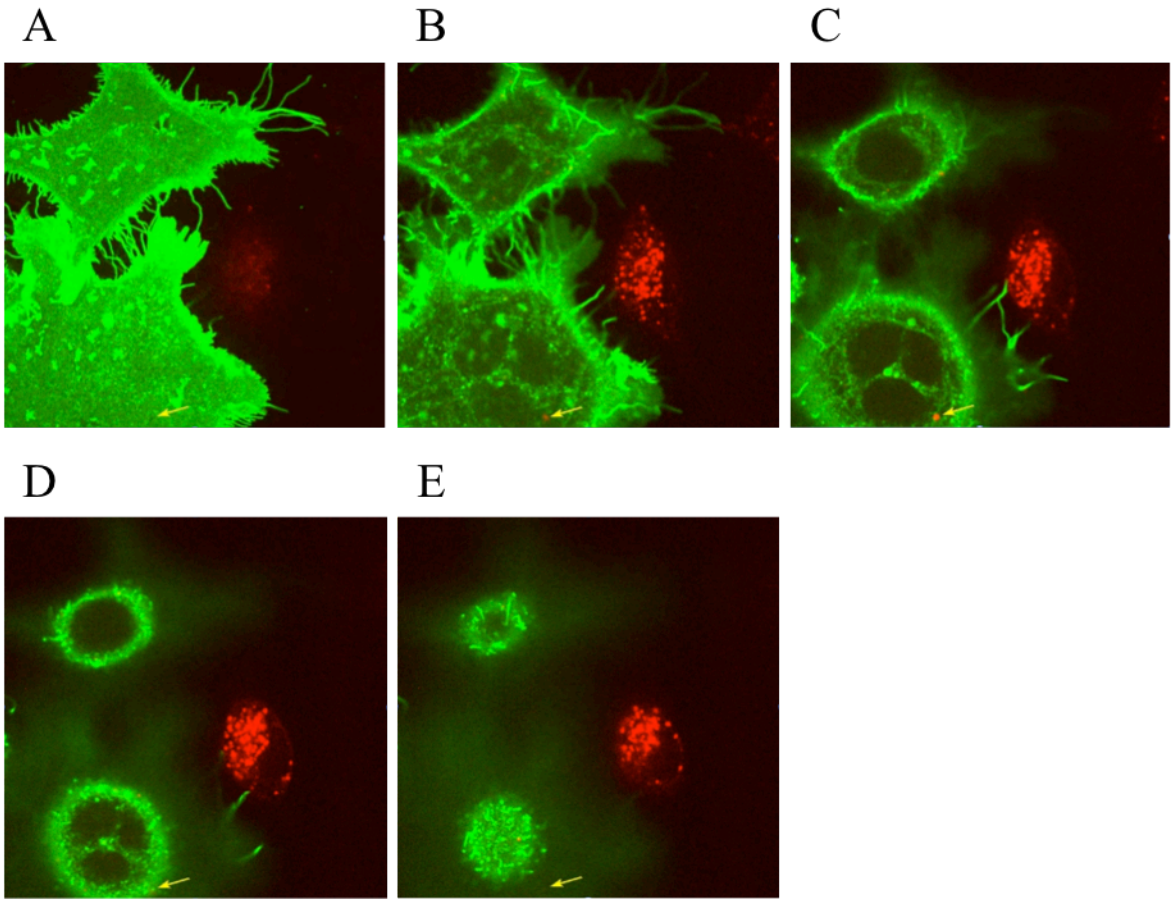

Figure 5.4: Live cell imaging Z-stack of CD9-GFP and CD63-RFP cells shows EVs exchange
Live cell imaging of CD9-GFP A549 cells co-cultured with CD63-RFP A549 cells over time. Z plane was scanned from bottom to top over time. Each image is a still from live cell imaging movie with each still 1 second apart. Placement of arrow held constant in XY plane and indicates CD63-RFP EV inside CD9-GFP cell.

Metabolic labeling of RNA to assess intercellular transfer

We decided to test whether RNA is transferred between cells using metabolic labeling of RNA in a co-culture system. Inspired by Gerald Kolodny's experiments from the 1970's (10), we decided to perform similar experiments using newer methods. One disadvantage of using radioactive uridine is that although the radioactivity can be detected, the radioactive RNA cannot be separated from non-radioactive RNA. The

radioactive RNA also cannot be imaged to assess its location inside of the cell. Thus, we decided to perform metabolic labeling of RNA using the chemically modified analog of uridine, 5-Ethynyl-Uridine (EU). Like normal uridine, EU can be incorporated into mRNA or other long (polymeric) RNA molecules during transcription. Since EU has an alkyne group, it is amenable to a click chemistry reaction using an azide group in the presence of copper. This means that RNA molecules containing EU are tagged in such a way that, using click chemistry, a biotin can be attached (allowing isolation using streptavidin beads). Alternatively, an azide-containing fluorescent dye can also be attached to image the EU-containing RNA in the cell (82).

We decided to use EU to see if RNA is transferred between two cell lines, human K562 leukemia cells and 293T human embryonic kidney cells. First, to label the donor K562 cells, we added EU to the media of K562 cells and cultured the cells in the presence of EU for 24 hour. We then removed the EU-containing media and washed the K562 cells. Next, the K562 cells were co-cultured with 293T cells for 14 hours. All of the cells were then fixed and permeabilized, followed by click coupling of EU to Alexa Flour 594 fluorescent dye (**Figure 5.5**). We also performed a series of controls where we labeled 293T cells with EU as positive control (**Figure 5.6A**) and 293T cells without EU as a negative control (**Figure 5.6B**). As an additional negative control, K562 cells with no EU labeling were also co-cultured with 293T cells (**Figure 5.6C**). All cells were then imaged by fluorescent microscopy. The K562 and 293T cells could be easily distinguished by cell morphology as the K562 cells are round suspension cells and the 293T are elongated adherent cells. After checking that there was no background fluorescence of Alexa Flour 594 in the controls where no EU was added (**Figure 5.6D**),

using the same microscopy settings, we observed distinct foci of labeled EU in acceptor 293T cells (**Figure 5.7**). We were able to observe fields of view where both the acceptor 293T cells and labeled donor K562 cells are visible and also fields of view acceptor 293T cells are in the image with the donor K562 cells out of the frame. These results demonstrate the labeled EU RNA in recipient cells.

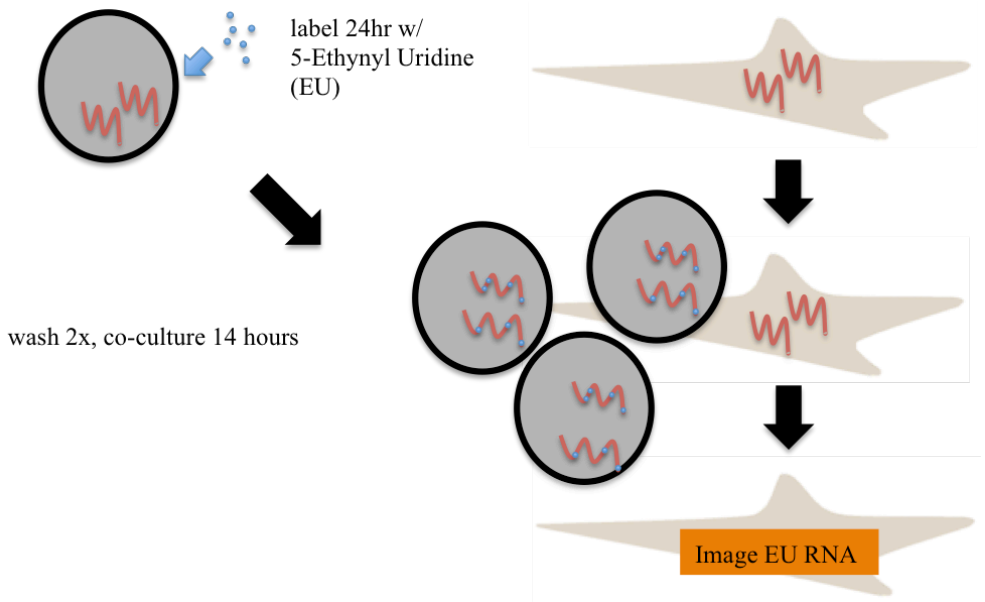

Figure 5.5: Outline of metabolic RNA labeling experiment to evaluate potential RNA transfer between cells
Outline of experimental setup. Round suspension K562 cells are labeled with 5-Ethynyl Uridine (EU), the free EU in media is washed off, and cells are added to unlabeled adherent 293T cells. The cells are then fixed, and a fluorescent dye is attached via Click Chemistry to the RNA. Potential labeled RNA could be detected in the adherent 293T cells.

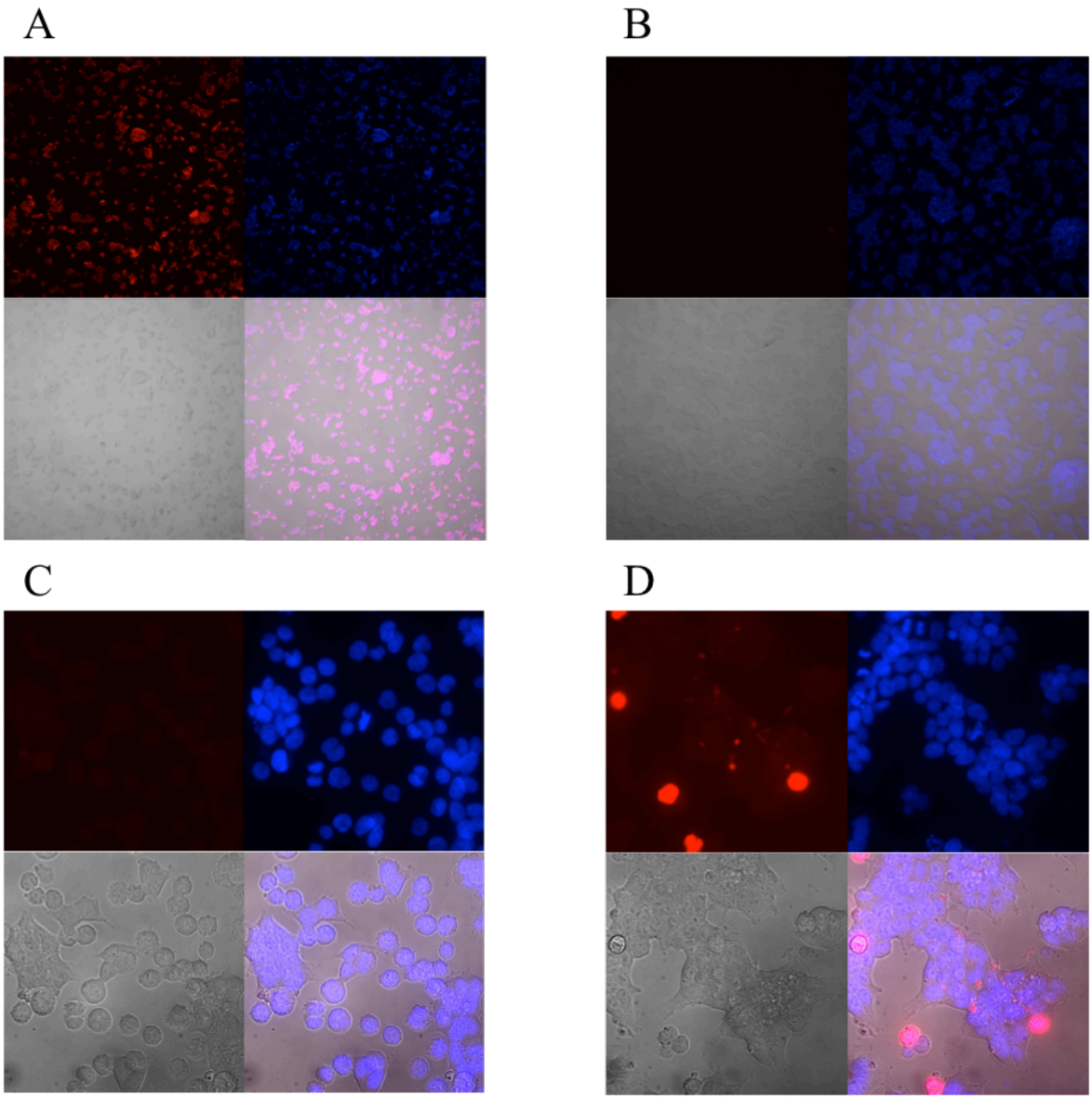

Figure 5.6: Metabolic RNA labeling experiment and controls to evaluate potential RNA transfer
In all experiments, blue is the Hoechst nuclear stain and red is the Alexa Flour 594 EU RNA label. **A**. 293T cells grown in the presence of EU. Top left: AlexaFlour594 label conjugated to EU. Top right: Hoechst DNA stain to label nucleus. Bottom left: Differential interference contrast (DIC). Bottom right: merge of three images, 100x magnification. **B.** 293T cells grown without EU. Top left: AlexaFlour594 label. Top right: Hoechst DNA stain to label nucleus. Bottom left: Differential interference contrast (DIC). Bottom right: merge. 100x magnification. **C.** 293T cells grown in co-culture with K562 cells not labeled with EU. Top left: AlexaFlour594 label. Top right: Hoechst DNA stain to label nucleus. Bottom left: Differential interference contrast (DIC). Bottom right: merge, 640x magnification. **D.** 293T cells grown in co-culture with EU-labeled K562 cells. Top left: AlexaFlour594 labeling. Top right: Hoechst DNA stain to label nucleus. Bottom left: Differential interference contrast (DIC). Bottom right: merge, 640x magnification.

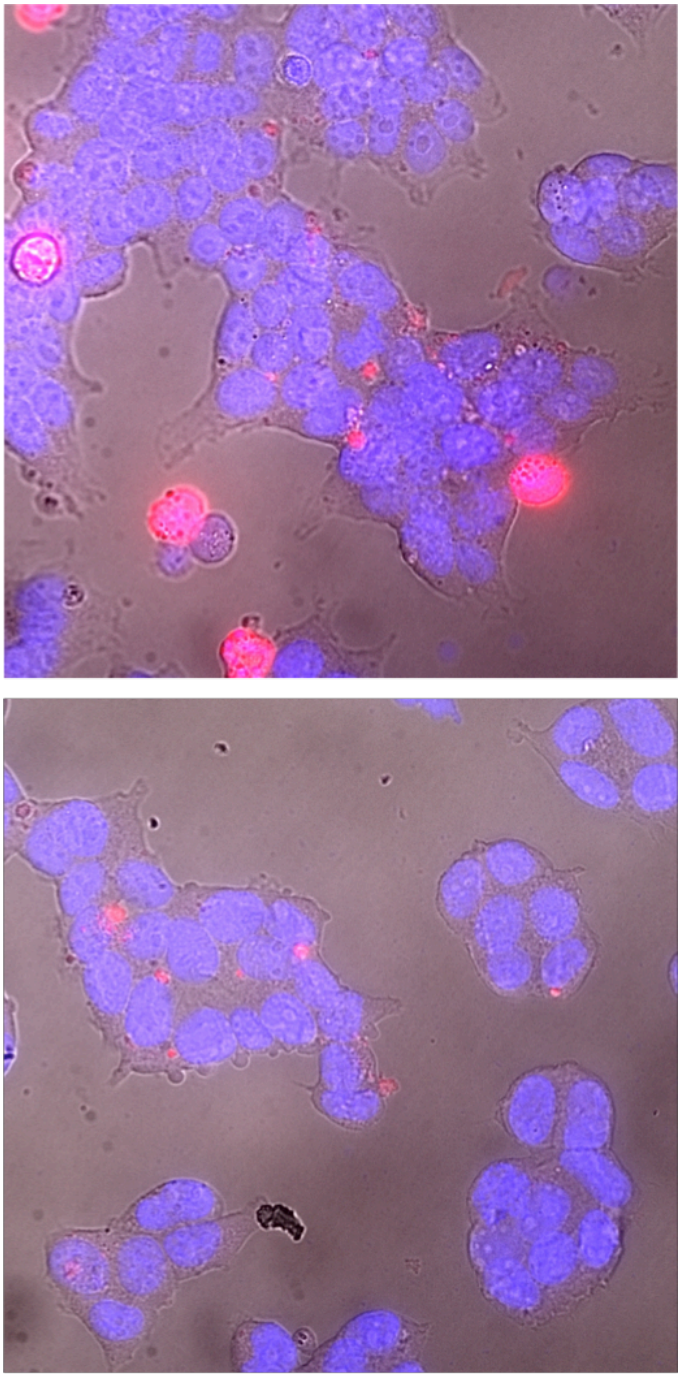

Figure 5.7: Metabolic RNA labeling to evaluate potential RNA transfer shows putative signal
Imaging the 293T cells that are co-cultured with EU-labeled K562 cells. **Top:** Image from Figure 5.6D showing both K562 cells and 293T cells. **Bottom:** Image from different field of same plate showing just 293T cells with some potentially transferred, labeled RNA. Merge of Alexa Flour 594 EU labeling, Hoechst DNA stain to label nucleus, and Differential interference contrast (DIC), 640x magnification.

To test if the effect was dependent on direct cell-cell contact, a transwell plate with 0.45 μm pores was used. Donor K562 cells with EU-labeled RNA were added to the top and unlabeled acceptor 293T cells were added to the bottom. As with the direct co-culture experiment, 293T cells were fixed and permeabilized after 14 hours of being cultured in the transwell plate together (but separated by the filter) with the labeled K562 cells. Click coupling was then performed to Alexa Flour 594 fluorescent dye and imaging was performed on the 293T cells. In the transwell system, no fluorescence was observed.

Human mouse cell co-culture

Due to the potential artifacts related to the metabolic labeling experiments, we came up with an alternative experimental approach to study transfer of RNA between cells. Since the human genome has a significant number of differences from that of the mouse, we decided this could be used to detect RNA transfer between human and mouse cells co-cultured *in vitro*. We reasoned that since some of the sequence differences between human and mouse are in coding regions, by sequencing the RNA of human cells after co-culture with mouse cells, we could detect if mouse RNAs have been transferred to human cells.

For this experiment, we needed to be able to separate the recipient cells from the donor cells. Thus, we infected K562 cells (human leukemia cell line) with a lentiviral construct encoding a nuclear GFP. We then sorted these cells using flow cytometry to have a pure population of GFP-positive cells. We co-cultured these cells with mouse RAW cells (a macrophage cell line) for 24 hours at 1:1 ratio. After 24 hours of co-

culture, we sorted the human K562 cells by flow cytometry away from the mouse cells (using GFP). We chose to use the mouse macrophage cell line as donor (as we didn't want a highly phagocytic cell type to be the acceptor cell). We then performed RNA-Seq on the population of human cells and aligned the sequencing reads to both human and mouse annotations so that we could differentiate between the two to detect mouse transcripts in human cells (**Figure 5.8A**).

We also included two controls conditions. As one control, we had just human cells that went through the same procedure as the human mouse co-culture to see if any reads from just the human cells mistakenly get aligned to the mouse annotations. As another control, we mixed human and mouse cells and immediately sorted them (not giving them an opportunity to interact in co-culture). We reasoned that this would act as a control for imperfect sorting (where a GFP-negative mouse cell could accidentally be sorted with the GFP-positive human cells) (**Figure 5.8B**).

We first examined the percentage of mouse genes detected in human cells in each condition. For this, we decided on an expression of 2 or greater using Trimmed Mean of M Values (TMM). Our K562 human only condition was meant to act as a negative control, and we expected our Mix 1 and 2 conditions (where cells were co-cultured for 24 hours) to be higher than Mix 0 (where cells were mixed and immediately sorted). This was not what we saw, as the Mix 0 condition had a slightly higher expression of mouse genes detected than the other conditions (**Figure 5.9A**).

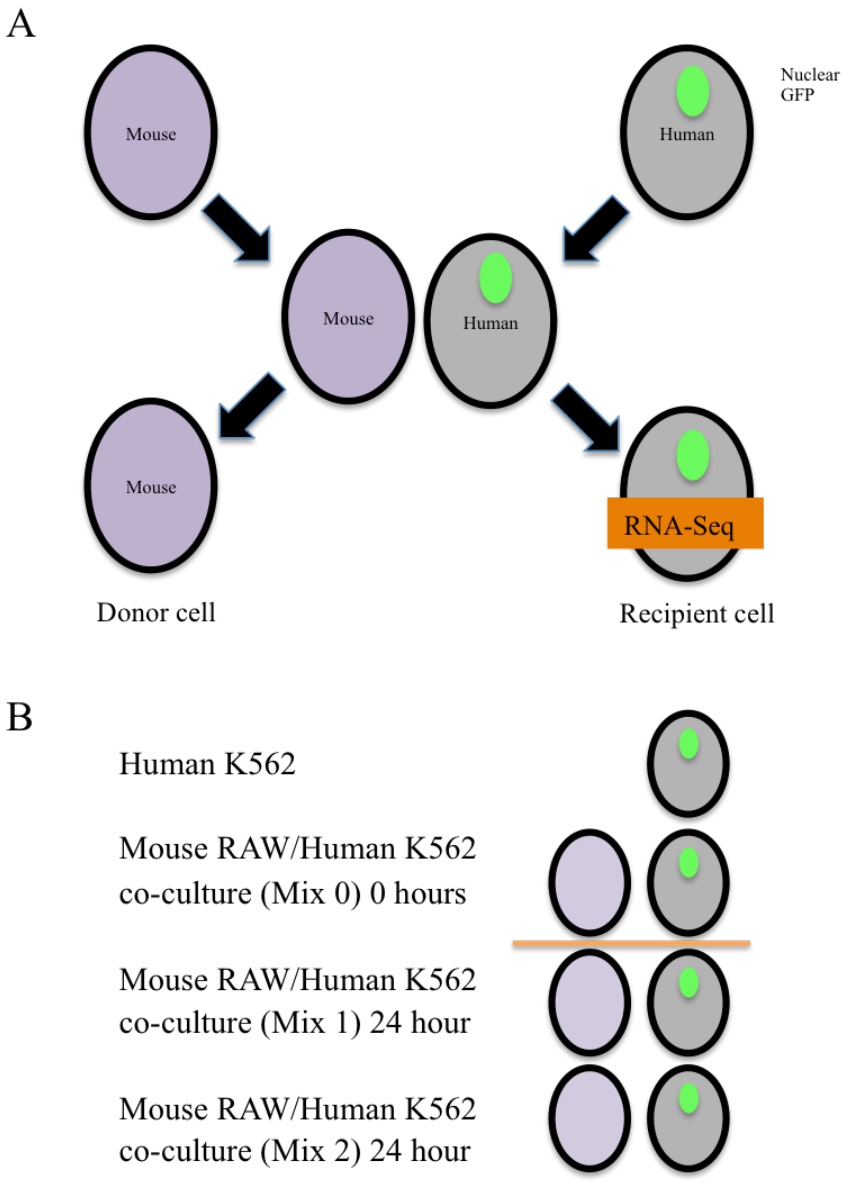

Figure 5.8: Outline of human-mouse co-culture experiment to evaluate potential RNA transfer between cells

Experimental setup: **A.** schematic of general procedure - human K562 cells expressing nuclear GFP and mouse RAW macrophage cells are co-cultured and then human K562 cells are separated from mouse RAW cells by flow cytometry and RNA-Seq is performed. **B.** Different experimental conditions – as controls, human K562 cells go through process by themselves, and human and mouse cell are mixed, immediately put on ice, and human cells are sorted

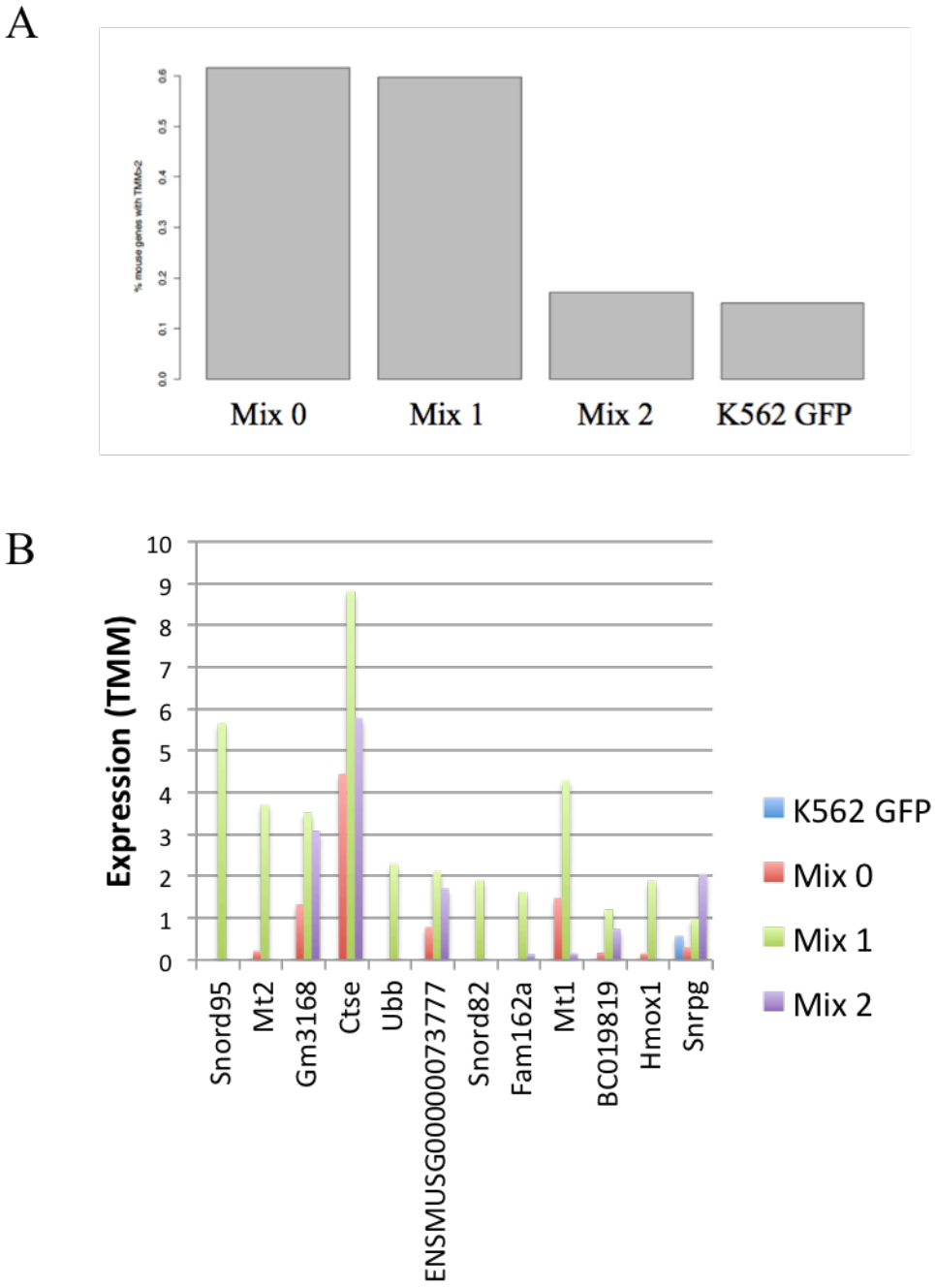

Figure 5.9: Human-mouse co-culture evaluates potential RNA transfer between cells
RNA-Seq results of human sorted K562 cells shown. **A**. Percentage of mouse genes with TMM of 2 or greater detected in human cells in the following conditions: K562 GFP (human only) cells, Mix 0 (mouse and human cells mixed for 0 hours), Mix 1 (replicate 1 of mouse and human cells mixed for 24 hours), and Mix 2 (replicate 2 of mouse and human cells mixed for 24 hours) **B**. Expression of top mouse transcripts expressed in human cells in: K562 GFP (human only) cells, Mix 0 (mouse and human cells mixed for 0 hours), Mix 1 (replicate 1 of mouse and human cells mixed for 24 hours), and Mix 2 (replicate 2 of mouse and human cells mixed for 24 hours)

Despite a lack of overall difference, we looked at the expression of specific mouse transcripts in each of the conditions for the mouse transcripts that were most highly detected in the human cells. We saw a few transcripts that were more highly expressed in Mix 1 and Mix 2 (where cells were co-cultured for 24 hours) than Mix 0 (where cells were mixed and immediately sorted) and did not show up in the human only control condition (**Figure 5.9B**). Interestingly, of the top 12 such transcripts, 3 are virally derived (likely from endogenous retroviruses in the mouse). Gm3168 encoded a Gag protein, Ctse encodes an envelope glycoprotein and ENSMUSG00000073777 encoded an envelope polyprotein.

Discussion

It is currently unclear whether EVs are transferred between cells, and if so, whether they transfer functional cargo to recipient cells. This is the main question in the EV field but has been difficult to answer, largely due to a lack of techniques to track EVs and their RNA cargo. We have developed two new techniques to study the transfer of RNA between cells and also investigated the transfer of EVs using live cell imaging. In one technique, we used metabolic labeling using EU to "mark" the RNA of a donor cell and then detect the marked RNA in recipient cells. In another technique, we co-cultured mouse and human cells and then looked for mouse transcripts in human cells by RNA-Seq. We also fused membrane proteins found on EVs with fluorescent proteins to visualize EV transfer between live cells.

Although we used cell lines for our experiments, the techniques we developed should be broadly applicable to studying RNA or EV transfer between any set of donor and acceptor cells. These techniques may also be extended to study RNA transfer *in vivo*. For example, one could imagine studying potential RNA transfer between xenograft human tumor cells in a mouse and mouse cells by looking at human RNAs in mouse cells. This could further be combined with a Cre-Lox reporter system to help determine which cells to look at for potential RNA transfer (if the human tumor cells have Cre and a LoxP reporter mouse is used).

In the EV live cell imaging experiments, we were clearly able to see EVs in the extracellular space as well as the uptake of EVs from one cell to another. It is important to note that most of the EVs we observed in the live cell imaging were larger than the isolated EVs we characterized previously. In our EV isolation experiments, we used a 0.22 μm filter, so we only analyzed EVs smaller than ~220 nm in diameter. For almost all of EVs we observed, we could not conclude that they came from live (as opposed to dead cells) since we started observing them after they had been released from donor cells. Despite these caveats, our experiments conclusively showed that cells in culture take up EVs. By using spinning-disk confocal microscopy, we were also able to conclude that the EVs that were taken up were truly inside recipient cells and not just stuck to the outside.

In our experiments, we were not, however able to determine where in recipient cells our EVs localized to. A crucial question is whether EVs end up in lysosomes after uptake by recipient cells. Once in a lysosome, it is unlikely that an EV is functional since we expect the EV and its cargo would be degraded. Thus, it is important to determine whether EVs get taken up by endocytosis, and, if so, whether EVs fuse with the

endosomal membrane. This would presumably be necessary for functional RNA cargo delivery since it would RNAs need to access the cytoplasm to carry out their functions.

Future experiments will use the labeling of various endocytic and lysosomal markers in recipient cells. This will allow us to analyze what compartments in the recipient cell EVs co-localize with. Additionally, it would be informative to tag RNA or protein cargo in the EVs in addition to a membrane protein. Then, it would be possible to track the co-localization (or lack thereof) of a transmembrane protein labeled with a fluorescent protein of one color with a cargo molecule labeled with another color to detect endosomal escape. Upon fusion of the EV membrane with the endosomal membrane of the recipient cell, I would expect the membrane protein fluorescence to disappear. At that point, it may be possible to still see a burst of the cargo protein fluorescence without membrane protein fluorescence before the cargo protein diffuses in the cytoplasm. New advances in microscopy, such as the development of light-sheet microscopy (83), will also allow improved interrogation of EV release and uptake in live cells.

In the metabolic labeling experiments, we were able to visualize RNA transfer between our K562 donor cells and HEK293 acceptor cells. However, we did not establish that the punctae of fluorescence we saw (EU-RNA conjugated to fluorescent dye) were in the cytosol of the recipient cells (as opposed to in lysosomes or stuck to the outside of the cell). Since RNA acts in the cytosol (or nucleus for some non-coding RNAs), RNA that is not in the cytosol does not have a chance to be functional. Future experiments could use confocal microscopy to ascertain that the RNA is inside the cell rather than stuck to the outside. Additionally, co-staining the recipient cells with other markers (such as

endocytic or lysosomal markers) could help determine whether the RNA is in the cytosol as opposed to the endosome or lysosome. It would also be interesting to attach biotin to EU-labeled RNA, and then use streptavidin to isolate it. This RNA could then be sequenced to see which particular transcripts get transferred.

In the human-mouse co-culture experiments, we were able to detect a very small number of mouse transcripts in human cells. The fact that several of the transferred transcripts were from virally derived genes indicates the utility of the experimental system, as we would expect these to be transferred if viral particles are being produced in the donor cells. Although there may be barriers to the transfer of RNA through EVs or other mechanisms between mouse and human cells (as opposed to cells of the same species), the advantage of this system is that no labeling is required.

Although in our experiments we were not able to confidently detect RNA transfer between cells, these experimental systems should pave the way for future investigation of RNA transfer. In the metabolic labeling experiments, we saw some contact-dependent RNA transfer but were not able to conclude that the RNA was in the cytosol of the recipient cells. We also cannot absolutely rule out that the EU nucleotide is transferred in monomeric form between donor and acceptor cells (for example, though gap junctions). In the human-mouse co-culture experiment, we saw only a few mouse transcripts transferred to human cells, and at very low levels. Nonetheless, both of these approaches warrant further investigation. In particular, the use of various primary cells that are known to interact (such as T cells and dendritic cells or neurons and glia) may result in more robust RNA transfer.

Chapter VI

Conclusion

In this thesis, I explore several aspects of EV biology pertaining to the RNA in EVs and whether EVs transfer RNA between mammalian cells. I also describe the development of several new methods to characterize EVs and their RNA content. We performed RNA-Seq to characterize the RNA contents of EVs and compare the RNA profiles of EVs to the profiles of donor cells. We found a strong correlation between the mRNA profile of cells and EVs. We also developed a new method using enzymatic treatments to differentiate the extracellular RNAs that are truly inside EVs from those outside of EVs. We further visualized single EVs with fluorescent dyes using TIRF imaging. Additionally, we developed an immuno-isolation protocol to capture EV subsets with specific protein markers.

Our work has significant applications towards the development of new molecular diagnostics. We have developed a simple computational framework for determining how to select protein markers for cell-type specific EV isolation. We then used this framework for the isolation of neuron-specific EV as a proof of principle. Working towards this goal, we established human iPS–derived neurons as a powerful *in vitro* system to study human neuronal EVs and develop methods for their isolation from biological fluids. We used this system to comprehensively characterize the full repertoire of membrane proteins in neuron EVs by mass spectrometry. We then applied our immuno-isolation protocol to isolate EVs using the neuron-specific markers we identified.

In the future, our work on isolating cell-type specific EVs could be extended to different cell types beyond neurons. One could imagine, one day, taking a sample of blood and isolating EVs from several different cell types. RNA-Seq could then be performed on each of those cell-type specific EVs. The resulting RNA-Seq profiles could

be used to assess the health of an individual at the molecular level. Additionally, one could analyze the protein contents of EVs in addition to the RNAs. This would be particularly useful for neurodegenerative diseases like Parkinson's or Alzheimer's, where a number of proteins isoforms and post-translational modifications are implicated in the disease process (84). A technical challenge that will have to be overcome is the low amount of material in any given subset of EVs, but new ultrasensitive methods for measuring RNAs and proteins, such as low input RNA-Seq (used for single cell RNA-Seq) (78) and Single Molecule Array (Simoa) "digital ELISA" technology (85), respectively, may help overcome this challenge.

One of my main interests upon the beginning of my thesis was studying whether EVs transfer RNA between cells as a mechanism of intercellular communication. Towards this end, I developed several experimental systems to study this question. First, we were able to set up a system for looking at EV transfer between cells using live cell imaging. Additionally, I came up with two new experimental frameworks for studying RNA transfer between cells. In one, I used metabolic labeling with a modified uridine to label RNA in donor cells and evaluate the presence of labeled RNA in unlabeled acceptor cells. In another set of experiments, I co-cultured mouse and human cells and looked for RNAs of one species in cells of the other species using RNA-Seq.

The results of my intercellular EV and RNA transfer experiments were not as conclusive as I would have liked. For the EV transfer live cell imaging experiments, I was clearly able to see EV transfer and EVs from one cell inside another cell. This was encouraging. However, I was not able to conclude that EVs transfer their cargo in recipient cells. It could be that the EVs that I observed were in endosomes (on their way

to lysosomes) or in lysosomes. It is likely that if EVs end up in lysosomes, their contents would be degraded, preventing RNA from reaching the cytoplasm (which would be necessary for the RNA to be functional) (86). Future experiments expanding on this work involve donor cells tagged with EV markers and recipient cells tagged with proteins marking different endosomal and lysosomal compartments. Additionally, one could label the cargo EVs in addition to the membrane to try to visualize endosomal escape.

The metabolic labeling experiments showed that RNA was transferred in my co-culture system. However, I could not conclude that the RNA was truly inside the recipient cells and not stuck to the outside. As with the live cell imaging experiment, I was also unable to rule out the possibility that if the labeled RNA is inside recipient cells, it may be in endosomes or lysosomes. Immunofluorescence experiments with markers of endosomes or lysosomes could help clarify this. Additionally, I also could not rule out a potential artifact of the experiment: it is possible that individual (monomeric) modified nucleotides (which were never incorporated into RNA molecules or after degradation of polymeric RNA molecules) are passed between donor and recipient cells. Gerald Kolodny, in his pioneering 1971 study of RNA transfer, thought about this potential artifact and used a drug that blocks transcription, Actinomycin D. After adding this drug to recipient cells, he was still able to see the labeled RNA signal (10). This is a good control, although blocking transcription will likely have many different effects in the cell.

An alternative experimental system that gets around the potential artifact of nucleotide transfer is the co-culture of human and mouse cells. An advantage of this system is that labeling RNA is not required, although a potential disadvantage is that human and mouse cells may have some interspecies barriers to interacting. I detected a

potential signal between the cells in my system, but the signal was low. It was reassuring to see that some of the top RNAs transferred were of viral origin, as there is evidence that some endogenous retroviruses form particles and bud from cells (87). In some instances, endogenous retroviruses have also been found to enter other cells (88, 89).

For both the metabolic labeling and mouse-human co-culture experiments, future studies will need to assess RNA transfer at different times, as we do not know at what conditions and timescales RNA transfer occurs (if it occurs at all). Furthermore, different types of donor and acceptor cells should be tried (with an emphasis on cell types that we know interact). As the question involves intercellular communication in mammals, some of these experiments will ultimately need to be done *in vivo* in mice. Although some variables will be harder to control, the experimental systems I've described should be amenable to transfer to an *in vivo* system. It would be useful to implant human tumors or human hematopoietic cells into mice and then performing RNA-Seq on various mouse cells. To help determine which cells to analyze, a Cre-Lox system could be used, where the human cells also express Cre and the mouse could be transgenic with a reporter that is expressed upon LoxP recombination.

Although it is perhaps naïve to have assumed that a single graduate student's thesis would come anywhere close to answering a question as broad as "what do EVs actually do," my work in the field allows me to speculate in a way that is at least slightly more informed than when I started. The pervading view of EV function in the field is that EVs transfer RNA and proteins between cells as part of a highly coordinated mechanism of intercellular communication (28, 90). Outside of the field, this notion is viewed with

skepticism (28, 91), and rightfully so. Extraordinary claims (such as a new form of intercellular communication) require extraordinary evidence.

I would consider my findings that the RNAs in EVs are generally not selectively packaged, with several caveats, an argument against the hypothesis of intercellular RNA communication through EVs. After all, why would a cell send another cell a sampling of its transcriptome? One would expect that in a coordinated system of intercellular communication, EVs would package specific RNAs. The caveats, however, are plentiful: EVs from more cell types need to be investigated, it is possible that a subset of EVs (for example, containing a fusogenic protein) is the important one that is functional, and the situation could be different *in vivo*. Nonetheless, at the conclusion of my thesis work, I am not certainly able to offer the world any evidence for functional RNA transfer between cells.

There are several other hypotheses of why EVs could be released by cells that are worth considering besides transferring RNA. These may be foundations for future theses. One such hypothesis is the "garbage bag" hypothesis that cells release unwanted proteins or other cellular components (lipids, RNAs, etc.). This hypothesis is that came to some of the early researchers in the field (92, 93). One theoretical argument against this hypothesis is that cells have a plethora of mechanisms to degrade various molecules and reuse the components. For example, the cell has all kinds of mechanisms for tagging proteins for degradation in the proteasome (94). Similarly, there are numerous, specific pathways for RNA degradation (95). Furthermore, when cells degrade proteins or RNAs, the monomeric subunits (amino acids or nucleotides) can be reused for transcription or translation. Nonetheless, perhaps there may be cases where it is easier for the cell to

throw away misfolded and aggregated proteins rather than try to degrade them (96). It is also possible that cells release damaged membrane in the form of EVs (97, 98).

Another reason for the existence of EVs could be that they are released from cells for a specific reason but do not transfer their luminal cargo. For example, perhaps EVs act through membrane protein on their surface to induce some response in a target cell through some receptor (48). This could particularly be the cause in the context of immunology for EVs that carry MHC, for example (99). In this case, the RNA cargo of EVs may not matter.

Another interesting possibility is that EVs are endogenous retroviruses, or are related to them. EVs have many features in common with viruses, and it is extremely challenging to separate EVs from viruses. As mammalian cells have a large portion of DNA that is of viral origin, some of this DNA encodes large open reading frames expresses functional proteins. There is significant evidence that some of the proteins form viral particles and bud from cells (87). Although there is considerable confusion regarding endogenous retrovirus annotations (100, 101), future work will investigate whether RNAs and proteins found in isolated EVs is enriched for components of endogenous retroviruses.

It is also important to note that "contaminating" exogenous retroviruses could contribute to EVs. It is unclear what proportion of cells in given organism, or in cell culture, are infected with viruses at any given point in time. Humans (in even a healthy state) have a "virome" that consists of many different viruses (102). This question could be investigated by aligning RNA-Seq data from EVs isolated from cell culture or human biological fluids to viral sequence reference databases.

The EV-virus connection has been made before. It has been speculated that the two are evolutionarily linked: either EVs have co-opted viral budding mechanisms or vice versa at some point in evolution (103, 104). Upon closer inspection, this question is even more complicated as viruses and EVs are hard to distinguish even conceptually. If we define a virus as a particle that contains each of the protein and RNA components that the viral genome encodes, any given cell that releases viral particles will also release incomplete viral particles (which have some, but not, all of the viral components) (105). For example, it has been shown that after expressing a single viral protein such as HIV Gag in an uninfected cell, the viral protein will be released in EVs (106). Thus, the distinction between EVs and viruses within an infected cell is not one that is clear. And this distinction becomes even less clear if we consider expression of endogenous retroviruses. Further development of techniques to image single EVs and their components will hopefully shed light on these questions.

Perhaps less exciting, it is also possible that some EVs are an artifact of isolation procedures (and are not naturally produced by cells). For example, I include a filtration step through a 0.22 μm filter in my EV isolation procedure but not all protocols include this step. My rationale for using a filter is that this gives a reproducible cutoff to the size of EVs, a parameter that I can control between experiments. Additionally, as the amount of RNA we are analyzing from a preparation of EVs is very low, if even one cell were to get into my preparation (escaping pelleting during the previous centrifugations), this could significantly skew my results. Thus using a filter should prevent against that as well. However, using a filter also raises the possibility that larger EVs (or even cells or parts of cells) could break during the filtration process itself, and therefore artificially

produce EVs of a smaller size (107). The fact that EVs with similar characteristics can be isolated using different isolation techniques provides some confidence that EVs are not just an artifact of the isolation procedure, but this remains an important consideration when choosing a particular isolation technique, and the lack of standardization of EV techniques continues to be a problem for reproducibility (49).

In our live cell imaging experiments, we were able to see EVs without performing any isolation procedure. Although most of the EVs we observed in those experiments were larger than the ones we isolated with a 0.22 μm filter, this was nonetheless proof that cells release EVs. One thing we were not able to distinguish, however, is what proportion of EVs is produced by dead cells (as opposed by to live cells). When a cell dies by apoptosis, the remains of the cell are released as vesicles called apoptotic bodies. These are generally thought to be larger than the EVs we analyze, but it is likely that apoptotic bodies can also be small and therefore overlap in size with the EVs that we presume are released by live cells (15).

There is, of course, significant evidence that live cells release EVs. When observing EV release by electron microscopy, budding at the plasma membrane or fusion of the MVB with the membrane can be seen without the large scale membrane blebbing found in apoptotic cells (18, 21). Additionally, observations of EV release with fluorescent reporters have been reported using live cell imaging (23). Nonetheless, it is disconcerting that when EVs are isolated from cell culture or a biological fluid, we have no way of knowing what proportion is coming from dying vs. live cells. It is conceivable that perhaps even the majority of EVs in a given preparation are actually from dead cells. Recent studies have reported that when a cell undergoes apoptosis, there is widespread

decay of mRNA (108). As part of the decay process involves non-templated uridylation at the 3' end of the mRNA (109), we could look whether we see enrichment of this uridylation in RNA isolated from EVs and compare that to what we see in the donor cells. If a strong enrichment of uridylation in EVs relative to cells (which in culture are always a mix of live and dead cells) is detected, this would suggest most of the EV RNAs come from dead cells.

Additionally, one could investigate the question of whether EVs come from mostly live or dead cells by sorting single cells into wells. Then, cell viability could be followed by microscopy and only media from cells that are alive could be analyzed for EV membrane proteins or RNAs by ultrasensitive methods such as Simoa (85) or digital droplet PCR (ddPCR) (110), respectively. Although this would be technically nontrivial, this would be a way of studying EVs only from live cells (since in a large cell culture dish there is always a significant number of dying cells).

As I've outline above, the field of EV research is clearly still in its infancy as there are many very basic questions completely unanswered. Despite evidence that all cell types release EVs, we still don't know what EVs actually do. Do they transfer functional RNA and protein contents between cells as a form of intercellular communication? And, if so, which cells send EVs to which cells? What are the molecular mechanisms involved in EV biogenesis? Are there specific proteins whose main role is EV secretion? How does RNA or protein cargo get selected for packaging into EVs? Many of these questions unanswered because we don't yet have the necessary tools. For example, we don't have a good tool for counting EVs (27) and being able to differentiate them from similarly sized complexes of aggregated proteins (11). In this thesis, I have

addressed fundamental questions relating to the RNA in EVs and developed several new methods for studying EVs. Collectively, I hope the work in this thesis represents a significant contribution to the experimentally challenging and confusing world of EV biology, and will be built upon by others to both understand the functional roles of EVs and, in parallel, accelerate their medical applications.

Chapter VI

Appendix

Appendix S1: Materials and Methods

Cell Culture

K562 cells (from ATCC) were grown in Gibco IMDM with Glutamax (Thermo Fisher Scientific) supplemented with Gibco Heat-Inactivated Fetal Bovine Serum (Thermo Fisher Scientific) and Gibco Penicillin Streptomycin (Thermo Fisher Scientific). For EV isolations, cells were switched to Gibco Aim V Serum-Free Medium (Thermo Fisher Scientific). A549, 293T, or RAW264.7 cells (all from ATCC) were grown in Gibco DMEM with Glutamax (Thermo Fisher Scientific) supplemented with Gibco Heat-Inactivated Fetal Bovine Serum (Thermo Fisher Scientific) and Gibco Penicillin Streptomycin (Thermo Fisher Scientific). For EV isolations, cells were switched to EV-depleted media (obtained by ultracentrifugation of media for 16 hours at 120,000xg and subsequent filtration through Corning 0.22 μm filter). Previously described iNGN cells were grown in mTeSR1 media (STEMCELL Technologies) on Matrigel (Corning) coated plates. Doxycycline (Sigma Aldrich) was diluted in PBS and added to MTeSR1 at a final concentration of 0.5 μg/mL to initiate differentiation. On Day 4 after Dox addition, media was switched to Gibco DMEM with Glutamax (Thermo Fisher Scientific) supplemented with B27 Serum-Free Supplement (Thermo Fisher Scientific) and Gibco Penicillin Streptomycin (Thermo Fisher Scientific).

EV Isolation

EV isolation from cell culture is described in great detail (46) and also reproduced in this thesis as Appendix S2. For CSF EV isolation, several samples of human CSF (BioIVT)

totaling 3 mL were pooled. Samples were centrifuged at 2000xg for 10 minutes to remove any potential residual cells. The pellet was left behind and the resulting supernatant was then applied to Corning CoStar X 0.44 μm filter and centrifuged again at 2000xg for 10 minutes. The filtered sample was then ultracentrifuged for 2 hours at 120,000xg.

Western Blotting

EV western blotting is described in great detail (46) and also reproduced in this thesis as Appendix S2. We used the iBlot Dry Blotting System (Thermo Fisher Scientific) for transfer. The following primary antibodies were used for western blot at the corresponding dilutions: M38 for CD81 (Thermo Fisher Scientific) at 1:666, h5c6 for CD63 (BD) at 1:1000, EPR18998 for L1CAM (Abcam) at 1:500, ab47441 for GJA1 at 1:500. For western blots of pulldown experiments, TrueBlot anti-mouse HRP or anti-rabbit HRP (Rockland) was used as a secondary at a concentration of 1:1000 in milk buffer.

EV Imaging by TIRF

EV imaging protocol is described in great detail (111) and also reproduced in this thesis as Appendix S3. For experiments with RNA labeling, Bodipy TR Ceramide or DiD and SYTO RNASelect or TOTO-1 were used to label EVs at the same time. All dyes are from Thermo Fisher Scientific. Samples were imaged on TIRF/LSM710 Confocal Microscope (Zeiss).

Metabolic RNA Labeling and Imaging

Cells were labeled using Click-iT RNA Alexa Flour 594 Imaging kit (Thermo Fisher Scientific). Metabolic RNA labeling was performed by adding EU to cell culture media to a final concentration of 2 mM. Cells were incubated for 24 hours with EU and then media containing EU was removed. Cells were washed twice with PBS, and then put in fresh media. After click labeling, cells were fixed and permeabilized using Click-iT Fixation/Permeabilization kit (Thermo Fisher Scientific). Cells were imaged on DMI6000B microscope (Leica).

Dynamic Light Scattering

Dynamic Light Scattering was performed by diluting EV samples 1:20 and loaded in a microcuvette (Malvern) into a Zetasizer Nano ZS (Malvern).

Transmission Electron Microscopy (TEM)

Procedure for visualizing EVs by TEM was based on previously described protocol (45). EV samples (undiluted) were stained with 2% uranyl formate on 400 mesh formar coated grid stabilized with evaporated carbon film. Grid was imaged on a JEM-1400 Series 120 kV transmission electron microscope (JEOL USA).

DNA/RNA Electrophoretic Size Analysis

RNA samples were analyzed using chips and reagents from RNA Pico 6000 kit (Agilent) and run on the Bioanalyzer (Agilent). DNA size was analyzed by agarose gel electrophoresis, either by 1.5% Agarose gel run in TAE buffer or by a 2% E-Gel EX

Agarose Gel (Thermo Fisher Scientific). 1.5% Agarose gel was stained with SYBR Gold Nucleic Acid Gel Stain (Thermo Fisher Scientific). Imaging of gel was performed on Gel Doc EZ Imager (Bio-Rad) or Typhoon FLA 9000 Gel Scanner (GE Healthcare).

DNA/RNA Extraction

DNA from cells or EVs was isolated using QIAamp DNA Mini kit (Qiagen). RNA from cells or EVs was extracted using miRvana miRNA Isolation kit, with phenol (Thermo Fisher Scientific). After extraction, RNA was treated with Turbo DNase Thermo Fisher Scientific together with Superase In RNase Inhibitor Thermo Fisher Scientific. RNA was then put through RNA Clean and Concentrator-5 kit (Zymo Research) before either qRT-PCR or RNA-Seq library construction.

RNA-Seq Library Preparation and Sequencing

For human/mouse co-culture experiments and K562 untreated EVs, RNA-Seq libraries using adapter ligation were performed as previously described (112). For proteinase-RNase experiments and CSF EV RNA-Seq, libraries were constructed using the SmartSeq2 method (78). All libraries were sequenced (paired end) using Illumina HiSeq2000, NextSeq500, or MiSeq.

RNA-Seq Analysis

Reads were aligned to the hg19 UCSC Known Genes annotations using RSEM v1.2.1 (113) to calculate TPM values. For calculating TMM normalization, edgeR was used

(114). For human mouse mixing experiment, UCSC human and mouse genome annotations were combined and RSEM was used to align to the joint annotation.

Enzymatic Treatments

After ultracentrifugation for EV isolation was finished, supernatant was removed and 150μL PBS was added to ultracentrifuge tube. Then 5 μL Proteinase K (New England BioLabs) was added to tube and incubated at 37C for 30 minutes with parafilm covering the top of the tube. PMSF (Sigma Aldrich) was then added to a final concentration of 1 mM and tubes were incubated at room temperature for 10 minutes. Then 0.5 μL of RNase A/T1 was added to each tube and tube was incubated at 37C for 30 minutes (again with parafilm covering the top of tube).

qRT-PCR

RNA was reverse transcribed using the SuperScript VILO cDNA Synthesis kit (Thermo Fisher Scientific). cDNA was then quantified by addition of qPCR Master Mix, 2x (KAPA Biosystems) together with primers and analysis on CFX96 Touch Real-Time PCR Detection System (Bio-Rad).

Live Cell Imaging

Cell media was switched to DMEM with no phenol red (Thermo Fisher Scientific) to reduce autofluorescence from media. Spinning-disk confocal fluorescence microscopy was done as previously described (115) using a Marianna system controlling an Axiovert 200M Fluorescence/Live Cell Imaging Microscope (Zeiss) with a Plan Apochromat 63x

objective (NA 1.4, Zeiss) and a CSU-XI spinning disk confocal head (Yokogawa Electric).

Mass Spectrometry

Mass Spectrometry was performed at the Broad Institute Proteomics Platform. EVs were lysed in RIPA buffer (Thermo Fisher Scientific). Samples were then run on an SDS gel and band corresponding in size to Albumin was cut out and discarded. Remaining samples was prepared for TNT labeling and run on Mass Spectrometer.

EV Immuno-isolation

Isolation Buffer was prepared by adding BSA to 7.4 pH PBS to final concentration of 1mg/mL and filtered through a 0.22 μm Steriflip Filter (Millipore). 500uL (2x10^8) Dynabeads Goat Anti-Mouse IgG beads (Thermo Fisher Scientific) was put into 2mL eppendorf tube and put on magnetic rack. Supernatant was removed and replaced with 250uL of Isolation Buffer off of the magnet. 10 μg primary antibody was coupled to beads overnight. The following antibodies were used for immuno-isolation: 5G3 (BD) for L1CAM, 1C51 for mCherry (Abcam), 9F9.F9 for GFP (Abcam), 1.3.3.22 (Thermo Fisher Scientific) for CD81, and h5c6 (BD) for CD63. On the next day, beads were washed twice with 1 mL of Isolation Buffer each time. EVs were then added (usually one pellet was in 150 μL) and Isolation Buffer was added to bring the volume to 0.5 mL. Immuno-isolation was performed on rotating rack either at 4C for 24 hours for L1CAM or for 1 hour at 37C for CD81 or CD63.

Appendix S2: Extracellular Vesicle Isolation and Analysis by Western Blotting

Chapter 12

Extracellular Vesicle Isolation and Analysis by Western Blotting

Emma J. K. Kowal, Dmitry Ter-Ovanesyan, Aviv Regev, and George M. Church

Abstract

Extracellular vesicles (EVs) are released by mammalian cells and are thought to be important mediators of intercellular communication. There are many methods for isolating EVs from cell culture media, but the most popular methods involve purification based on ultracentrifugation. Here, we provide a detailed protocol for isolating EVs by differential ultracentrifugation and analyzing EV proteins (such as the tetraspanins CD9, CD63 and CD81) by western blotting.

Key words Exosomes, Extracellular vesicles, Exosome isolation, Extracellular vesicle isolation, Ultracentrifugation, Immunoblotting, Western blot, Tetraspanins, CD63, CD81, CD9

1 Introduction

Extracellular vesicles (EVs) are involved in intercellular communication. All mammalian cell types secrete heterogeneous vesicles of a variety of sizes [1]. Here, we focus on small EVs, which are often called exosomes. Although the exact definition of exosomes varies in different papers and remains debated [2], we define an exosome as any EV between 30 and ~200 nanometers (nm). The upper limit is imposed by using a 0.22 μm filter.

There are many different protocols for isolating EVs, which yield vesicles of varying purity (all protocols, to some degree co-isolate soluble proteins) [3]. We describe an ultracentrifugation-based protocol, which remains one of the most commonly used protocols for isolating extracellular vesicles from cell culture media [4]. There are many variations on this protocol, and our protocol includes a 0.22 μm filtration step. This cutoff provides a specific size

Emma J.K. Kowal and Dmitry Ter-Ovanesyan contributed equally to this work.

Winston Patrick Kuo and Shidong Jia (eds.), *Extracellular Vesicles: Methods and Protocols*, Methods in Molecular Biology, vol. 1660, DOI 10.1007/978-1-4939-7253-1_12,

range for the isolated extracellular vesicles, which enhances reproducibility in EV analysis across cell types or conditions.

EVs can be characterized by a wide variety of techniques, including profiling the proteins they contain. Tetraspanins are a group of proteins that contain four transmembrane domains and certain characteristic features. The tetraspanins CD9, CD63 and CD81 are transmembrane proteins that are commonly found in extracellular vesicles across cell types [5]. In addition to our EV isolation protocol, we describe a detailed protocol for analysis of these characteristic EV markers by western blotting.

2 Materials

Store all materials at room temperature unless otherwise stated.

2.1 Cell Culture

1. Cells and cultureware.
2. Fetal bovine serum (FBS)-depleted media or defined media without FBS (*see* **Note 1**).

2.2 EV Isolation

1. PBS without Ca^{2+}/Mg^{2+}.
2. HEPES buffer (optional) (*see* **Note 2**).
3. 50 mL Falcon tubes (Fisher Scientific).
4. 0.22 μm Steriflip filter tubes (Fisher Scientific).
5. Ultracentrifuge and rotor.
6. Polyallomer ultracentrifuge tubes (Beckman Coulter).

2.3 Western Blot

1. Sample Buffer: Bolt 4× LDS Sample Buffer (Thermo Fisher Scientific). Store at 4 °C.
2. Bolt 10× Reducing Buffer (optional) (Thermo Fisher Scientific) (For proteins that require reducing conditions, not tetraspanins; *see* **Note 3**).
3. RIPA buffer (optional) (*see* **Note 4**).
4. A660 or BCA protein quantification assay (optional) (*see* **Note 5**).
5. Running buffer: 100 mL 20× MES SDS running buffer (Thermo Fisher Scientific), 1900 mL deionized water.
6. 4–12% Bis-Tris Gels (Thermo Fisher Scientific). Store at 4 °C.
7. Gel tank (XCell SureLock® Mini, Thermo Fisher Scientific) and electrophoresis equipment.
8. MagicMark XP Western protein standard (Thermo Fisher Scientific). Store at −20 °C.
9. SeeBluePlus2 protein ladder (Thermo Fisher Scientific). Store at 4 °C.

10. XCell II Blot Module and sponges (Thermo Fisher Scientific) (*see* **Note 6**).
11. Methanol.
12. Transfer buffer: 100 mL Bolt 20× transfer buffer (Thermo Fisher Scientific), 400 mL methanol, 1500 mL deionized water.
13. PVDF or nitrocellulose membranes (Thermo Fisher Scientific).
14. Milk powder.
15. Tween 20.
16. PBST: PBS with 0.1% vol/vol Tween 20. Store at 4 °C.
17. Cold room with a tilting rocker (not orbital).
18. Plastic containers to hold membranes, such as PerfectWestern™ containers.
19. Flat tweezers for handling membranes.
20. Antibodies to proteins of interest.
21. HRP-conjugated secondary antibody for visualization (Bethyl Laboratories).
22. HRP substrate, such as SpectraQuant™-HRP CL Chemiluminescent detection reagent (BridgePath Scientific).

3 Methods

3.1 EV Isolation

1. Culture cells under standard conditions to 50–70% confluency.

Day 1
For suspension cells:

1. Spin down desired total number of cells (*see* **Note 7**) in six 50 mL Falcon tubes at 300 × *g* for 5 min.
2. Aspirate media and resuspend each cell pellet in 40 mL FBS-depleted or defined media without FBS (*see* **Note 1**). Transfer contents of each Falcon tube to T75 flask and return to incubator.

For adherent cells:

1. Aspirate media from twelve 15 cm plates.
2. Add 20 mL FBS-depleted or defined media without FBS per plate (*see* **Note 1**). Return cells to incubator.

Day 2

1. After 24 h, take off all media and divide among 50 mL falcon tubes.
2. Spin at 300 × *g* for 10 min at RT (to pellet the cells).

3. Transfer supernatant to new 50 mL tubes leaving cell pellet behind. If cell protein is to be analyzed alongside EVs, one cell pellet can at this step be resuspended in the desired lysis buffer (*see* **Notes 4** and **5**).
4. Spin at 2000 × *g* for 10 min at RT (to pellet any dead cells).
5. Transfer supernatant to new 50 mL tubes leaving cell pellet behind.
6. Spin supernatant at 16,500 × *g* for 20 min at 4 °C (to pellet large EVs).
7. Transfer supernatant to new 50 mL tubes, leaving pellet behind.
8. Pass supernatant through Steriflip 0.22 μm filter.
9. Transfer supernatant to polyallomer ultracentrifuge tubes. Centrifuge at 120,000 × *g* (26,500 RPM with SW32Ti rotor) for 70 min at 4 °C.
10. Remove most of supernatant, leaving ~2 cm of media above pellet. Add 5 mL PBS to each tube. Vortex on medium speed for a few seconds. Fill to top of each tube with PBS.
11. Again, centrifuge at 120,000 × *g* for 70 min at 4 °C.
12. Aspirate all of supernatant with Pasteur pipet without touching bottom of tube where pellet is located (*see* **Note 8**).
13. Resuspend pellet either in PBS or directly in the desired lysis buffer for western blot (*see* **Notes 4** and **5**).

3.2 Western Blot

14. Add 100 μL 1× Sample Buffer to each pellet, or add 4× sample buffer to a final concentration of 1× (i.e., add 25 μL 4× sample buffer to 75 μL sample) in a pre-isolated EV sample. Vortex on high speed to mix. If in ultracentrifuge tubes pipet up and down to further disrupt pellet, then transfer to Eppendorf tubes.
15. Incubate at 70 °C for 10 min.
16. Make 2 L of 1× MES SDS running buffer (100 mL buffer into 1900 mL deionized water).
17. Make 5% milk buffer: 2.5 g dried milk into 50 mL PBST (PBS + 0.1% v/v Tween 20). Tumble at 4° for an hour (*see* **Note 9**).
18. Prepare 4–12% bis-tris gel in gel tank. Add 1× MES running buffer to top of gel. Do not forget to rinse wells.
19. Load wells. For ladder use 3 μL MagicMark + 6 μL SeeBlue-Plus2, in separate lanes if possible (*see* **Note 10**).
20. Run 40 min at 150 V, 22 min at 200 V, or until blue dye reaches gel foot.

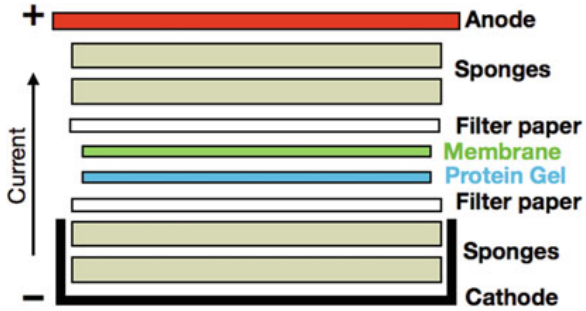

Fig. 1 Schematic of membrane transfer sandwich. This should be constructed from the bottom (cathode) up, using as many sponges as necessary to put even pressure across the surface of the membrane with no air bubbles, and all internal components except gel pre-soaked in transfer buffer

21. While gel is running, prepare for transfer (see XCell surelock manufacturer instructions [6] for more detail).
22. Make 2 L transfer buffer (100 mL Bolt 20× transfer buffer, 400 mL methanol, 1500 mL water).
23. If using PVDF membranes, place one membrane in empty tip box lid with a few milliliters methanol to activate it. Rinse several times with transfer buffer, dumping excess into large sandwich making tray, then rock gently in hand for several minutes. For nitrocellulose membranes, simply soak in transfer buffer for a minute.
24. Soak sponges in transfer buffer, squeezing out bubbles as much as possible (*see* **Note 11**). Briefly immerse filter papers in transfer buffer as well.
25. Build sandwich up from the bottom in the following order: anode, sponges, filter paper, gel, transfer membrane, filter paper and sponges (*see* Fig. 1, **Note 12**).
26. When sandwich is ready for gel, take gel out of tank and rinse it off. Crack open plastic casing. Cut off wells and foot so that remainder is completely flat and lay carefully on filter paper.
27. Squeeze sandwich together in holder and insert into gel tank. If reusing the same tank make sure to pour out gel running buffer and rinse with deionized water.
28. Use fresh transfer buffer to fill in sandwich from the top. Open and close clamp several times to let the buffer soak down through.
29. Fill the rest of the gel box with deionized water, which will serve as a heat sink.
30. Put on lid and run 1.5–2 h at 30 V, tapping firmly on occasion to remove bubbles (*see* **Note 11**).

31. When done, turn off current, pull out sandwich in holder, put it back in large tray (minus transfer buffer) then unpack it carefully. Peel away filter paper very slowly to check for protein transfer (*see* **Note 13**).
32. As soon as you peel off membrane, take a blade and cut off upper right hand corner to mark "top" face (face which was touching gel).
33. Place membrane in PerfectWestern box containing 5–10 mL milk buffer (as much as necessary to cover membrane completely). If using PVDF membranes, ensure that the membrane does not dry out at any step.
34. To block, place membrane in milk buffer on rocker in the cold room and let rock at least half an hour. Conduct all further steps in the cold room if possible.
35. After at least half an hour, pour off block and add 10 mL primary antibody diluted 1:1000 in milk buffer (*see* **Note 14**). Leave overnight rocking in the cold room.

Day 3:

1. Pour off primary, take PBST, pour in, swish, pour off, 2×, then do three washes in PBST of ~10 min each, rocking in the cold room.
2. Add 10 mL secondary antibody diluted 1:2000 in milk buffer (*see* **Note 14**). Leave rocking in the cold room for at least 1 h.
3. Pour off secondary, take PBST, pour in, swish, pour off, 2×, then do three washes in PBST of ~10 min each, rocking in the cold room.
4. Bring the membrane (in fresh PBST), equal volumes of each component of HRP substrate (reagent A and B; *see* Subheading 2.3, **item 21**) and an empty falcon tube to the imaging stage.
5. Mix reagent A and B together immediately before use. Pour PBST off membrane and pour A/B mix on. Let sit for a minute then image, using tweezers to handle membrane (*see* **Note 15**).

4 Notes

1. Since fetal bovine serum contains bovine EVs, it is important for downstream analysis that media from which EVs will be isolated is either FBS-free or has been depleted of vesicles by overnight ultracentrifugation at 120,000 × *g*. A convenient formulation is to make media with 2× FBS and ultracentrifuge it overnight, then remove and keep the supernatant, diluting it 1:1 in the base media to bring it to 1×. Some cells will still not like this media and so we advise collecting EVs for 24 h.

2. For storage of EVs at −80 °C we recommend the addition of HEPES buffer to a final concentration of 20 mM to stabilize pH over freeze–thaw cycles (to PBS or other buffers).
3. Protein gel electrophoresis can be either denaturing or non-denaturing ("native," i.e., retaining the original folded structure) and either reducing (where Cys-Cys disulfide bonds are specifically broken) or nonreducing. Though reducing can help to solubilize a concentrated or complex sample, tetraspanins such as CD63, CD81 and CD9 require nonreducing electrophoresis for western blotting, as the epitope recognized by antibodies to these proteins usually relies on several disulfide bonds to fold properly and be recognized.
4. Transmembrane proteins, particularly those with four or more membrane-spanning regions, can be difficult to extract from lysates. We have had success extracting tetraspanins with LDS sample buffer alone (Subheading 2.3, **item 1**) but other proteins may require some optimization of lysis buffer for efficient extraction. RIPA buffer is one of the harsher common buffers and is well suited for this purpose. When extracting membrane proteins from cells, it is often helpful to centrifuge the lysate at high speed (>12,000 × *g*) for 10 min and take the supernatant, leaving behind the membrane and insoluble material which can interfere with electrophoresis.
5. Many common protein quantification assays (such as A660 and BCA) rely on a colorimetric readout, and are thus incompatible with the bromophenol blue-containing LDS sample buffer. This protocol does not explicitly describe how to quantify protein in a lysate, but note that if you do wish to quantify the protein in your samples, you should lyse the cells or vesicles in RIPA (Subheading 2.3, **item 2**) or another clear buffer, quantify, and then add 4× LDS sample buffer to 1× concentration prior to immunoblotting.
6. The reagents listed as subheading 2.3, **items 10–13** are required for a traditional wet transfer of proteins to a membrane. These can be substituted with other materials of your choice for dry or semidry transfer. For example, we have found the iBlot dry blotting system from Thermo Fisher is convenient and effective, though not all labs may have the required equipment.
7. The total number of cells per isolation should be determined by the total volume of media from which you are able to isolate EVs. The limiting factor will likely be the volume capacity of your ultracentrifuge tubes (e.g., the SW32Ti rotor can hold six tubes with a volume of ~38 mL each, so the max volume per isolation is 228 mL). Start with a few extra milliliters of media per flask to account for some loss throughout the

centrifugation steps and culture the number of cells necessary to achieve 50–70% confluence in this volume.

8. The pellet at this stage will most likely not be visible. It is possible to remove all but 20–30 μL of the supernatant by tilting the tube to pool the liquid on one side and carefully avoiding touching the center of the tube bottom. We have also found that it is helpful to remove all but ~2 cm of supernatant and wait 30 s before aspirating the final few milliliters, as otherwise some liquid clings to the sides of the tube and makes the final residual volume >50 μL.
9. The proteins in the milk buffer associate with proteins in the membrane and block nonspecific antibody interactions. There are many formulations of blocking solution available but we have found milk to be cheap and effective. It is important to make this buffer fresh (it should be a few days old at most and stored at 4 °C with rotation).
10. MagicMark XP is a protein standard ladder containing IgG binding sites (you will see it on the final western blot, not in the gel), while SeeBlue is a prestained protein standard ladder which you should see in the gel and membrane but not in the final blot. These can be mixed if necessary but will run better in separate wells. SeeBlue is useful for evaluating how far the gel has run and if the transfer was successful (*see* **Note 13**) as well as for horizontally cutting the membrane in order to blot for proteins of different molecular weights, e.g., CD63 and CD81 (*see* Fig. 2).
11. Air bubbles anywhere in the sandwich can prevent successful transfer of proteins to the membrane in that spot, so it's important to squeeze the sandwich tightly and firmly tap the XCell mini tank periodically (as many times as is convenient) while transfer occurs.
12. Use as many sponges as necessary to form a tight sandwich. Generally at least three sponges on either side of the gel and membrane (six total) will suffice, but the tighter the better. *See* Fig. 1 for schematic.
13. Carefully peel away the top corner of the membrane closest to where the SeeBlue ladder was run and check for the location of the colored bands. If the transfer worked, some or all of them should now be on the membrane instead of the gel. Specifically, check that the SeeBlue bands in the molecular weight range of your protein of interest (for example, the 28 kDa band is close to the size of CD81) are on the membrane. If they are still on the gel, you can carefully reconstruct the sandwich (ensure that the gel and membrane do not shift relative to one another) and run it slightly longer. Keep in mind that running the transfer for too long will cause the lower molecular weight bands to

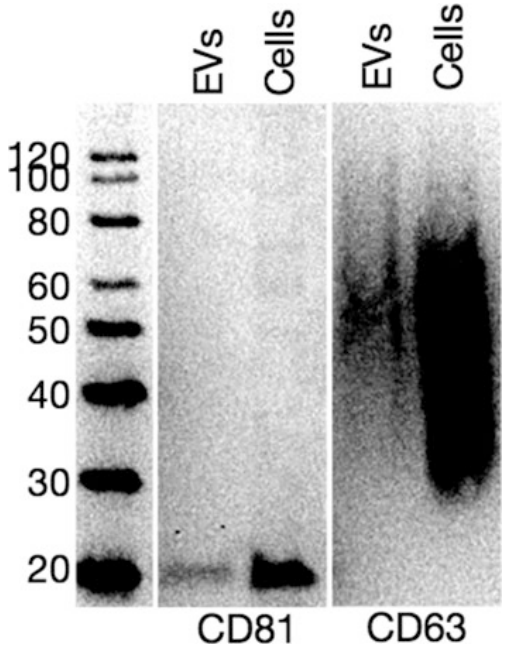

Fig. 2 Western blot showing CD81 and CD63 blotting on K562 EV lysate (7 μg) and cell lysate (86 μg), resuspended in RIPA and quantified before addition of LDS Sample Buffer. Note that CD63 appears as a smear in the range of 30–60 kDa; this is due to heavy glycosylation and is expected [7]. Each membrane was blocked for 30 min at 4 °C in milk buffer, then incubated with primary antibody diluted in 10 mL milk buffer for 12 h (1:1000 dilution mouse anti-human CD81, clone M38, or 1:1000 dilution mouse anti-human CD63, clone TS63), washed three times for 10 min each in PBST, then incubated for 2 h with 10 mL secondary antibody (Rabbit anti-mouse HRP, 1:2000 dilution in milk buffer), washed three times for 10 min each in PBST, then imaged on a Bio-Rad ChemiDoc MP system with SpectraQuant'™-HRP CL Chemiluminescent detection reagent

pass through the membrane onto the filter paper, at which point they cannot be recovered.

14. As different antibodies have different affinities for their targets, it is often necessary to experimentally determine the optimal antibody dilutions for immunoblotting. Generally these fall within 1:100 and 1:5000 and are lower (i.e., more dilute) for the secondary antibody. We recommend starting with a higher dilution (more concentrated) to ensure a strong signal and diluting further as necessary to eliminate background or conserve reagents.
15. If using Image Lab software to visualize the blot, it can be set to "signal accumulation mode" to determine optimal exposure time by monitoring blot over the course of imaging.

Acknowledgment

This work was supported by US National Institutes of Health National Human Genome Research Institute grant P50 HG005550.

References

1. Tkach M, Thery C (2016) Communication by extracellular vesicles: where we are and where we need to go. Cell 164(6):1226–1232
2. Gould SJ, Raposo G (2013) As we wait: coping with an imperfect nomenclature for extracellular vesicles. J Extracell Vesicles 2. doi:10.3402/jev.v2i0.20389
3. Witwer KW, Buzas EI, Bemis LT, Bora A, Lasser C, Lotvall J, Nolte-'t Hoen EN, Piper MG, Sivaraman S, Skog J, Thery C, Wauben MH, Hochberg F (2013) Standardization of sample collection, isolation and analysis methods in extracellular vesicle research. J Extracell Vesicles 2. doi:10.3402/jev.v2i0.20360
4. Thery C, Amigorena S, Raposo G, Clayton A (2006) Isolation and characterization of exosomes from cell culture supernatants and biological fluids. Curr Protoc Cell Biol Chapter 3:Unit 3.22
5. Kowal J, Arras G, Colombo M, Jouve M, Morath JP, Primdal-Bengtson B, Dingli F, Loew D, Tkach M, Thery C (2016) Proteomic comparison defines novel markers to characterize heterogeneous populations of extracellular vesicle subtypes. Proc Natl Acad Sci U S A 113(8):E968–E977
6. XCell SureLock® Mini-Cell. https://tools.thermofisher.com/content/sfs/manuals/surelock_man.pdf. Accessed 27 Apr 2016
7 Ageberg M, Lindmark A (2003) Characterisation of the biosynthesis and processing of the neutrophil granule membrane protein CD63 in myeloid cells. Clin Lab Haematol 25 (5):297–306

Appendix S3: Imaging of Isolated Extracellular Vesicles Using Fluorescence Microscopy

Chapter 19

Imaging of Isolated Extracellular Vesicles Using Fluorescence Microscopy

Dmitry Ter-Ovanesyan, Emma J. K. Kowal, Aviv Regev, George M. Church, and Emanuele Cocucci

Abstract

High-resolution fluorescence microscopy approaches enable the study of single objects or biological complexes. Single object studies have the general advantage of uncovering heterogeneity that may be hidden during the ensemble averaging which is common in any bulk conventional biochemical analysis. The implementation of single object analysis in the study of extracellular vesicles (EVs) may therefore be used to characterize specific properties of vesicle subsets which would be otherwise undetectable. We present a protocol for staining isolated EVs with a fluorescent lipid dye and attaching them onto a glass slide in preparation for imaging with total internal reflection fluorescence microscopy (TIRF-M) or other high-resolution microscopy techniques.

Key words Exosomes, Extracellular vesicles, EVs, Imaging, Microscopy, TIRF

1 Introduction

Over the last decade, interest in extracellular vesicles (EVs) has significantly grown due to their role in normal physiology, as well as pathological processes. EVs are thought to signal with recipient cells by interaction with their surface ligands or by transferring their contents (such as RNA or protein) into the recipient cell's cytoplasm [1]. Furthermore, as EVs are secreted into all biological fluids, they also hold great promise as novel biomarkers [2].

One of the major challenges in understanding the role of EVs in intercellular communication is characterizing the composition of individual EVs. When EVs are isolated in bulk, information regarding EV heterogeneity is lost. Existing EV isolation techni-

Dmitry Ter-Ovanesyan and Emma J.K. Kowal contributed equally to this work.

Winston Patrick Kuo and Shidong Jia (eds.), *Extracellular Vesicles: Methods and Protocols*, Methods in Molecular Biology, vol. 1660, DOI 10.1007/978-1-4939-7253-1_19,

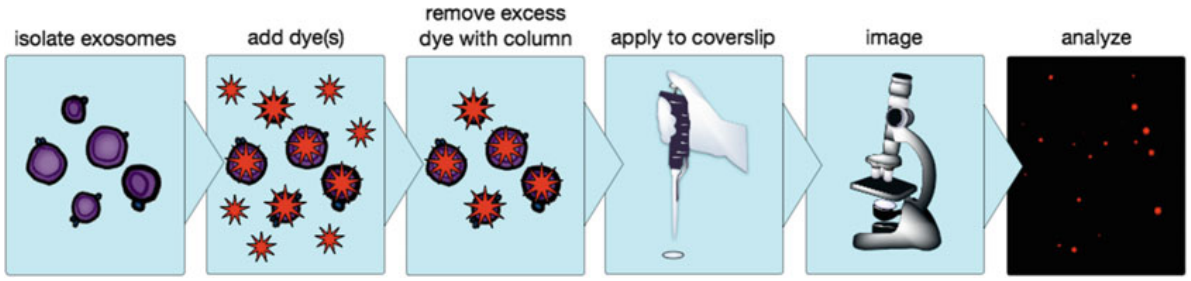

Fig. 1 Conceptual overview of the protocol. Schematic of EV staining and imaging procedure

ques, such as ultracentrifugation [3], result in a diverse mixture of vesicles from different cellular compartments [4] and are often contaminated by nonvesicular components such as extracellular protein complexes [5].

In recent years, high-resolution imaging has contributed greatly to the understanding of cell biology, permitting the detailed visualization of complex processes such as endocytosis [6], or the composition of single objects such as viruses [7]. In particular, total internal reflection fluorescence microscopy (TIRF-M) has been widely applied since it permits a high signal to noise ratio, the detection of single molecules, and a facile calibration of measurements to the single molecule level. These approaches can be efficiently applied to the study of EVs and identify different subpopulation of EVs present in a given sample. Although flow cytometry-based methods are able to characterize EV subpopulations, using flow cytometry for EV detection presents many technical challenges [8, 9] and is much less sensitive than TIRF-M.

Here, we provide a protocol for imaging isolated EVs by fluorescence microscopy. Although we have found TIRF-M to be best suited for these studies, other microscopes such as confocal [10, 11] and STED microscopes [12] can be used as well. We provide detailed instructions for staining EVs with a fluorescent membrane dye and attaching them to a glass slide (Fig. 1). This basic approach can be easily combined with other more specific staining, such as antibodies or nucleic acid dyes to study the heterogeneity of EV composition. Though colocalization does not strictly indicate that a given molecule is encapsulated within the lipid membrane, since it could also be adhered to the outside of the vesicle, use of this technique after various enzymatic treatments could provide this information. Additionally, EVs isolated from cells expressing fluorescent fusion proteins can be visualized using high-resolution microscopy [10, 11]. In conclusion, the high sensitivity of TIRF-M and its ability to make quantitative measurements provides a highly promising approach to study EV composition, as well as other diffraction-limited objects such as viruses or nanoparticles.

2 Materials

Store all materials at room temperature unless otherwise stated.

1. Glass coverslips. # 1.5 round 25 mm glass coverslips (Warner Instruments).
2. Coverslip rack. Teflon rack to vertically hold glass coverslips during cleaning procedures (C-14784, Thermo Fisher Scientific).
3. Coverslip holder for imaging. Attofluor Cell Chamber (A-7816, Thermo Fisher Scientific).
4. Total Internal Reflection Microscopy System. The imaging setup described here is composed of a Zeiss Axio Imager Z2 microscope equipped with a 63× Oil immersion objective (1.46 NA, Carl Zeiss) and a TIRF slider with manual angle and focus controls (Carl Zeiss). The illumination is supplied by solid state and argon ion lasers at 405 nm, 458/488/514 nm, 561 nm and 639 nm (power ~ 2–5 mW at the objective depending on laser). The excitation light is coupled through an acousto-optical tunable filter into a single mode optical fiber, carried to the TIRF slider and reflected into the objective using a single- or multi-band dichroic mirror (various; Semrock). The emission light is collected by the objective, passes the dichroic mirror and a single- or multi-band emission filter (various; Semrock), and is projected onto an electron multiplying charge-coupled device (EMCCD) camera (ImagEM-1K BackThinned EMCCD, Hamamatsu) for a final pixel size of 206 nm. Microscope operation and image acquisition are controlled by the Zen Blue software (Carl Zeiss). Any equivalent setup is suitable for the experiments described in this chapter.
5. EVs (*see* **Note 1**) isolated fresh, stored at 4 °C, or thawed from storage at −80 °C (*see* **Note 2**).
6. Vybrant DiD Cell-Labeling Solution (V-22887, Thermo Fisher Scientific).
7. Other fluorescent dyes (*see* **Note 3**) stored according to respective manufacturer recommendations.
8. Diluted dye stocks (*see* **Note 4**) stored according to respective manufacturer recommendations. For DiD, make a 50 nM stock in DMSO and store at room temperature in the dark.
9. EV Spin Columns, MW 3000 (4484449, Thermo Fisher Scientific) (*see* **Note 5**).
10. Fluorescent beads (*see* **Note 6**). 0.1 μm carboxylated beads (Ex/Em: 505/515 nm; F-8803, Thermo Fisher Scientific) stored at 4 °C.

11. Fluorescent bead solution. Dilute the fluorescent beads (2.10) to obtain ~4x10^7 beads in 100 μL of PBS, which according to the manufacturer (*see* 2.10) corresponds to a 10^5-fold dilution. To do this, prepare two consecutive dilutions, first 1:1000 to obtain a 1 mL stock solution, then 1:100 to obtain the working solution. Store all bead solutions at 4 °C or on ice during the experiment.
12. Bottle-top filter unit. Reusable bottle top filter unit (DS0320–5033, Nalgene) with removable membrane of 0.2 μm pore size for vacuum filtration.
13. 100% Ethanol. Filter 1 L of denatured ethanol (9401–03, JT Baker) into a bottle using a vacuum-based bottle-top filter unit (2.10). Fill a glass jar with the filtered ethanol such that it will entirely cover a rack loaded with glass coverslips (2.1 and 2.2).
14. Dulbecco's Phosphate Buffer Saline, no calcium, no magnesium (PBS, Thermo Fisher Scientific).

3 Methods

3.1 Clean Glass Coverslip Preparation

1. Place coverslips in rack (one per sample to be imaged, plus controls; *see* **Note 7**) and submerge rack in filtered 100% ethanol.
2. Sonicate for 20–30 min on low power.
3. Remove rack from ethanol and, without touching coverslips, adsorb excess ethanol by placing rack onto a Kimwipes or other tissue.
4. Place the rack with coverslips in 120 °C oven until dry; a lower temperature is acceptable but will take longer.
5. Immediately before applying sample to be imaged, expose the rack of coverslips to air plasma inside a glow discharge unit operated at 50 mA for 2 min.

3.2 Sample Preparation

1. Prepare one clean 1.5 mL tube of 50 μL PBS (*see* **Note 8**).
2. Prepare one tube of 50 μL EVs. If you are testing other dyes in addition to DiD, prepare one tube of EVs per dye and dye combination to be tested (*see* **Note 7** on experimental design).
3. Add 1 μL of 50 nM DiD stock to PBS and to EVs. If using other dyes, add to appropriate tubes, making sure to add all dyes in use to control PBS tube.
4. Tap or gently vortex tubes to mix.
5. Incubate all samples for 20 min at 37 °C in the dark.
6. While incubating, prepare spin columns (*see* **Note 5**) according to manufacturer instructions [13], reproduced here:

7. Tap the column to settle the dry gel into the bottom of the spin column.
8. Hydrate the column with 650 µL PBS.
9. Cap, vortex, tap out air bubbles, and leave at RT 5–15 min.
10. Place columns in 2 mL collection tubes and spin at 750 RCF for 2 min at RT. Keep track of the orientation of the column in the rotor.
11. Discard collection tube and immediately apply the EV sample directly to the center of the gel bed at the top of the column IMPORTANT! Do not disturb the gel surface or contact the sides of the column with the pipette tip or reaction mixture.
12. Place column in 1.5 mL elution tube and place in rotor, maintaining same orientation as previous spin.
13. Spin at 750 RCF for 2 min at RT.
14. Discard column, retrieve EV sample from tube.
15. Samples can be imaged immediately or stored at 4 °C in the dark for up to 24 h.

3.3 Sample Addition to Coverslips and Imaging

1. Tape a clean strip of Parafilm onto bench and carefully lay down coverslip(s).
2. If using beads to visualize the focal plane (*see* **Note 6**), add 1 µL working fluorescent bead solution (*see* 2.1.11) to sample and invert several times to mix.
3. Add 50–100 µL sample to each coverslip and wait for 5 min for EVs to adsorb. Monitor the coverslips to ensure that they do not dry out completely, as this will create salt crystals which will interfere with imaging. If necessary, add several drops of PBS. (*see also* **Note 8**).
4. Using tweezers, turn the coverslip on its side and dab against Kimwipes or other tissue to wick off excess liquid, again without drying completely.
5. Place the coverslip carefully into bottom of holder with sample oriented up and make sure it is centered (tap around edges with tweezers, it should not lift on opposite side; *see* **Note 9**) before screwing holder together.
6. Gently add 1 mL PBS directly to coverslip.

3.4 Imaging

1. Place the holder with coverslip and PBS on the microscope stage.
2. Find the focal plane (*see* **Note 6**). In the DiD-stained EV sample, you should see a distribution of diffraction-limited punctae across the field of view (as in Fig. 2, right panel).

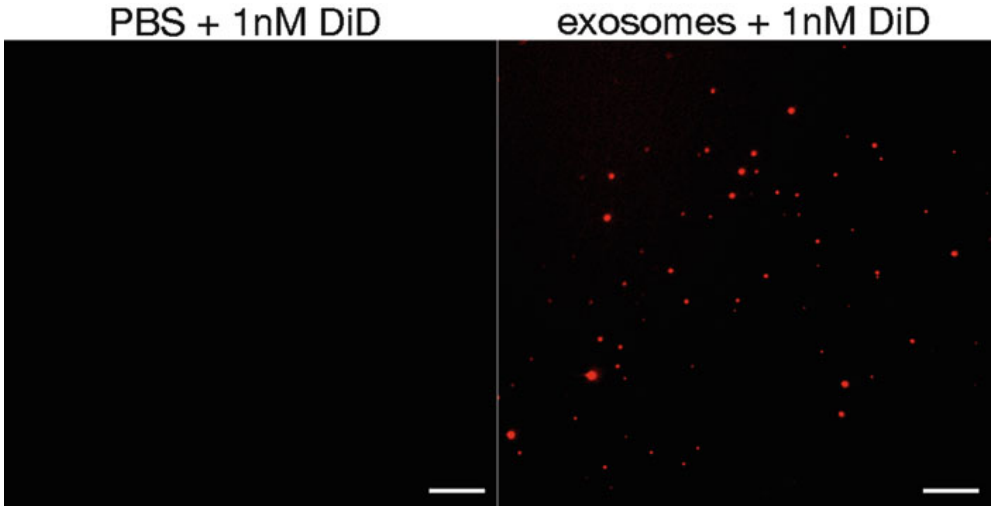

Fig. 2 Imaging of DiD-labeled extracellular vesicles. K562 EVs and PBS control incubated with 1 nM DiD, then imaged in far-red (Em filter 688/48). No signal is visible in the PBS slide while the EVs are clearly visible above background. Images shown are representative of three coverslips, twenty fields of view, in each case. (*Scale bars* = 10 μm)

3. Acquire several images in each channel of interest. Ensure that the PBS + dyes control sample is devoid of signal in each channel (as in Fig. 2, left panel).
4. For colocalization studies, ensure that vesicles labeled with one dye alone do not give signal in other channels (as in Fig. 3, bottom panels) and use caution when interpreting results (*see* **Note 10**).

4 Notes

1. EVs can be derived from any source of interest, i.e., cell culture or biological fluids. We find that EVs collected by standard ultracentrifugation protocols [3] from 250 mL of 50% confluent K562 cells over 24 h are sufficient to cover 50 coverslips with a reasonable concentration of particles/field.
2. EVs stored at 4 °C for under a week look similar to freshly isolated vesicles. For storage at −80 °C we recommend the addition of 20 mM HEPES buffer to stabilize the pH at ~7.4 over freeze-thaw cycles.
3. This protocol specifically outlines use of a lipid dye (DiD) to label EV membranes, but it can be used in combination with other dyes to label EV protein and RNA, or with transgenic cell lines to label specific molecules of interest [10, 11]. DiD in particular is conveniently combined with other probes as it emits in far-red, minimizing chance of bleed-through into other commonly used channels. Based on our tests, the spin

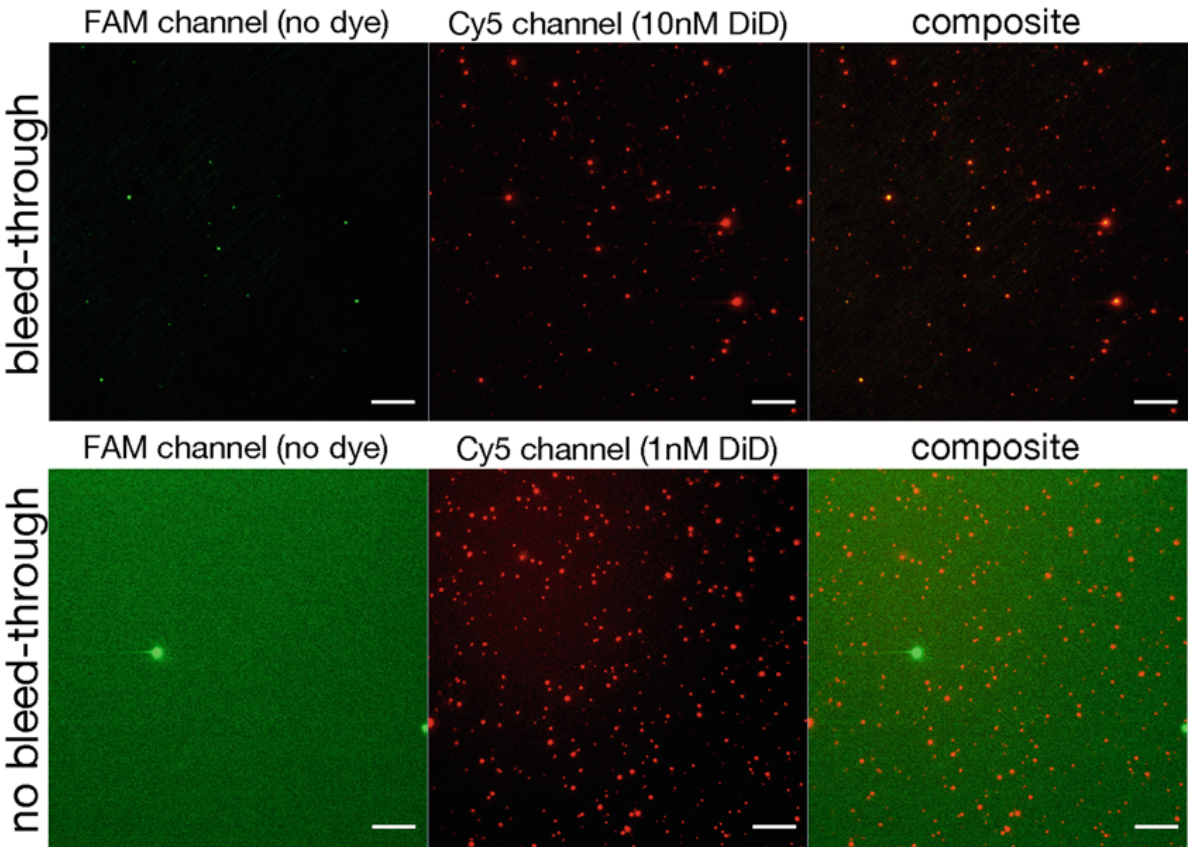

Fig. 3 Imaging of DiD-labeled EVs together with fluorescent beads. Distinguishing EV signal from bleed-through. *Top*: K562 EV sample demonstrating bleed-through between channels. *Left*: green (Em filter 525/50), *Center*: far-red (Em filter 688/48), *Right*: merge. EVs stained with 10 nM DiD appear to colocalize with objects in the green channel (emission filter) despite absence of green fluorophores in the sample. *Bottom*: K562 EV sample demonstrating no bleed-through between channels. *Left*: green (Em filter 525/50), *Center*: far-red (Em filter 688/48), *Right*: merge. Decreasing the concentration of DiD to 1 nM in the staining relieves bleed-through, while GFP-coated beads are still visible. Green channel is deliberately overexposed to demonstrate absence of any signal from DiD-stained objects. Images shown are representative of three coverslips, twenty fields of view, in each case. (*Scale bars* = 10 μm)

columns (2.1.9) did not effectively clear unbound fluorescent antibodies. When using multiple dyes or labeling strategies it is important to perform controls outlined in **Note 7**.

4. We recommend making dye stocks at a concentration equal to the desired final concentration times the volume of the sample, such that each dye can be provided to each sample in 1 μL of stock solution—for example, use a 150 nM stock of DiD with 30 μL EV samples for a final concentration of 5 nM. This is both for convenience and to avoid disrupting vesicle membranes with high concentrations of stock solvent.
5. The purpose of these spin columns is to remove contaminating fluorescent components from the dyed sample (i.e., free or aggregated dye, which should be in complexes smaller than

3 kDa). We found that the spin columns were more effective than dialysis and more convenient than ultracentrifugation.

6. It can be difficult to find the correct focal plane while imaging using signal from the vesicles alone, especially for initial experiments, and so we recommend the use of beads (with Ex/Em spectra distinct from any dyes in use) to aid in finding the correct plane. This is particularly crucial for control experiments with no labeled vesicles (*see* **Note 8**).
7. As EVs are diffraction-limited objects and this technique is very sensitive, there are many potential sources of false positive signal. It is important that for a given set of parameters (EV and dye concentration, laser power, TIRF angle, gain and exposure time) a number of controls is performed, and several images are taken across the coverslip in each channel of interest and at the correct focal plane (*see* **Note 9**). A sample of PBS and dyes only (no EVs) should be prepared and imaged to ensure that the dye itself is not forming micelles or aggregates which escape the spin column, as these would appear as fluorescent punctae indistinguishable from EVs (*see* Fig. 2, left vs. right). If objects are seen in this control, potential fixes are: decreasing the concentration of dye, cleaning and handling coverslips meticulously, filtering PBS to ensure it is free of contaminants, loading the spin column without disturbing the gel bed, or centrifuging dye stocks at high speed to remove precipitates. For colocalization experiments, a separate aliquot of EVs should be labeled with each dye alone and imaged to ensure that there is no bleed-through of fluorescence from the expected channel into another (*see* Fig. 3, top vs. bottom). If bleed-through is seen, exposure time may be lowered in the channel where bleed-through is observed or the concentration of the dye is decreased. Another potential solution is finding a narrower emission band filter for that channel.
8. The manufacturer's protocol [13] for the EV Spin Columns suggests a sample volume of 20–100 μL, but in our hands, samples lower than 40 μL applied to the column do not consistently elute at input volume and often come out 50% more dilute (i.e., 20 μL input yields 30 μL or more stained sample). This should be taken into account when considering desired final sample concentration for imaging.
9. If the coverslip is not flat it will be difficult to keep the focal plane while panning across the sample. If repeated adjustments of the coverslip in the holder do not fix a tilted sample, check that the microscope stage is flat.
10. The diffraction of light limits the resolution of imaging instruments. Therefore objects smaller than the diffraction limit, which approximately corresponds to half of the emitted

wavelength in a fluorescent sample, corresponds to the point spread function of the imaging system. Since a large fraction of EVs is smaller than the diffraction limit (~250 nm) more than one vesicle might be present in a single detected point spread function. Thus, this technique cannot strictly distinguish between one vesicle and two vesicles stuck together. Furthermore, as small EVs are diffraction-limited objects, colocalization does not strictly indicate that a given molecule is encapsulated within the lipid membrane, since it could also be adhered to the outside of the vesicle. Use of this technique in concert with enzymatic protection assays would be necessary to elucidate the contents of EVs.

Acknowledgment

This work was supported by US National Institutes of Health National Human Genome Research Institute Grant P50 HG005550, The Ohio State Cancer Center (P30-CA016058), and an intramural fund (IRP46050-502339) granted to EC.

References

1. Tkach M, Thery C (2016) Communication by extracellular vesicles: where we are and where we need to go. Cell 164(6):1226–1232
2. Revenfeld AL, Baek R, Nielsen MH, Stensballe A, Varming K, Jorgensen M (2014) Diagnostic and prognostic potential of extracellular vesicles in peripheral blood. Clin Ther 36 (6):830–846
3. Thery C, Amigorena S, Raposo G, Clayton A (2006) Isolation and characterization of exosomes from cell culture supernatants and biological fluids. Curr Protoc Cell Biol Chapter 3:Unit 3.22
4. Cocucci E, Meldolesi J (2015) Ectosomes and exosomes: shedding the confusion between extracellular vesicles. Trends Cell Biol 25 (6):364–372
5. Cvjetkovic A, Lotvall J, Lasser C (2014) The influence of rotor type and centrifugation time on the yield and purity of extracellular vesicles. J Extracell Vesicles 3
6. Cocucci E, Aguet F, Boulant S, Kirchhausen T (2012) The first five seconds in the life of a clathrin-coated pit. Cell 150(3):495–507
7. Chou YY, Vafabakhsh R, Doganay S, Gao Q, Ha T, Palese P (2012) One influenza virus particle packages eight unique viral RNAs as shown by FISH analysis. Proc Natl Acad Sci U S A 109(23):9101–9106
8. van der Pol E, Coumans F, Varga Z, Krumrey M, Nieuwland R (2013) Innovation in detection of microparticles and exosomes. J Thromb Haemost 11(Suppl 1):36–45
9. Nolan JP, Moore J (2016) Extracellular vesicles: great potential, many challenges. Cytometry B Clin Cytom 90:324–325
10. Fang Y, Wu N, Gan X, Yan W, Morrell JC, Gould SJ (2007) Higher-order oligomerization targets plasma membrane proteins and HIV gag to exosomes. PLoS Biol 5(6):e158
11. Lai CP, Kim EY, Badr CE, Weissleder R, Mempel TR, Tannous BA, Breakefield XO (2015) Visualization and tracking of tumour extracellular vesicle delivery and RNA translation using multiplexed reporters. Nat Commun 6:7029
12. Koliha N, Wiencek Y, Heider U, Jungst C, Kladt N, Krauthauser S, Johnston IC, Bosio A, Schauss A, Wild S (2016) A novel multiplex bead-based platform highlights the diversity of extracellular vesicles. J Extracell Vesicles 5:29975
13. Exosome Spin Columns. https://tools.thermofisher.com/content/sfs/manuals/MAN0008464_Rev01_PI_08Aug2013.pdf. Accessed 4 Apr 2016

Appendix S4: Primer Sequences

Primer Sequences for qRT-PCR (All sequences 5' > 3')

Gene	**Forward Primer**	**Reverse Primer**
SRP14	GGGTACTGTGGAGGGCTTTG	AGGAGGTTTGAATAAGCCATCTGA
B2M	GTATGCCTGCCGTGTGAAC	AAAGCAAGCAAGCAGAATTTGG
ACTB	CGGCATCGTCACCAACTG	AACATGATCTGGGTCATCTTCTC
GAPDH	GGTGGTCTCCTCTGACTTCAACA	GTTGCTGTAGCCAAATTCGTTGT

Appendix S5: References

1. Mandel P, Metais P. Les acides nucléiques du plasma sanguin chez l'homme. Comptes rendus des seances de la Societe de biologie et de ses filiales. 1948;142(3-4):241-3.
2. Mitchell PS, Parkin RK, Kroh EM, Fritz BR, Wyman SK, Pogosova-Agadjanyan EL, et al. Circulating microRNAs as stable blood-based markers for cancer detection. Proceedings of the National Academy of Sciences of the United States of America. 2008;105(30):10513-8.
3. Tsui NB, Ng EK, Lo YM. Stability of endogenous and added RNA in blood specimens, serum, and plasma. Clinical chemistry. 2002;48(10):1647-53.
4. Baj-Krzyworzeka M, Szatanek R, Weglarczyk K, Baran J, Urbanowicz B, Branski P, et al. Tumour-derived microvesicles carry several surface determinants and mRNA of tumour cells and transfer some of these determinants to monocytes. Cancer immunology, immunotherapy : CII. 2006;55(7):808-18.
5. Ratajczak J, Miekus K, Kucia M, Zhang J, Reca R, Dvorak P, et al. Embryonic stem cell-derived microvesicles reprogram hematopoietic progenitors: evidence for horizontal transfer of mRNA and protein delivery. Leukemia. 2006;20(5):847-56.
6. Valadi H, Ekstrom K, Bossios A, Sjostrand M, Lee JJ, Lotvall JO. Exosome-mediated transfer of mRNAs and microRNAs is a novel mechanism of genetic exchange between cells. Nature cell biology. 2007;9(6):654-9.
7. Skog J, Wurdinger T, van Rijn S, Meijer DH, Gainche L, Sena-Esteves M, et al. Glioblastoma microvesicles transport RNA and proteins that promote tumour growth and provide diagnostic biomarkers. Nature cell biology. 2008;10(12):1470-6.
8. Raposo G, Stoorvogel W. Extracellular vesicles: exosomes, microvesicles, and friends. The Journal of cell biology. 2013;200(4):373-83.
9. Dinger ME, Mercer TR, Mattick JS. RNAs as extracellular signaling molecules. Journal of molecular endocrinology. 2008;40(4):151-9.
10. Kolodny GM. Evidence for transfer of macromolecular RNA between mammalian cells in culture. Experimental cell research. 1971;65(2):313-24.
11. Shurtleff MJ, Temoche-Diaz MM, Schekman R. Extracellular vesicles and cancer: caveat Lector. Annual Review of Cancer Biology. 2018;2:395-411.
12. Arroyo JD, Chevillet JR, Kroh EM, Ruf IK, Pritchard CC, Gibson DF, et al. Argonaute2 complexes carry a population of circulating microRNAs independent of vesicles in human plasma. Proceedings of the National Academy of Sciences of the United States of America. 2011;108(12):5003-8.
13. Turchinovich A, Weiz L, Langheinz A, Burwinkel B. Characterization of extracellular circulating microRNA. Nucleic Acids Res. 2011;39(16):7223-33.
14. Thery C, Boussac M, Veron P, Ricciardi-Castagnoli P, Raposo G, Garin J, et al. Proteomic analysis of dendritic cell-derived exosomes: a secreted subcellular compartment distinct from apoptotic vesicles. Journal of immunology (Baltimore, Md : 1950). 2001;166(12):7309-18.

15. Akers JC, Gonda D, Kim R, Carter BS, Chen CC. Biogenesis of extracellular vesicles (EV): exosomes, microvesicles, retrovirus-like vesicles, and apoptotic bodies. Journal of neuro-oncology. 2013;113(1):1-11.
16. Allan D, Billah MM, Finean JB, Michell RH. Release of diacylglycerol-enriched vesicles from erythrocytes with increased intracellular (Ca2+). Nature. 1976;261(5555):58-60.
17. Trams EG, Lauter CJ, Salem N, Jr., Heine U. Exfoliation of membrane ecto-enzymes in the form of micro-vesicles. Biochimica et biophysica acta. 1981;645(1):63-70.
18. Harding C, Heuser J, Stahl P. Receptor-mediated endocytosis of transferrin and recycling of the transferrin receptor in rat reticulocytes. The Journal of cell biology. 1983;97(2):329-39.
19. Pan BT, Johnstone RM. Fate of the transferrin receptor during maturation of sheep reticulocytes in vitro: selective externalization of the receptor. Cell. 1983;33(3):967-78.
20. Lutz HU, Liu SC, Palek J. Release of spectrin-free vesicles from human erythrocytes during ATP depletion. I. Characterization of spectrin-free vesicles. The Journal of cell biology. 1977;73(3):548-60.
21. Pan BT, Teng K, Wu C, Adam M, Johnstone RM. Electron microscopic evidence for externalization of the transferrin receptor in vesicular form in sheep reticulocytes. The Journal of cell biology. 1985;101(3):942-8.
22. Gould SJ, Raposo G. As we wait: coping with an imperfect nomenclature for extracellular vesicles. Journal of extracellular vesicles. 2013;2.
23. Verweij FJ, Bebelman MP, Jimenez CR, Garcia-Vallejo JJ, Janssen H, Neefjes J, et al. Quantifying exosome secretion from single cells reveals a modulatory role for GPCR signaling. The Journal of cell biology. 2018;217(3):1129-42.
24. Bobrie A, Colombo M, Raposo G, Thery C. Exosome secretion: molecular mechanisms and roles in immune responses. Traffic (Copenhagen, Denmark). 2011;12(12):1659-68.
25. Colombo M, Moita C, van Niel G, Kowal J, Vigneron J, Benaroch P, et al. Analysis of ESCRT functions in exosome biogenesis, composition and secretion highlights the heterogeneity of extracellular vesicles. Journal of cell science. 2013;126(Pt 24):5553-65.
26. Ostrowski M, Carmo NB, Krumeich S, Fanget I, Raposo G, Savina A, et al. Rab27a and Rab27b control different steps of the exosome secretion pathway. Nature cell biology. 2010;12(1):19-30; sup pp 1-13.
27. van der Pol E, Hoekstra AG, Sturk A, Otto C, van Leeuwen TG, Nieuwland R. Optical and non-optical methods for detection and characterization of microparticles and exosomes. Journal of thrombosis and haemostasis : JTH. 2010;8(12):2596-607.
28. Sverdlov ED. Amedeo Avogadro's cry: what is 1 microg of exosomes? BioEssays : news and reviews in molecular, cellular and developmental biology. 2012;34(10):873-5.
29. Tkach M, Thery C. Communication by Extracellular Vesicles: Where We Are and Where We Need to Go. Cell. 2016;164(6):1226-32.

30. Wiklander OP, Nordin JZ, O'Loughlin A, Gustafsson Y, Corso G, Mager I, et al. Extracellular vesicle in vivo biodistribution is determined by cell source, route of administration and targeting. Journal of extracellular vesicles. 2015;4:26316.
31. Lai CP, Mardini O, Ericsson M, Prabhakar S, Maguire C, Chen JW, et al. Dynamic biodistribution of extracellular vesicles in vivo using a multimodal imaging reporter. ACS nano. 2014;8(1):483-94.
32. Smyth T, Kullberg M, Malik N, Smith-Jones P, Graner MW, Anchordoquy TJ. Biodistribution and delivery efficiency of unmodified tumor-derived exosomes. Journal of controlled release : official journal of the Controlled Release Society. 2015;199:145-55.
33. Ridder K, Keller S, Dams M, Rupp AK, Schlaudraff J, Del Turco D, et al. Extracellular vesicle-mediated transfer of genetic information between the hematopoietic system and the brain in response to inflammation. PLoS biology. 2014;12(6):e1001874.
34. Ridder K, Sevko A, Heide J, Dams M, Rupp AK, Macas J, et al. Extracellular vesicle-mediated transfer of functional RNA in the tumor microenvironment. Oncoimmunology. 2015;4(6):e1008371.
35. Zomer A, Maynard C, Verweij FJ, Kamermans A, Schafer R, Beerling E, et al. In Vivo imaging reveals extracellular vesicle-mediated phenocopying of metastatic behavior. Cell. 2015;161(5):1046-57.
36. Lai CP, Kim EY, Badr CE, Weissleder R, Mempel TR, Tannous BA, et al. Visualization and tracking of tumour extracellular vesicle delivery and RNA translation using multiplexed reporters. Nature communications. 2015;6:7029.
37. Mateescu B, Kowal EJ, van Balkom BW, Bartel S, Bhattacharyya SN, Buzas EI, et al. Obstacles and opportunities in the functional analysis of extracellular vesicle RNA - an ISEV position paper. Journal of extracellular vesicles. 2017;6(1):1286095.
38. Kim YK, Yeo J, Kim B, Ha M, Kim VN. Short structured RNAs with low GC content are selectively lost during extraction from a small number of cells. Molecular cell. 2012;46(6):893-5.
39. Gill S, Catchpole R, Forterre P. Extracellular membrane vesicles (EVs) in the three domains of life and beyond. FEMS microbiology reviews. 2018.
40. Melnyk CW, Molnar A, Baulcombe DC. Intercellular and systemic movement of RNA silencing signals. The EMBO journal. 2011;30(17):3553-63.
41. Hunter CP, Winston WM, Molodowitch C, Feinberg EH, Shih J, Sutherlin M, et al. Systemic RNAi in Caenorhabditis elegans. Cold Spring Harbor symposia on quantitative biology. 2006;71:95-100.
42. Xu R, Rai A, Chen M, Suwakulsiri W, Greening DW, Simpson RJ. Extracellular vesicles in cancer - implications for future improvements in cancer care. Nature reviews Clinical oncology. 2018;15(10):617-38.
43. Thompson AG, Gray E, Heman-Ackah SM, Mager I, Talbot K, Andaloussi SE, et al. Extracellular vesicles in neurodegenerative disease - pathogenesis to biomarkers. Nature reviews Neurology. 2016;12(6):346-57.
44. Hill AF, Pegtel DM, Lambertz U, Leonardi T, O'Driscoll L, Pluchino S, et al. ISEV position paper: extracellular vesicle RNA analysis and bioinformatics. Journal of extracellular vesicles. 2013;2.

45. Thery C, Amigorena S, Raposo G, Clayton A. Isolation and characterization of exosomes from cell culture supernatants and biological fluids. Current protocols in cell biology / editorial board, Juan S Bonifacino [et al]. 2006;Chapter 3:Unit 3.22.
46. Kowal EJK, Ter-Ovanesyan D, Regev A, Church GM. Extracellular Vesicle Isolation and Analysis by Western Blotting. Methods Mol Biol. 2017;1660:143-52.
47. Thorvaldsdottir H, Robinson JT, Mesirov JP. Integrative Genomics Viewer (IGV): high-performance genomics data visualization and exploration. Briefings in bioinformatics. 2013;14(2):178-92.
48. Cossetti C, Iraci N, Mercer TR, Leonardi T, Alpi E, Drago D, et al. Extracellular vesicles from neural stem cells transfer IFN-gamma via Ifngr1 to activate Stat1 signaling in target cells. Molecular cell. 2014;56(2):193-204.
49. Soekmadji C, Hill AF, Wauben MH, Buzas EI, Di Vizio D, Gardiner C, et al. Towards mechanisms and standardization in extracellular vesicle and extracellular RNA studies: results of a worldwide survey. Journal of extracellular vesicles. 2018;7(1):1535745.
50. Kahlert C, Melo SA, Protopopov A, Tang J, Seth S, Koch M, et al. Identification of double-stranded genomic DNA spanning all chromosomes with mutated KRAS and p53 DNA in the serum exosomes of patients with pancreatic cancer. The Journal of biological chemistry. 2014;289(7):3869-75.
51. Lee TH, Chennakrishnaiah S, Audemard E, Montermini L, Meehan B, Rak J. Oncogenic ras-driven cancer cell vesiculation leads to emission of double-stranded DNA capable of interacting with target cells. Biochemical and biophysical research communications. 2014;451(2):295-301.
52. Thakur BK, Zhang H, Becker A, Matei I, Huang Y, Costa-Silva B, et al. Double-stranded DNA in exosomes: a novel biomarker in cancer detection. Cell research. 2014;24(6):766-9.
53. Wei Z, Batagov AO, Schinelli S, Wang J, Wang Y, El Fatimy R, et al. Coding and noncoding landscape of extracellular RNA released by human glioma stem cells. Nature communications. 2017;8(1):1145.
54. Hung ME, Leonard JN. A platform for actively loading cargo RNA to elucidate limiting steps in EV-mediated delivery. Journal of extracellular vesicles. 2016;5:31027.
55. Tosar JP, Cayota A, Eitan E, Halushka MK, Witwer KW. Ribonucleic artefacts: are some extracellular RNA discoveries driven by cell culture medium components? Journal of extracellular vesicles. 2017;6(1):1272832.
56. Wei Z, Batagov AO, Carter DR, Krichevsky AM. Fetal Bovine Serum RNA Interferes with the Cell Culture derived Extracellular RNA. Scientific reports. 2016;6:31175.
57. Hinger SA, Cha DJ, Franklin JL, Higginbotham JN, Dou Y, Ping J, et al. Diverse Long RNAs Are Differentially Sorted into Extracellular Vesicles Secreted by Colorectal Cancer Cells. Cell reports. 2018;25(3):715-25.e4.
58. Koh W, Pan W, Gawad C, Fan HC, Kerchner GA, Wyss-Coray T, et al. Noninvasive in vivo monitoring of tissue-specific global gene expression in humans. Proceedings of the National Academy of Sciences of the United States of America. 2014;111(20):7361-6.

59. Ngo TTM, Moufarrej MN, Rasmussen MH, Camunas-Soler J, Pan W, Okamoto J, et al. Noninvasive blood tests for fetal development predict gestational age and preterm delivery. Science (New York, NY). 2018;360(6393):1133-6.
60. van der Pol E, Coumans F, Varga Z, Krumrey M, Nieuwland R. Innovation in detection of microparticles and exosomes. Journal of thrombosis and haemostasis : JTH. 2013;11 Suppl 1:36-45.
61. Nolan JP, Moore J. Extracellular vesicles: Great potential, many challenges. Cytometry Part B, Clinical cytometry. 2016;90(4):324-5.
62. Puzar Dominkus P, Stenovec M, Sitar S, Lasic E, Zorec R, Plemenitas A, et al. PKH26 labeling of extracellular vesicles: Characterization and cellular internalization of contaminating PKH26 nanoparticles. Biochimica et biophysica acta Biomembranes. 2018;1860(6):1350-61.
63. Fiandaca MS, Kapogiannis D, Mapstone M, Boxer A, Eitan E, Schwartz JB, et al. Identification of preclinical Alzheimer's disease by a profile of pathogenic proteins in neurally derived blood exosomes: A case-control study. Alzheimer's & dementia : the journal of the Alzheimer's Association. 2015;11(6):600-7.e1.
64. Goetzl EJ, Boxer A, Schwartz JB, Abner EL, Petersen RC, Miller BL, et al. Altered lysosomal proteins in neural-derived plasma exosomes in preclinical Alzheimer disease. Neurology. 2015;85(1):40-7.
65. Kapogiannis D, Boxer A, Schwartz JB, Abner EL, Biragyn A, Masharani U, et al. Dysfunctionally phosphorylated type 1 insulin receptor substrate in neural-derived blood exosomes of preclinical Alzheimer's disease. FASEB J. 2015;29(2):589-96.
66. Goetzl EJ, Kapogiannis D, Schwartz JB, Lobach IV, Goetzl L, Abner EL, et al. Decreased synaptic proteins in neuronal exosomes of frontotemporal dementia and Alzheimer's disease. Faseb j. 2016;30(12):4141-8.
67. Shi M, Kovac A, Korff A, Cook TJ, Ginghina C, Bullock KM, et al. CNS tau efflux via exosomes is likely increased in Parkinson's disease but not in Alzheimer's disease. Alzheimer's & dementia : the journal of the Alzheimer's Association. 2016;12(11):1125-31.
68. Melo SA, Luecke LB, Kahlert C, Fernandez AF, Gammon ST, Kaye J, et al. Glypican-1 identifies cancer exosomes and detects early pancreatic cancer. Nature. 2015;523(7559):177-82.
69. Jeong S, Park J, Pathania D, Castro CM, Weissleder R, Lee H. Integrated Magneto-Electrochemical Sensor for Exosome Analysis. ACS nano. 2016;10(2):1802-9.
70. Reategui E, van der Vos KE, Lai CP, Zeinali M, Atai NA, Aldikacti B, et al. Engineered nanointerfaces for microfluidic isolation and molecular profiling of tumor-specific extracellular vesicles. Nature communications. 2018;9(1):175.
71. Busskamp V, Lewis NE, Guye P, Ng AH, Shipman SL, Byrne SM, et al. Rapid neurogenesis through transcriptional activation in human stem cells. Mol Syst Biol. 2014;10:760.
72. UniProt: the universal protein knowledgebase. Nucleic Acids Res. 2017;45(D1):D158-d69.
73. Chiasserini D, van Weering JR, Piersma SR, Pham TV, Malekzadeh A, Teunissen CE, et al. Proteomic analysis of cerebrospinal fluid extracellular vesicles: a comprehensive dataset. Journal of proteomics. 2014;106:191-204.

74. Schutzer SE, Liu T, Natelson BH, Angel TE, Schepmoes AA, Purvine SO, et al. Establishing the proteome of normal human cerebrospinal fluid. PloS one. 2010;5(6):e10980.
75. Zhang Y, Chen K, Sloan SA, Bennett ML, Scholze AR, O'Keeffe S, et al. An RNA-sequencing transcriptome and splicing database of glia, neurons, and vascular cells of the cerebral cortex. J Neurosci. 2014;34(36):11929-47.
76. Zhang Y, Sloan SA, Clarke LE, Caneda C, Plaza CA, Blumenthal PD, et al. Purification and Characterization of Progenitor and Mature Human Astrocytes Reveals Transcriptional and Functional Differences with Mouse. Neuron. 2016;89(1):37-53.
77. Kowal J, Arras G, Colombo M, Jouve M, Morath JP, Primdal-Bengtson B, et al. Proteomic comparison defines novel markers to characterize heterogeneous populations of extracellular vesicle subtypes. Proceedings of the National Academy of Sciences of the United States of America. 2016;113(8):E968-77.
78. Picelli S, Bjorklund AK, Faridani OR, Sagasser S, Winberg G, Sandberg R. Smart-seq2 for sensitive full-length transcriptome profiling in single cells. Nature methods. 2013;10(11):1096-8.
79. Kiefel H, Bondong S, Hazin J, Ridinger J, Schirmer U, Riedle S, et al. L1CAM: a major driver for tumor cell invasion and motility. Cell adhesion & migration. 2012;6(4):374-84.
80. Regev A, Teichmann SA, Lander ES, Amit I, Benoist C, Birney E, et al. The Human Cell Atlas. eLife. 2017;6.
81. Charrin S, Jouannet S, Boucheix C, Rubinstein E. Tetraspanins at a glance. Journal of cell science. 2014;127(Pt 17):3641-8.
82. Jao CY, Salic A. Exploring RNA transcription and turnover in vivo by using click chemistry. Proceedings of the National Academy of Sciences of the United States of America. 2008;105(41):15779-84.
83. Power RM, Huisken J. A guide to light-sheet fluorescence microscopy for multiscale imaging. Nature methods. 2017;14(4):360-73.
84. Eftekharzadeh B, Hyman BT, Wegmann S. Structural studies on the mechanism of protein aggregation in age related neurodegenerative diseases. Mechanisms of ageing and development. 2016;156:1-13.
85. Rissin DM, Kan CW, Campbell TG, Howes SC, Fournier DR, Song L, et al. Single-molecule enzyme-linked immunosorbent assay detects serum proteins at subfemtomolar concentrations. Nature biotechnology. 2010;28(6):595-9.
86. Heusermann W, Hean J, Trojer D, Steib E, von Bueren S, Graff-Meyer A, et al. Exosomes surf on filopodia to enter cells at endocytic hot spots, traffic within endosomes, and are targeted to the ER. The Journal of cell biology. 2016;213(2):173-84.
87. Mager DL, Stoye JP. Mammalian Endogenous Retroviruses. Microbiology spectrum. 2015;3(1):Mdna3-0009-2014.
88. Contreras-Galindo R, Kaplan MH, Dube D, Gonzalez-Hernandez MJ, Chan S, Meng F, et al. Human Endogenous Retrovirus Type K (HERV-K) Particles Package and Transmit HERV-K-Related Sequences. Journal of virology. 2015;89(14):7187-201.

89. Dewannieux M, Blaise S, Heidmann T. Identification of a functional envelope protein from the HERV-K family of human endogenous retroviruses. Journal of virology. 2005;79(24):15573-7.
90. Maas SLN, Breakefield XO, Weaver AM. Extracellular Vesicles: Unique Intercellular Delivery Vehicles. Trends in cell biology. 2017;27(3):172-88.
91. Turchinovich A, Tonevitsky AG, Cho WC, Burwinkel B. Check and mate to exosomal extracellular miRNA: new lesson from a new approach. Frontiers in molecular biosciences. 2015;2:11.
92. Johnstone RM. Revisiting the road to the discovery of exosomes. Blood cells, molecules & diseases. 2005;34(3):214-9.
93. Harding CV, Heuser JE, Stahl PD. Exosomes: looking back three decades and into the future. The Journal of cell biology. 2013;200(4):367-71.
94. Varshavsky A. The Ubiquitin System, Autophagy, and Regulated Protein Degradation. Annual review of biochemistry. 2017;86:123-8.
95. Moore MJ. From birth to death: the complex lives of eukaryotic mRNAs. Science (New York, NY). 2005;309(5740):1514-8.
96. Cheng L, Zhao W, Hill AF. Exosomes and their role in the intercellular trafficking of normal and disease associated prion proteins. Molecular aspects of medicine. 2018;60:62-8.
97. Jimenez AJ, Maiuri P, Lafaurie-Janvore J, Divoux S, Piel M, Perez F. ESCRT machinery is required for plasma membrane repair. Science (New York, NY). 2014;343(6174):1247136.
98. Gong YN, Guy C, Olauson H, Becker JU, Yang M, Fitzgerald P, et al. ESCRT-III Acts Downstream of MLKL to Regulate Necroptotic Cell Death and Its Consequences. Cell. 2017;169(2):286-300.e16.
99. Zeng F, Morelli AE. Extracellular vesicle-mediated MHC cross-dressing in immune homeostasis, transplantation, infectious diseases, and cancer. Seminars in immunopathology. 2018;40(5):477-90.
100. Gifford RJ, Blomberg J, Coffin JM, Fan H, Heidmann T, Mayer J, et al. Nomenclature for endogenous retrovirus (ERV) loci. Retrovirology. 2018;15(1):59.
101. Blomberg J, Benachenhou F, Blikstad V, Sperber G, Mayer J. Classification and nomenclature of endogenous retroviral sequences (ERVs): problems and recommendations. Gene. 2009;448(2):115-23.
102. Virgin HW. The virome in mammalian physiology and disease. Cell. 2014;157(1):142-50.
103. Wurdinger T, Gatson NN, Balaj L, Kaur B, Breakefield XO, Pegtel DM. Extracellular vesicles and their convergence with viral pathways. Advances in virology. 2012;2012:767694.
104. Izquierdo-Useros N, Puertas MC, Borras FE, Blanco J, Martinez-Picado J. Exosomes and retroviruses: the chicken or the egg? Cellular microbiology. 2011;13(1):10-7.
105. Nolte-'t Hoen E, Cremer T, Gallo RC, Margolis LB. Extracellular vesicles and viruses: Are they close relatives? Proceedings of the National Academy of Sciences of the United States of America. 2016;113(33):9155-61.

106. Fang Y, Wu N, Gan X, Yan W, Morrell JC, Gould SJ. Higher-order oligomerization targets plasma membrane proteins and HIV gag to exosomes. PLoS biology. 2007;5(6):e158.
107. Witwer KW, Buzas EI, Bemis LT, Bora A, Lasser C, Lotvall J, et al. Standardization of sample collection, isolation and analysis methods in extracellular vesicle research. Journal of extracellular vesicles. 2013;2.
108. Liu X, Fu R, Pan Y, Meza-Sosa KF, Zhang Z, Lieberman J. PNPT1 Release from Mitochondria during Apoptosis Triggers Decay of Poly(A) RNAs. Cell. 2018;174(1):187-201.e12.
109. Thomas MP, Liu X, Whangbo J, McCrossan G, Sanborn KB, Basar E, et al. Apoptosis Triggers Specific, Rapid, and Global mRNA Decay with 3' Uridylated Intermediates Degraded by DIS3L2. Cell reports. 2015;11(7):1079-89.
110. Hudecova I. Digital PCR analysis of circulating nucleic acids. Clinical biochemistry. 2015;48(15):948-56.
111. Ter-Ovanesyan D, Kowal EJK, Regev A, Church GM, Cocucci E. Imaging of Isolated Extracellular Vesicles Using Fluorescence Microscopy. Methods Mol Biol. 2017;1660:233-41.
112. Schwartz S, Mumbach MR, Jovanovic M, Wang T, Maciag K, Bushkin GG, et al. Perturbation of m6A writers reveals two distinct classes of mRNA methylation at internal and 5' sites. Cell reports. 2014;8(1):284-96.
113. Li B, Dewey CN. RSEM: accurate transcript quantification from RNA-Seq data with or without a reference genome. BMC bioinformatics. 2011;12:323.
114. Robinson MD, McCarthy DJ, Smyth GK. edgeR: a Bioconductor package for differential expression analysis of digital gene expression data. Bioinformatics (Oxford, England). 2010;26(1):139-40.
115. Cocucci E, Aguet F, Boulant S, Kirchhausen T. The first five seconds in the life of a clathrin-coated pit. Cell. 2012;150(3):495-507.